8-2011

LIPID METABOLISM IN *Trypanosoma brucei*: MOLECULAR CHARACTERIZATION OF FATTY ACID SYNTHESIS AND UPTAKE

Patrick Vigueira
Clemson University, pviguei@gmail.com

LIPID METABOLISM IN *Trypanosoma brucei*: MOLECULAR CHARACTERIZATION OF FATTY ACID SYNTHESIS AND UPTAKE

A Dissertation
Presented to
the Graduate School of
Clemson University

In Partial Fulfillment
of the Requirements for the Degree
Doctor of Philosophy
Biological Sciences

---

by
Patrick A. Vigueira
August 2011

Accepted by:
Kimberly S. Paul, Committee Chair
James C. Morris
Lesly A. Temesvari
Matthew W. Turnbull

ABSTRACT

My doctoral studies focused on the fatty acid metabolism of the deadly protozoan parasite, *Trypanosoma brucei*. Fatty acid metabolism in *T. brucei* can be broadly divided into two pathways, synthesis and uptake. In Chapters 2-4 I describe experiments investigating the parasite's fatty acid synthesis pathway. Chapter 2 contains the initial characterization of acetyl-CoA carboxylase (ACC) in *T. brucei*. Knockdown of TbACC by RNA interference (RNAi) reduced parasite virulence in a mouse model, suggesting that TbACC has the potential to be utilized as a drug target. Chapters 3 and 4 explore the effects of two known ACC inhibitors, the aryloxyphenoxypropionate herbicide, haloxyfop and the green tea catechin, (−)-epigallocatechin-3-gallate (EGCG) on TbACC activity and parasite growth. Both compounds inhibited TbACC enzymatic activity and parasite growth *in vitro*. In Chapters 5 and 6 contain research that utilizes forward and reverse-genetic techniques to study *T. brucei* fatty acid uptake. In Chapter 5 I begin to characterize the role of the parasite's acyl-CoA synthetase genes in fatty acid uptake and growth. Further, I demonstrate that fatty acid uptake is in part a protein mediated process. Chapter 6 describes an RNAi screen for genes involved in *T. brucei* fatty acid uptake. Together these studies build upon our knowledge of the unique fatty acid metabolism of *T. brucei*, bringing us one step closer to a potential cure for this horrible disease.

DEDICATION

To my family:

My loving parents, who taught me the value of education and always encouraged me to strive for excellence.

My beautiful wife Cindy for her constant support and companionship.

ACKNOWLEDGMENTS

First, I would like to thank Dr. Kim Paul for giving me the opportunity to work in her lab and the freedom to pursue experiments of my own design.

In addition, I would like to thank Dr. Jim Morris, Dr. Lesly Temesvari, and Dr. Matthew W. Turnbull for serving on my committee. I appreciate your willingness to share your time and expertise.

I would also like to thank Dr. Meredith Morris for her helpful advice and friendly smile and Dr. Hap Wheeler for his support of Biological Sciences graduate students. The members of the Paul, Morris, Turnbull, Temesvari, Chapman, Childress and Mount labs were always available for helpful discussion over lunch or beer.

The value of a clean and functional facility cannot be overestimated. I thank Mr. Mark for his daily efforts towards keeping Jordan Hall spick and span. Finally, I would like to thank Mr. Mike Moore for his hard work, patience, and sense of humor. Without him, I am convinced that the building would have crumbled to the ground long ago.

TABLE OF CONTENTS

Table of Contents (Continued)

Page

Table of Contents (Continued)

Page

LIST OF TABLES

LIST OF FIGURES

List of Figures (Continued)

CHAPTER ONE

LITERATURE REVIEW

AFRICAN TRYPANOSOMIASIS

Trypanosoma brucei is an early-branching protozoan parasite transmitted by the tsetse fly to its mammalian hosts. The parasite threatens over 6.2 million square miles in sub-Saharan Africa (FAO, Food and Agricultural Organization of the United Nations, 2007) where it causes fatal disease in humans. Between 1998 and 2004 annual cases of African sleeping sickness were estimated to number 50,000 to 70,000 (WHO, 2010). More recently, in 2009, less than 10,000 cases were reported. In some regions the infection rate of human African trypanosomiasis (HAT) is especially high, causing greater morbidity and mortality than either HIV/AIDS or malaria (WHO, 2010).

Two subspecies of the parasite cause disease in humans. *T. b. gambiense* is most common on the western side of the Nile rift valley and causes a chronic infection that leads to death over a ~3 year period. *T. b. rhodesiense* is found primarily on the eastern side of the Nile rift valley and causes an acute infection that can result in death in as little as 3 weeks (Brun *et al.*, 2010). *T. b. brucei* is the subspecies we utilize for laboratory experiments. Humans are resistant to infection by *T. b. brucei* because they possess a specialized type of high density lipoprotein called trypanolytic factor (TLF) causes parasite lysis when it is taken up via endocytosis (Wheeler, 2010). Cattle and other livestock lack TLF and are therefore sensitive to infection by *T. b. brucei* and a related

parasite, *Trypanosoma congolense*. These parasites are the causative agents of a devastating livestock disease called nagana (Baumgaertner *et al.*, 2008). The disease makes agriculture in this lush, fertile landscape nearly impossible and results in $4.5 billion dollars of trypanosome-related agricultural losses each year. Much of the economic turmoil in this poverty-stricken region of sub-Saharan Africa stems from the inability to establish an efficient agricultural system in this uncultivatable “green desert” (FAO, Food and Agricultural Organization of the United Nations, 2007).

HAT manifests two distinct clinical stages. In early-stage infections parasites are restricted to the bloodstream and lymph. Typical early-stage symptoms include fever, headache, and swollen lymph nodes. Late-stage symptoms occur after the parasite has invaded the central nervous system. Severe insomnia is often induced by disruptions of circadian rhythms. This disruption causes the lethargic coma-like state that is characteristic of the infection and the origin of the term “sleeping sickness”. Late-stage HAT may also bring about psychological conditions ranging from apathy to irritability (Brun *et al.*, 2010).

African Trypanosomiasis Treatment

There is no vaccine for African trypanosomiasis because the antigenic variability of the parasite confounds vaccine development (Brun *et al.*, 2010; Horn *et al.*, 2010). Thus, current control options center on prevention and chemotherapy. Prevention methods such as trapping, insecticide treatment, and

behavioral changes (e.g. grazing at night) are costly and/or potentially toxic to humans and cattle, while ultimately yielding incomplete protection (Enserink, 2007).

Successful treatment of HAT is dependent upon proper diagnosis of the parasite subspecies and disease phase. Hemolymphatic infections are diagnosed using either card agglutination tests or microscopic examination of blood and lymph node aspirates. However, detection of late-stage HAT requires a lumbar puncture to acquire cerebrospinal fluid (CSF) for analysis. Despite the invasive nature of a lumbar puncture, CSF screening is considered a necessary step in the diagnostic process, as two of the approved drugs are not suitable for last-stage treatment because they do not efficiently cross the blood-brain barrier (Fairlamb, 2003; WHO, 2010; Brun *et al.*, 2010).

The five compounds currently available for treating sleeping sickness each have substantial limitations (Fairlamb, 2003; Brun *et al.*, 2010). Patients with an early-stage infection are treated with either Suramin or Pentamidine. Suramin is the front-line drug for early-stage *T. b. rhodesiense* infections. Besides having immediate life-threating side-effects, the trypanocidal activity of Suramin is slow and the mode of action remains a mystery. It is widely considered to have multiple cellular targets, a notion supported by the fact that drug resistance in field isolates has not been reported. Early-stage *T. b. gambiense* infections are typically treated with Pentamidine. The drug has relatively high trypanocidal activity, and resistance in field isolates has not been reported. The compound is

taken up by at least three cell membrane transporters and causes a disruption in kinetoplast DNA replication by inhibiting mitochondrial topoisomerase II. Pentamidine is also believed to reduce polyamine biosynthesis by inhibiting production of *S*-adenosylmethionine. However, Pentamidine has limited use because it does not cross the blood-brain barrier and has limited efficacy against *T. b. rhodesiense*.

Late-stage *T. b. gambiense* infections can be treated with Eflornithine. The compound perturbs polyamine biosynthesis by irreversibly inhibiting ornithine decarboxylase. Treatment with Eflornithine is reasonably effective, but the medically-intensive administration (four daily infusions over 1-2 weeks) and high cost often force care-givers to utilize Melarsoprol, a much less desirable alternative. Because Melarsoprol is relatively inexpensive compared to Eflornithine, it is the most common chemotherapeutic agent for treatment of late-stage *T. b. gambiense* and *T. b. rhodesiense* infections. It is a highly-toxic, organic derivative of arsenic. Melarsoprol kills 5% of patients receiving treatment (McNeil, 2000). Drug administration is extremely painful because the water-insoluble compound is dissolved in propylene glycol. Due to its widespread use, reports of Melarsoprol resistance are common. Treatment failures as high as 30% have been reported in some regions (Fairlamb, 2003; WHO, 2010; Brun *et al.*, 2010).

Nifurtimox, a drug approved for treatment of *Trypanosoma cruzi* infection, has also been utilized in combination with either Eflornithine or Melarsoprol to

treat late-stage cases of sleeping sickness. The results of the clinical trials have been somewhat conflicting, but a recent review of 9 different Nifurtimox-combination therapy trials concluded that a Nifurtimox-Eflornithine combination was better tolerated than a Nifurtimox-Melarsoprol combination or Melarsoprol alone. Additionally, rates of relapse, a typical complication in treating late-stage HAT, were low when Nifurtimox-Eflornithine combination therapy was utilized. Thus, Nifurtimox combination therapies represent a new weapon in the battle against sleeping sickness (Fairlamb, 2003; Lutje *et al.*, 2010).

New drugs for the treatment of sleeping sickness are desperately needed. Of the 5 currently used compounds, Eflornithine was developed most recently, first synthesized in 1977. Suramin has been in use for over 90 years (Fairlamb, 2003). These facts highlight the desperate need for new drugs and drug targets, making research into trypanosome biology of critical importance. My research represents progress towards developing new treatments for sleeping sickness.

Trypanosoma brucei LIFE CYCLE

Within an infected mammalian host, the parasite lives and divides extracellularly in the blood stream and in late-stage infections, the cerebrospinal fluid. Rapid division occurs via binary fission, resulting in parasite titers exceeding $1x10^9$ parasites/mL. This spike in parasitemia is followed by a developmental shift to the nonproliferative short stumpy form. As the infection progresses, parasites begin to cross the blood-brain barrier and accumulate in

the brain, eventually leading to coma and death (Matthews, 2005; Lee *et al.*, 2007).

The insect life stage begins when the tsetse fly takes a blood meal containing short stumpy forms from an infected mammal. The parasites replicate for a period in the insect's midgut before traversing the midgut epithelium into the hemolymph. They then navigate through the hemolymph to invade the salivary glands where they undergo another developmental shift into metacyclic forms. These metacyclic form parasites can then be transmitted to another mammalian host when the fly takes its next blood meal (Matthews, 2005; Lee *et al.*, 2007) (Fig. 1.1).

Parasite Surface Coats

The surface coat proteins of the parasite are important for survival throughout its life cycle. In the mammalian bloodstream form (BF), the surface coat is composed of 10^7 identical copies of variant surface glycoprotein (VSG) (Ferguson *et al.*, 1984). Each VSG molecule is attached to the cell membrane by a glycosylphosphatidylinositol (GPI) anchor whose fatty acid moiety is exclusively the 14-carbon fatty acid, myristate (Ferguson *et al.*, 1984). This dense VSG coat allows the parasite to vary its surface antigens throughout the duration of an infection. Over 1000 genes code for the proteinaceous portion of VSG, giving the parasite a huge antigenic repertoire (Ferguson *et al.*, 1999). This process of antigenic variation allows the trypanosome to be a very successful parasite; the

mammalian adaptive immune system is unable to mount an efficient attack against the ever-changing parasite surface coat.

The insect midgut, procyclic form (PF) parasites also depend heavily on their surface coat protein, procyclin (Richardson *et al.*, 1988; Roditi *et al.*, 1989). Procyclin may play a major role in protecting the trypanosome against proteolytic degradation while in the midgut of the tsetse fly (Acosta-Serrano *et al.*, 2001). Each of the 10^6 procyclins per cell is attached to the cell membrane by a lyso-GPI anchor, each requiring two fatty acid molecules, either 16 or 18-carbons in length (Butikofer *et al.*, 1997). The parasite's dependence upon GPI-anchored surface coat proteins during two life cycle stages highlights the high demand for copious quantities of fatty acids throughout its life cycle (Morita *et al.*, 2000; Paul *et al.*, 2001).

Host Microenvironments

As the parasite moves through its life cycle, it encounters a number of diverse microenvironments: the mammalian blood and brain/CSF; and the insect midgut, hemolymph and salivary glands. Each of these environments is unique in their nutrient content. One example of a dramatic shift in environmental fatty acid availability occurs when the parasite moves across the blood-brain barrier; the CSF contains 99.8% less lipids than the blood (Roheim *et al.*, 1979). Fatty acids are extremely important to the parasite. Besides constituting critical GPI anchor components for essential cell surface proteins, fatty acids play both functional roles (cell signaling molecules) and structural roles (principal elements of cellular

membranes) within the cell. Because of the extremely variable conditions and high demand for fatty acids, the parasite encounters host microenvironments where the available fatty acids are insufficient. To compensate, *T. brucei* can synthesize its own fatty acids. Thus, the parasites must have the ability to efficiently regulate its mechanism for *de novo* synthesis of fatty acids to meet its changing nutrient demands.

FATTY ACID SYNTHESIS

Fatty acid synthesis (FAS) occurs in cycles of four enzymatic reactions that result in the extension of a growing acyl chain by two carbons with each successive cycle. The first reaction in the cycle involves the condensation of an acyl chain with a malonyl group, the two-carbon donor molecule; this reaction is catalyzed by a ketoacyl synthase. The ketoacyl intermediate then undergoes a reduction by ketoacyl reductase, dehydration by a dehydratase and final reduction by enoyl reductase, yielding a fatty acyl chain two carbons greater in length (Lee *et al.*, 2007) (Fig. 1.2). While all FAS includes the same four basic reactions, different types of FAS pathways have a number of important distinctions.

FAS pathways are separated into two groups: the eukaryotic type I and the prokaryotic-origin type II. The type I FAS pathway includes one or two very large multifunctional proteins, while the type II pathway utilizes four separate proteins, each with a discrete enzymatic function. Many eukaryotic organisms possess both pathways. However, the type II pathway is typically restricted to

organelles of prokaryotic origin (e.g., mitochondria, apicoplasts and chloroplasts) (Goodman *et al.*, 2007; Lee *et al.*, 2007; Stephens *et al.*, 2007). Some eukaryotes also utilize microsomal elongases (ELO) as a component of their FAS machinery. ELO pathways utilize the same cycle of enzymatic reactions as type I or type II FAS, but typically extend only long chain fatty acids (16 to 18 carbons) to very long chain fatty acids, greater than 20 carbons in length (Toke *et al.*, 1996; Oh *et al.*, 1997; Moon *et al.*, 2001). ELO pathways are also distinct because they are associated with organellar membranes and utilize Coenzyme-A (CoA) rather than acyl carrier protein as a carrier molecule for acyl intermediates.

T. brucei Fatty Acid Synthesis

Unlike most eukaryotes *T. brucei* lacks the typical components of the cytosolic type I FAS. In lieu of the conventional FAS pathway, the parasite depends completely upon an ELO pathway for the bulk synthesis of its fatty acids (Lee *et al.*, 2006). This ELO pathway is set apart from others by the ability to synthesize fatty acids *de novo* from a 4-carbon primer, butyryl-CoA. The *T. brucei* ELO pathway consists of four different ketoacyl-CoA synthases with distinct, yet overlapping specificities for acyl-CoA chain lengths: ELO1 (C4:0 – C10:0), ELO 2 (C10:0 – C14:0), ELO 3 (C14:0 – C18:0). There is a fourth enzyme in the pathway, ELO4, but its use is restricted to elongation of long chain unsaturated fatty acids. The two reductases in the pathway have also been identified; the genome codes for two ketoacyl-CoA reductases and a single

enoyl-CoA reductase. The pathway's dehydratase has yet to be identified (Lee *et al.*, 2006; Lee *et al.*, 2007).

The distinct yet overlapping activities of the ELO proteins allows for a very efficient FAS mechanism in *T. brucei*. The modulation of each ELO's enzymatic activity allows for the preferential production of specific chain length fatty acids, providing *T. brucei* the ability to adjust to its ever-changing environmental conditions and demands for fatty acids (Lee *et al.*, 2007). In addition, the need for a dedicated FAS and elongation pathways is essentially eliminated, because the ELO pathway serves both purposes.

T. brucei also possess a second FAS pathway, a mitochondrial type II pathway. It consists of one acyl carrier protein (ACP), one ketoacyl-ACP synthase, three ketoacyl-ACP reductases, one or more currently unidentified dehydratases, and two enoyl-ACP reductases. Mitochondrial FAS is only responsible for 10% of total the FAS in the parasite and its primary products are C16:0 and C8:0. The C8:0 product is synthesized as a precursor for lipoic acid, which is an important prosthetic group for multiple mitochondrial enzymes (Lee *et al.*, 2007; Stephens *et al.*, 2007).

Both the mitochondrial and cytoplasmic FAS pathways of *T. brucei* are essential for parasite growth. In both PF and BF parasites, reduction of ACP by RNAi or conditional knockout resulted in reduced mitochondrial FAS and slowed parasite growth in culture (Stephens *et al.*, 2007). *T. brucei* exhibits a condition and stage-specific requirement for cytoplasmic FAS. Reduction of enoyl-CoA

reductase by conditional knockout caused a growth phenotype only when PF parasites were cultured in low-lipid media (Lee *et al.*, 2006). This is not the case in BF parasites; enoyl-CoA reductase was essential for growth in normal media and in a mouse model (Soo Hee Lee, personal communication).

ACETYL-COA CARBOXYLASE

FAS requires a substantial amount of malonyl-CoA, as it donates two carbons to the growing acyl-chain. Malonyl-CoA is generated by the carboxylation of acetyl-CoA, a reaction catalyzed by acetyl-CoA carboxylase (ACC). This is an ATP dependent reaction and therefore, is considered the first committed step in FAS (Barber *et al.*, 2005).

The *T. brucei* genome codes for a single ACC gene, which was determined by homology to other ACCs (Aslett *et al.*, 2010; TbGeneDB). TbACC is a large multidomain enzyme, consisting of biotin carboxylase, biotin-carboxyl carrier protein (BCCP), and carboxyl-transferase (CT) domains. The ACC reaction proceeds forward in two steps. First, the carboxylation of the biotin prosthetic group proceeds by adding a CO_2 group from a bicarbonate molecule. This is followed by the carboxyl transfer step, combining CO_2 and acetyl-CoA, resulting in the creation of the two-carbon donor malonyl-CoA (Lee *et al.*, 2008).

Regulation of Acetyl-CoA Carboxylase

The enzymatic activity of ACC is controlled by multiple post-translational modifications. Reversible phosphorylation is the best understood mechanism and is conserved in all described ACCs (Barber *et al.*, 2005). Increased

phosphorylation causes a reduction in ACC activity. Both AMP-activated protein kinase (AMPK) and protein kinase A phosphorylate ACC and have direct impact on activity (Barber *et al.*, 2005; Brownsey *et al.*, 2006). Regulation of TbACC by phosphorylation has yet to be demonstrated. However, experiments in our lab have demonstrated that TbACC is indeed phosphorylated (Sunayan Ray, personal communication).

Regulation of ACC activity by polymerization has also been reported. In its basal state ACC exists as a dimer, but it is also capable of forming higher order polymers (Kleinschmidt *et al.*, 1969; Mackall *et al.*, 1978; Thampy *et al.*, 1985; Barber *et al.*, 2005). *in vitro* treatment of chicken liver extracts with supraphysiological concentrations of citrate causes the enzyme to polymerize into long filaments and increases enzymatic activity (Beaty *et al.*, 1985). In mouse liver the polymerization process is facilitated by the MIG12 protein. The presence of MIG12 lowers the citrate concentration needed to induce ACC polymerization and elevated activity (Kim *et al.*, 2010). These filamentous polymers dissociate in response to ACC's product, malonyl-CoA (Beaty *et al.*, 1983). ACC polymers in the form of planar arrays have also been reported in yeast and are believed to be active polymers (Schneiter *et al.*, 1996).

Mammalian Acetyl-CoA Carboxylase

The mammalian genome contains two ACCs: ACC1 and ACC2. While both catalyze the conversion of acetyl-CoA to malonyl-CoA, their products serve very different functions in the cell. ACC1 is predominately involved in creating

malonyl-CoA to be used in fatty acid synthesis, while the malonyl-CoA produced by ACC2 is involved in regulating cellular energy usage. Malonyl-CoA is an allosteric inhibitor of carnitine palmitoyltransferase 1 (CPT1), the enzyme responsible for transporting long-chain fatty acids (LCFA) into the mitochondrion (Harada *et al.*, 2007). By inhibiting CPT1, high malonyl-CoA concentrations reduce the rate of FA beta-oxidation within the mitochondrion. Low malonyl-CoA levels activate CPT1 and increase the amount of LCFA available to the beta-oxidation pathway. By this mechanism cells avoids futile cycling, preventing simultaneous synthesis and oxidation of FA. This balance is believed to be regulated by AMPK. Activation of AMPK causes increased phosphorylation and inhibition of ACC (Bouzakri *et al.*, 2008).

Acetyl-CoA Carboxylase Inhibitors

As a consequence of the huge cost associated with the development of pharmaceuticals and the dire economic status of sub-Saharan Africa, critics contend that even the identification of a perfect drug target would not result in a commercially available therapy for African trypanosome infections. African trypanosomiasis and similar infectious diseases are very low priorities for pharmaceutical companies, so called “orphan diseases.” However, recent research has implicated the human ACC pathway as playing a role in diabetes, obesity, and some cancers, effectively sparking the interest of drug companies (Lopaschuk *et al.*, 2006; Tong *et al.*, 2006; Choi *et al.*, 2007; Folmes *et al.*, 2007). As a result, multiple drugs targeting human ACC are in the drug development

pipeline, and many of their analogs have been synthesized in the process (Cheng *et al.*, 2006; Corbett *et al.*, 2007). These compounds have the potential to inhibit TbACC, thereby reducing the problem of African trypanosomiasis being an "unprofitable" disease.

In addition to its potential use as a drug target for human disease, ACC has long been recognized as a valuable target for chemical intervention in crop management and fungicides. Current allosteric ACC inhibitors can be divided into three distinct classes (Tong *et al.*, 2006).

Class 1 inhibitors work by preventing transfer of the carboxyl group from the BCCP domain to the acetyl-CoA substrate. The cyclohexanediones and aryloxyphenoxypropionates, also known as DIMs and FOPs, are members of this class. Haloxyfop targets the plastid ACCs of grasses by binding the CT domain and causing conformational changes that render the enzyme inactive (Delye *et al.*, 2003; Zhang *et al.*, 2004b; Xiang *et al.*, 2009). Another class 1 inhibitor, 5-(tetradecyloxy)-2-furancarboxylic acid (TOFA) accomplishes the same goal by a different mechanism. Upon entering the cell, TOFA is converted to a CoA thioester and competes for the acetyl-CoA binding pocket (Halvorson *et al.*, 1984; Tong *et al.*, 2006).

Class 2 inhibitors are substituted bipiperidylcarboxamides. CP-640186 is the best characterized of the class 2 inhibitors. It interacts with ACC near the BCCP domain and interferes with the biotin moiety (Zhang *et al.*, 2004a).

Class 3 inhibitors are polyketide fungicides. Soraphen A is the best characterized class 3 compound. It binds ACC near the ATP binding pocket and interferes with the carboxylation of the biotin moiety by preventing the dimerization of the BC domain (Shen *et al.,* 2004; Tong *et al.*, 2006).

Many other naturally occurring products are also being explored as inhibitory molecules. They are attractive because they are readily available and many are currently approved for human consumption. The green tea catechin (−)-epigallocatechin-3-gallate (EGCG) inhibits ACC activity in a non-allosteric manner. EGCG activates AMPK and thereby increases ACC phosphorylation, resulting in decreased ACC activity (Moon *et al.*, 2007a; Moon *et al.*, 2007b; Huang *et al.*, 2009).

In the third and fourth chapters of this dissertation I demonstrate the effectiveness of haloxyfop and EGCG as TbACC inhibitors. Both molecules are commercially available and have well-characterized modes of action, making them useful tools in my efforts to characterize TbACC. These studies add to my initial characterization of TbACC (Chapter 2) and build upon previously published studies of haloxyfop and EGCG in related protozoan parasites. Taken together the experiments described in Chapters 2-4 significantly extend our knowledge of *T. brucei* FAS.

EXTRACELLULAR LIPID UPTAKE

Mammalian lipid acquisition mechanisms can vary by tissue and cell type. In this section I will present a generalized review of the best-characterized mechanisms of lipid uptake.

A primary route of lipid acquisition is through endocytosis of lipoproteins. Lipoproteins are made up of a polar surface layer, containing phospholipids, apolipoproteins, and cholesterol and a nonpolar inner core that contains triglycerides and cholesterol esters (Wasan *et al.*, 2008). Lipoproteins are internalized by endocytosis and transported to the lysosome, where the components are liberated. In addition to bulk uptake of lipoproteins, specific phospholipids can be acquired from donor lipoprotein particles and inserted directly into the cell membrane (Engelmann *et al.*, 2010).

A second major mechanism of lipid acquisition is through uptake of FAs. FAs have very low aqueous solubility, and therefore are usually associated with membranes or proteins, typically albumin in the mammalian bloodstream. To become internalized, FAs must first dissociate from albumin and partition into the outer leaflet of the phospholipid bilayer. This is followed by a flip-flop that changes the orientation of the FA carboxyl head group from the outer to the inner lipid-water interface. The FAs can then partition into the cell and become bound, activated, or incorporated into more complex lipid species (Glatz *et al.*, 2010). This process follows biphasic kinetics. Partitioning into the lipid bilayer occurs quickly, but internalization is much slower (Mellors *et al.*, 1989). The flip-flop

mechanism is widely considered the rate-limiting step in the uptake process (Kampf *et al.*, 2007a; Kampf *et al.*, 2007b).

Uptake of FA is known to occur both by protein-mediated active transport and passive diffusion (Glatz *et al.*, 2010). Fatty acid transport protein 1 (FATP1) is localized to the cellular membrane and actively moves fatty acids into the cell. Other proteins, such as CD36 and the peripheral membrane fatty acid binding protein, function by facilitating diffusion, binding FAs, and concentrating them on membrane surface. Bound fatty acids are more easily partitioned into the membrane than albumin-associated FAs, thus uptake rates are greatly increased.

Lipid rafts, specifically caveolae, also appear to play a role in the FA uptake process. Caviolin exhibits high-affinity FA binding. However, its major role in FA uptake is to provide a plasma membrane docking site for CD36. CD36 is predominantly localized to caveolae but is dispersed throughout the plasma membrane when lipid rafts are disrupted by cholesterol depletion. This mislocalization is accompanied by a reduction in FA uptake (Ehehalt *et al.*, 2006; Glatz *et al.*, 2010).

Non-plasma membrane associated proteins also play a role in the uptake of fatty acids. Before an internalized FA can be broken down for energy or incorporated into a more complex lipid species, it must first be activated. The activation process involves esterification to CoA by a family of enzymes called acyl-CoA synthetases (ACS). Before a FA is activated or bound by a protein, it

can leave the cell by outward passive diffusion. Esterification to CoA makes the resulting acyl-CoA membrane-impermeant. Thus, ACS increases retention of FAs that are internalized by facilitated or passive diffusion (Milger *et al.*, 2006).

Lipid Uptake in Trypanosoma brucei

Multiple mechanisms for lipid uptake have been described in *T. brucei*. In the mammalian bloodstream the parasite can take up both high and low density lipoproteins via endocytosis (Coppens *et al.*, 1995; Green *et al.*, 2003). This process is enhanced by a lipoprotein scavenger receptor (Green *et al.*, 2003; Thomson *et al.*, 2009). PF *T. brucei* also likely utilizes a similar mechanism to take up lipophorin (LP) from the tsetse hemolymph. Uptake of LP has been demonstrated in the related parasite, *Trypanosoma rangeli* (Folly *et al.*, 2003) and the malaria parasite, *Plasmodium gallinaceum* (Atella *et al.*, 2009). In addition to endocytosis of lipoproteins, *T. brucei* has a specialized mechanism for acquisition of phospholipids. This process involves the coordinated activity of three proteins and has been validated *in vitro* for uptake of lysophosphatidylcholine (Bowes *et al.*, 1993).

To date little is known about the mechanisms of FA uptake in *T. brucei*. Proteins involved in uptake of FAs in *T. brucei* have not yet been identified and characterized. Early studies demonstrate that FA uptake follows similar biphasic kinetics as described in humans (Voorheis,1980). This similarity in kinetics suggests that, like in human FA uptake, both protein-mediated active transport and passive diffusion are likely occurring. The *T. brucei* genome does contain 5

ACSs, and some early characterization of the genes has been completed (Jiang *et al.*, 2000; Jiang *et al.*, 2001; Jiang *et al.*, 2004). However, characterization of the enzymes in intact cells has not been previously undertaken. In Chapter 5 of this dissertation, I present the first experiments examining the role of the TbACS genes in *T. brucei* FA uptake and growth.

Additionally, because FA uptake likely plays a key role in the growth and virulence of the parasite, I performed an RNAi library screen to identify novel genes involved in this process. In Chapter 6 of this dissertation I describe the screen and provide suggestions for improvements.

RNA INTERFERENCE IN *Trypanosoma brucei*

A number of genetic tools are available for use in *T. brucei*. The initial description of RNAi in *Caenorhabditis elegans* (Fire *et al.*, 1998) was followed quickly by its discovery in *T. brucei* (Ngo *et al.*, 1998). Soon after, a number of genetic tools were developed to take advantage of the parasite's RNAi machinery to study the function of genes in forward and reverse genetic experiments (Shi *et al.*, 2000; Wang *et al.*, 2000; LaCount *et al.*, 2002; Morris *et al.*, 2002). The last decade has seen a steady increase in the use of RNAi as a substitute for traditional knockouts or dominant negative mutants.

The popularity of RNAi over traditional gene knockouts can be attributed to a number of factors. First, compared to creating deletion mutants through gene knockouts, RNAi is quick and less labor intensive. Specifically, creating an RNAi mutant involves a single cloning reaction and one stable transfection, whereas

creating knockouts requires multiple rounds of cloning and transfection, due to the diploid genome of *T. brucei.*

Second, RNAi provides researchers a tool to study essential genes (Motyka *et al.*, 2004; Balana-Fouce *et al.*, 2007). With the exception of low-level leaky expression, uninduced RNAi mutants have identical gene expression to their parental cell lines. Induction of RNAi is achieved by addition of tetracycline to the growth media, initiating synthesis of dsRNA and degradation of target mRNA. The resulting phenotype can be effectively studied prior to the death of the cell. Deletion of essential genes is not possible because it results in death of the organism. An alternative approach, termed conditional knockout, involves stably transfecting an ectopic gene copy prior to native gene deletion. Conditional knockouts are even more labor intensive, and high ectopic gene expression levels can become toxic to the cell.

While RNAi has proven to be a very powerful tool, it comes with its own set of drawbacks. RNAi does not necessarily provide complete abolishment of the target protein. Even when mRNA is degraded below the level of detection, stable proteins can persist for the duration of an experiment. The level of protein required for parasite growth or function of a metabolic pathway can vary widely between genes and growth conditions (Krieger *et al.*, 2000; Albert *et al.*, 2005; Caceres *et al.*, 2010; Vigueira *et al.*, 2011). Thus, RNAi may provide insufficient knockdown to yield phenotypes for some genes. In these cases, alternative strategies such as knockout, dominant negative, or transposon mutagenesis

would need to be employed. A second limiting factor of RNAi is the rather rapid reversion of mutants upon induction. Knockdown of essential genes, resulting in death of the parasite, can promote selection for individuals that have mutated or deleted the RNAi vector thereby rendering it nonfunctional (Motyka *et al.*, 2004). This phenomenon is most common in animal models, because drug selection for maintenance of the dsRNA expression system is no longer imposed on the parasite.

The *T. brucei* RNAi system has proven to be a very useful tool in my research. I have utilized RNAi in reverse-genetics experiments to study the function of TbACC and TbACS (see Chapters 2, 5). I have also used an RNAi library (Morris *et al.*, 2002) to perform a forward-genetics screen for genes involved in fatty acid uptake (see Chapter 6).

In the future, I expect that the popularity of RNAi as a tool for research will continue to grow. Recently, an exciting publication described the creation of an efficient RNAi library in BF *T. brucei* (Alsford *et al.,* 2011). This library was utilized to identify genes essential for BF parasite growth *in vitro*, an important first step in the development of new drug targets. In addition, great strides have been made towards the creation of an inducible RNAi system in a related trypanosome, *Leishmania braziliensis* (Lye *et al.,* 2010). RNAi has been, and will continue to be a valuable weapon in our fight against trypanosome infections.

FIGURES

Figure 1.1: *T. brucei* life cycle. *T. brucei* is transmitted between mammalian hosts by the blood-feeding tsetse fly. Figure adapted from Lee S.H., Stephens J.L., and Englund P.T. (2007) A fatty-acid synthesis mechanism specialized for parasitism. *Nat Rev Microbiol* **5:** 287-297.

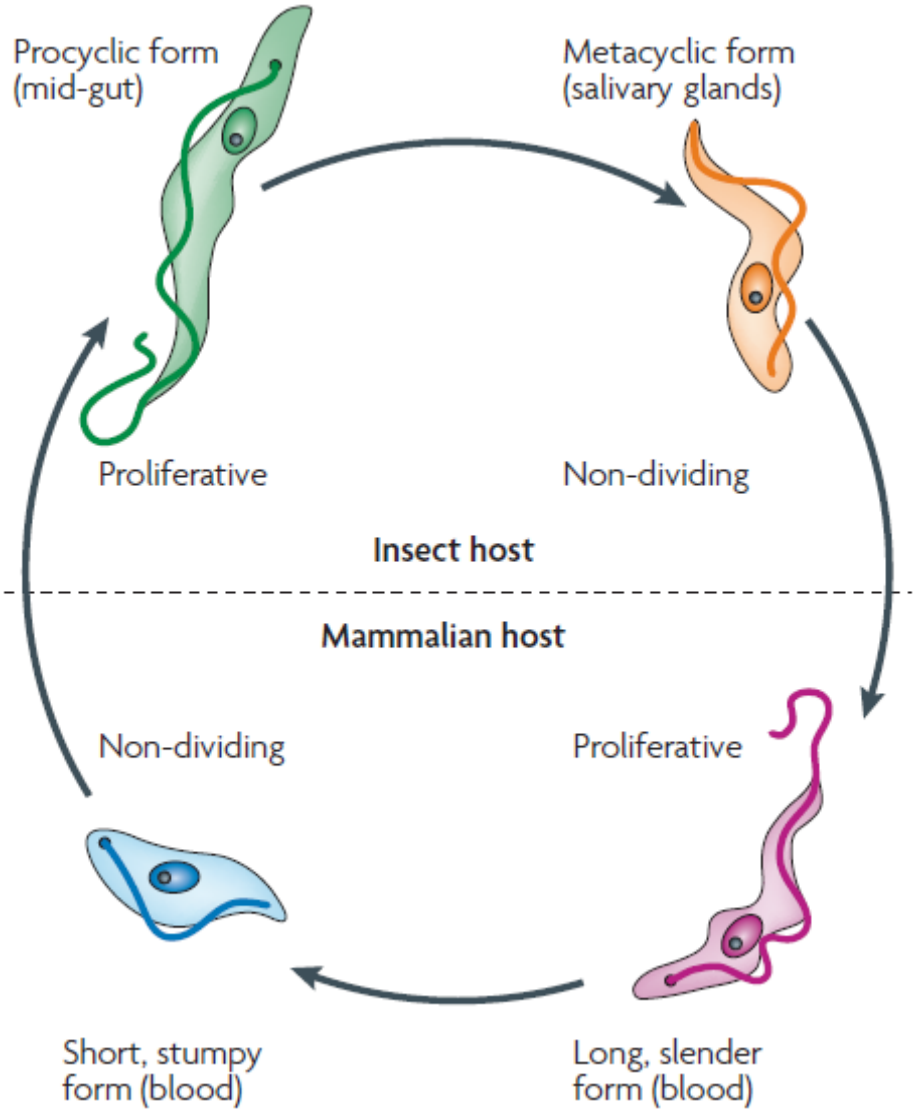

Figure 1.2: Enzymatic reactions of fatty acid synthesis by the *T. brucei* elongase pathway. Each cycle of four enzymatic reactions adds an additional 2 carbons in length to the acyl-CoA product. Figure adapted from Lee S.H., Stephens J.L., and Englund P.T. (2007) A fatty-acid synthesis mechanism specialized for parasitism. *Nat Rev Microbiol* **5:** 287-297.

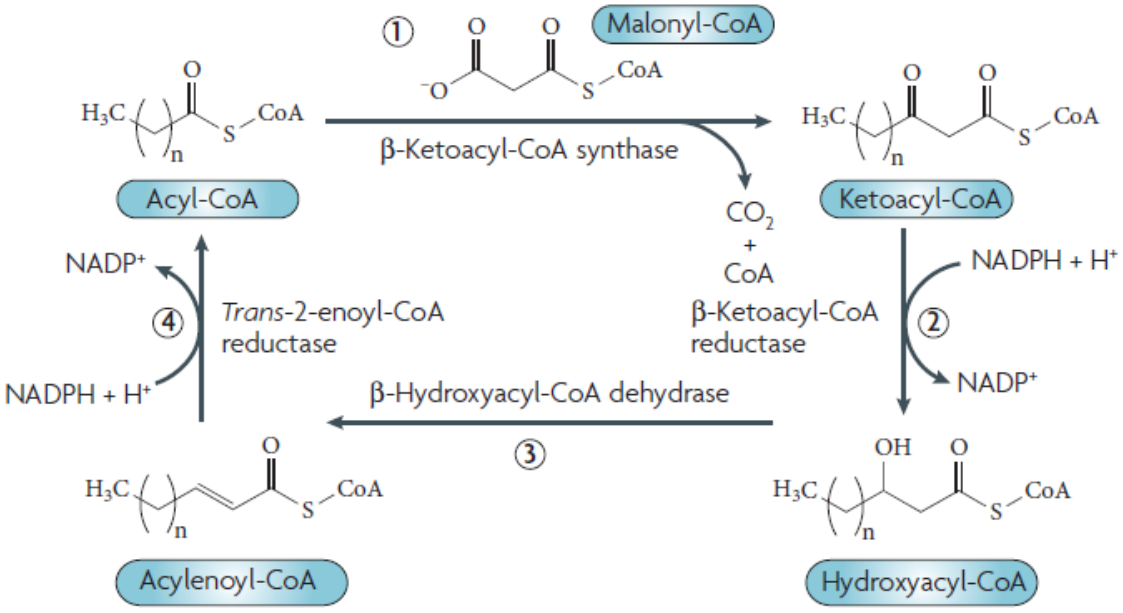

REFERENCES

Acosta-Serrano, A., E. Vassella, M. Liniger, C. Kunz Renggli, R. Brun, I. Roditi and Englund, P. T. (2001) The surface coat of procyclic *Trypanosoma brucei*: programmed expression and proteolytic cleavage of procyclin in the tsetse fly. *Proc Natl Acad Sci U S A* **98**: 1513-1518.

Albert M.A., Haanstra J.R., Hannaert V., Van Roy J., Opperdoes F.R., Bakker B.M., and Michels P.A. (2005) Experimental and *in silico* analyses of glycolytic flux control in bloodstream form *Trypanosoma brucei*. *J Biol Chem* **280:** 28306-28315.

Alsford S., Turner D.J., Obado S.O., Scnchez-Flores A., Glover L., Berriman M., Hertz-Fowler C., and Horn D. (2011) High-throughput phenotyping using parallel sequencing of RNA interference targets in the African trypanosome. Genome Res *21:* 915-924.

Aslett M., Aurrecoechea C., Berriman M., Brestelli J., Brunk B.P., Carrington M*., et al.* (2010) TriTrypDB: A functional genomic resource for the Trypanosomatidae. *Nucleic Acids Res* **38:** D457-62.

Atella G.C., Bittencourt-Cunha P.R., Nunes R.D., Shahabuddin M., and Silva-Neto M.A. (2009) The major insect lipoprotein is a lipid source to mosquito stages of malaria parasite. *Acta Trop* **109:** 159-162.

Balana-Fouce R., and Reguera R.M. (2007) RNA interference in *Trypanosoma brucei*: A high-throughput engine for functional genomics in trypanosomatids? *Trends Parasitol* **23:** 348-351.

Barber M.C., Price N.T., and Travers M.T. (2005) Structure and regulation of acetyl-CoA carboxylase genes of metazoa. *Biochim Biophys Acta* **1733:** 1-28.

Baumgaertner J., Gilioli G., Tikubet G., and Gutierrez A.P. (2008) Eco-social analysis of an east African agro-pastoral system: Management of tsetse and bovine trypanosomiasis. *Ecol Econ* **65:** 125-135.

Beaty N.B., and Lane M.D. (1985) Kinetics of citrate-induced activation and polymerization of chick liver acetyl-CoA carboxylase. *Ann N Y Acad Sci* **447:** 23-37.

Beaty N.B., and Lane M.D. (1983) The polymerization of acetyl-CoA carboxylase. *J Biol Chem* **258:** 13051-13055.

Bouzakri K., Austin R., Rune A., Lassman M.E., Garcia-Roves P.M., Berger J.P., *et al.* (2008) Malonyl CoenzymeA decarboxylase regulates lipid and glucose metabolism in human skeletal muscle. *Diabetes* **57:** 1508-1516.

Bowes A.E., Samad A.H., Jiang P., Weaver B., and Mellors A. (1993) The acquisition of lysophosphatidylcholine by African trypanosomes. *J.Biol.Chem.* **268:** 13885-13892.

Brownsey R.W., Boone A.N., Elliott J.E., Kulpa J.E., and Lee W.M. (2006) Regulation of acetyl-CoA carboxylase. *Biochem Soc Trans* **34:** 223-7.

Brun R., Blum J., Chappuis F., and Burri C. (2010) Human African trypanosomiasis. *Lancet* **375:** 148-159.

Butikofer P., Ruepp S., Boschung M., and Roditi I. (1997) 'GPEET' procyclin is the major surface protein of procyclic culture forms of *Trypanosoma brucei brucei* strain 427. *Biochem. J.* **326:** 415-423.

Caceres A.J., Michels P.A., and Hannaert V. (2010) Genetic validation of aldolase and glyceraldehyde-3-phosphate dehydrogenase as drug targets in *Trypanosoma brucei*. *Mol Biochem Parasitol* **169:** 50-54.

Cheng J.F., Huang Y., Penuliar R., Nishimoto M., Liu L., Arrhenius T., *et al.* (2006) Discovery of potent and orally available malonyl-CoA decarboxylase inhibitors as cardioprotective agents. *J Med Chem* **49:** 4055-4058.

Choi C.S., Savage D.B., Abu-Elheiga L., Liu Z.X., Kim S., Kulkarni A., *et al.* (2007) Continuous fat oxidation in acetyl-CoA carboxylase 2 knockout mice increases total energy expenditure, reduces fat mass, and improves insulin sensitivity. *Proc Natl Acad Sci U S A* **104:** 16480-16485.

Coppens I., Levade T., and Courtoy P.J. (1995) Host plasma low density lipoprotein particles as an essential source of lipids for the bloodstream forms of *Trypanosoma brucei*. *J.Biol.Chem.* **270:** 5736-5741.

Corbett J.W., and H. H.J.,Jr. (2007) Inhibitors of mammalian acetyl-CoA carboxylase. *Recent Patents Cardiovasc Drug Discov* **2:** 162-80.

Delye C., Zhang X.Q., Chalopin C., Michel S., and Powles S.B. (2003) An isoleucine residue within the carboxyl-transferase domain of multidomain acetyl-coenzyme A carboxylase is a major determinant of sensitivity to aryloxyphenoxypropionate but not to cyclohexanedione inhibitors. *Plant Physiol* **132:** 1716-1723.

Ehehalt R., Fullekrug J., Pohl J., Ring A., Herrmann T., and Stremmel W. (2006) Translocation of long chain fatty acids across the plasma membrane--lipid rafts and fatty acid transport proteins. *Mol Cell Biochem* **284:** 135-140.

Engelmann B., and Wiedmann M.K. (2010) Cellular phospholipid uptake: Flexible paths to coregulate the functions of intracellular lipids. *Biochim Biophys Acta* **1801:** 609-616.

Enserink M. (2007) Entomology. welcome to Ethiopia's fly factory. *Science* **317:** 310-313.

Fairlamb A.H. (2003) Chemotherapy of human African trypanosomiasis: Current and future prospects. *Trends Parasitol* **19:** 488-494.

FAO, Food and Agricultural Organization of the United Nations. (2007) Ethiopian fly factory guns for "poverty insect".

Ferguson M.A., and Cross G.A. (1984) Myristylation of the membrane form of a *Trypanosoma brucei* variant surface glycoprotein. *J Biol Chem* **259:** 3011-5.

Ferguson M.A., Brimacombe J.S., Brown J.R., Crossman A., Dix A., Field R.A.*, et al.* (1999) The GPI biosynthetic pathway as a therapeutic target for African sleeping sickness. *Biochim Biophys Acta* **1455:** 327-40.

Fire A., Xu S., Montgomery M.K., Kostas S.A., Driver S.E., and Mello C.C. (1998) Potent and specific genetic interference by double-stranded RNA in *Caenorhabditis elegans*. *Nature* **391:** 806-811.

Folly E., Cunha e Silva N.L., Lopes A.H., Silva-Neto M.A., and Atella G.C. (2003) *Trypanosoma rangeli* uptakes the main lipoprotein from the hemolymph of its invertebrate host. *Biochem Biophys Res Commun* **310:** 555-561.

Folmes C.D., and Lopaschuk G.D. (2007) Role of malonyl-CoA in heart disease and the hypothalamic control of obesity. *Cardiovasc Res* **73:** 278-287.

Glatz J.F., Luiken J.J., and Bonen A. (2010) Membrane fatty acid transporters as regulators of lipid metabolism: Implications for metabolic disease. *Physiol Rev* **90:** 367-417.

Goodman C.D., and McFadden G.I. (2007) Fatty acid biosynthesis as a drug target in apicomplexan parasites. *Curr Drug Targets* **8:** 15-30.

Green H.P., Del Pilar Molina Portela M., St Jean E.N., Lugli E.B., and Raper J. (2003) Evidence for a *Trypanosoma brucei* lipoprotein scavenger receptor. *J Biol Chem* **278:** 422-427.

Halverson D.L., and McCune S.A. (1984) Inhibition of fatty acid synthesis in isolated adipocytes by 5-(tetradecyloxy)-2-furoic acid. *Lipids* **11:** 851-856.

Harada N., Oda Z., Hara Y., Fujinami K., Okawa M., Ohbuchi K.*, et al.* (2007) Hepatic de novo lipogenesis is present in liver-specific ACC1-deficient mice. *Mol Cell Biol* **27:** 1881-8.

Horn D., and McCulloch R. (2010) Molecular mechanisms underlying the control of antigenic variation in African trypanosomes. *Curr Opin Microbiol* **13:** 700-705.

Huang C.H., Tsai S.J., Wang Y.J., Pan M.H., Kao J.Y., and Way T.D. (2009) EGCG inhibits protein synthesis, lipogenesis, and cell cycle progression through activation of AMPK in p53 positive and negative human hepatoma cells. *Mol Nutr Food Res* **53:** 1156-1165.

Jiang D.W., and Englund P.T. (2001) Four *Trypanosoma brucei* fatty acyl-CoA synthetases: Fatty acid specificity of the recombinant proteins. *Biochem J* **358:** 757-761.

Jiang D.W., Ingersoll R., Myler P.J., and Englund P.T. (2000) *Trypanosoma brucei*: Four tandemly linked genes for fatty acyl-CoA synthetases. *Exp Parasitol* **96:** 16-22.

Jiang D.W., Werbovetz K.A., Varadhachary A., Cole R.N., and Englund P.T. (2004) Purification and identification of a fatty acyl-CoA synthetase from *Trypanosoma brucei*. *Mol Biochem Parasitol* **135:** 149-152.

Kampf J.P., and Kleinfeld A.M. (2007a) Is membrane transport of FFA mediated by lipid, protein, or both? an unknown protein mediates free fatty acid transport across the adipocyte plasma membrane. *Physiology (Bethesda)* **22:** 7-14.

Kampf J.P., Parmley D., and Kleinfeld A.M. (2007b) Free fatty acid transport across adipocytes is mediated by an unknown membrane protein pump. *Am J Physiol Endocrinol Metab* **293:** E1207-14.

Kim C.W., Moon Y.A., Park S.W., Cheng D., Kwon H.J., and Horton J.D. (2010) Induced polymerization of mammalian acetyl-CoA carboxylase by MIG12 provides a tertiary level of regulation of fatty acid synthesis. *Proc Natl Acad Sci U S A* **107:** 9626-9631.

Kleinschmidt A.K., Moss J., and Lane D.M. (1969) Acetyl coenzyme A carboxylase: Filamentous nature of the animal enzymes. *Science* **166:** 1276-1278.

Krieger S., Schwarz W., Ariyanayagam M.R., Fairlamb A.H., Krauth-Siegel R.L., and Clayton C. (2000) Trypanosomes lacking trypanothione reductase are avirulent and show increased sensitivity to oxidative stress. *Mol Microbiol* **35:** 542-552.

LaCount D.J., Barrett B., and Donelson J.E. (2002) *Trypanosoma brucei* FLA1 is required for flagellum attachment and cytokinesis. *J Biol Chem* **277:** 17580-17588.

Lee C.K., Cheong H.K., Ryu K.S., Lee J.I., Lee W., Jeon Y.H., and Cheong C. (2008) Biotinoyl domain of human acetyl-CoA carboxylase: Structural insights into the carboxyl transfer mechanism. *Proteins* **72:** 613-24.

Lee S.H., Stephens J.L., and Englund P.T. (2007) A fatty-acid synthesis mechanism specialized for parasitism. *Nat Rev Microbiol* **5:** 287-297.

Lee S.H., Stephens J.L., Paul K.S., and Englund P.T. (2006) Fatty acid synthesis by elongases in trypanosomes. *Cell* **126:** 691-699.

Lopaschuk G.D., and Stanley W.C. (2006) Malonyl-CoA decarboxylase inhibition as a novel approach to treat ischemic heart disease. *Cardiovasc Drugs Ther* **20:** 433-439.

Lutje V., Seixas J., and Kennedy A. (2010) Chemotherapy for second-stage human African trypanosomiasis. *Cochrane Database Syst Rev* **8:** CD006201.

Lye L.F., Owens K., Shi H., Murta S.M., Vieira A.C., Turco S.J., Tschudi C., Ullu E., and Beverley S.M. (2010) Retention and loss of RNA interference pathways in trypanosomatid protozoans. PLoS Pathog **10:** e1001161.

Mackall J.C., Lane M.D., Leonard K.R., Pendergast M., and Kleinschmidt A.K. (1978) Subunit size and paracrystal structure of avian liver acetyl-CoA carboxylase. *J Mol Biol* **123:** 595-606.

Matthews K.R. (2005) The developmental cell biology of *Trypanosoma brucei*. *J Cell Sci* **118:** 283-90.

McNeil D.G.J. (2000) Drug makers and 3rd world: Study in neglect. *New York Times* .

Mellors A., and Samad A. (1989) The aquisition of lipids by African trypanosomes. *Parasitology Today* **5:** 239-244.

Milger K., Herrmann T., Becker C., Gotthardt D., Zickwolf J., Ehehalt R.*, et al.* (2006) Cellular uptake of fatty acids driven by the ER-localized acyl-CoA synthetase FATP4. *J Cell Sci* **119:** 4678-4688.

Moon H.S., Lee H.G., Choi Y.J., Kim T.G., and Cho C.S. (2007a) Proposed mechanisms of (-)-epigallocatechin-3-gallate for anti-obesity. *Chem Biol Interact* **167:** 85-98.

Moon H.S., Chung C.S., Lee H.G., Kim T.G., Choi Y.J., and Cho C.S. (2007b) Inhibitory effect of (-)-epigallocatechin-3-gallate on lipid accumulation of 3T3-L1 cells. *Obesity (Silver Spring)* **15:** 2571-2582.

Moon Y.A., Shah N.A., Mohapatra S., Warrington J.A., and Horton J.D. (2001) Identification of a mammalian long chain fatty acyl elongase regulated by sterol regulatory element-binding proteins. *J Biol Chem* **276:** 45358-45366.

Morita Y.S., Paul K.S., and Englund P.T. (2000) Specialized fatty acid synthesis in African trypanosomes: Myristate for GPI anchors. *Science* **288:** 140-143.

Morris J.C., Wang Z., Drew M.E., and Englund P.T. (2002) Glycolysis modulates trypanosome glycoprotein expression as revealed by an RNAi library. *Embo J* **21:** 4429-38.

Motyka S.A., and Englund P.T. (2004) RNA interference for analysis of gene function in trypanosomatids. *Curr Opin Microbiol* **7:** 362-8.

Ngo H., Tschudi C., Gull K., and Ullu E. (1998) Double-stranded RNA induces mRNA degradation in *Trypanosoma brucei*. *Proc Natl Acad Sci U S A* **95:** 14687-92.

Oh C.S., Toke D.A., Mandala S., and Martin C.E. (1997) ELO2 and ELO3, homologues of the saccharomyces cerevisiae ELO1 gene, function in fatty acid elongation and are required for sphingolipid formation. *J Biol Chem* **272:** 17376-17384.

Paul K.S., Jiang D., Morita Y.S., and Englund P.T. (2001) Fatty acid synthesis in African trypanosomes: A solution to the myristate mystery. *Trends Parasitol* **17:** 381-7.

Richardson J.P., Beecroft R.P., Tolson D.L., Liu M.K., and Pearson T.W. (1988) Procyclin: An unusual immunodominant glycoprotein surface antigen from the procyclic stage of African trypanosomes. *Mol.Biochem.Parasitol.* **31:** 203-216.

Roditi I., Schwarz H., Pearson T.W., Beecroft R.P., Liu M.K., Richardson J.P.*, et al.* (1989) Procyclin gene expression and loss of the variant surface glycoprotein during differentiation of *Trypanosoma brucei*. *J.Cell.Biol.* **108:** 737-746.

Roheim P.S., Carey M., Forte T., and Vega G.L. (1979) Apolipoproteins in human cerebrospinal fluid. *Proc Natl Acad Sci U S A* **76:** 4646-9.

Schneiter R., Hitomi M., Ivessa A.S., Fasch E.V., Kohlwein S.D., and Tartakoff A.M. (1996) A yeast acetyl coenzyme A carboxylase mutant links very-long-chain fatty acid synthesis to the structure and function of the nuclear membrane-pore complex. *Mol Cell Biol* **16:** 7161-72.

Shen, Y., S. L. Volrath, S. C. Weatherly, T. D. Elich and Tong, L. (2004) A mechanism for the potent inhibition of eukaryotic acetyl-coenzyme A carboxylase by soraphen A, a macrocyclic polyketide natural product. *Mol Cell* **16**: 881-891.

Shi H., Djikeng A., Mark T., Wirtz E., Tschudi C., and Ullu E. (2000) Genetic interference in *Trypanosoma brucei* by heritable and inducible double-stranded RNA. *RNA* **6:** 1069-1076.

Stephens J.L., Lee S.H., Paul K.S., and Englund P.T. (2007) Mitochondrial fatty acid synthesis in *Trypanosoma brucei*. *J Biol Chem* **282:** 4427-4436.

TbGeneDB. *Trypanosoma brucei* GeneDB.

Thampy K.G., and Wakil S.J. (1985) Activation of acetyl-CoA carboxylase. purification and properties of a Mn2+-dependent phosphatase. *J Biol Chem* **260:** 6318-23.

Thomson R., Samanovic M., and Raper J. (2009) Activity of trypanosome lytic factor: A novel component of innate immunity. *Future Microbiol* **4:** 789-796.

Toke D.A., and Martin C.E. (1996) Isolation and characterization of a gene affecting fatty acid elongation in *Saccharomyces cerevisiae*. *J Biol Chem* **271:** 18413-18422.

Tong L., and J. H.H.,Jr. (2006) Acetyl-coenzyme A carboxylases: Versatile targets for drug discovery. *J Cell Biochem* **99:** 1476-88.

Vigueira P.A., and Paul K.S. (2011) Requirement for acetyl-CoA carboxylase in *Trypanosoma brucei* is dependent upon the growth environment. *Mol Microbiol* **80:** 117-132.

Voorheis H.P. (1980) Fatty acid uptake by bloodstream forms of *Trypanosoma brucei* and other species of the kinetoplastida. *Mol Biochem Parasitol* **1:** 177-186.

Wang Z., Morris J.C., Drew M.E., and Englund P.T. (2000) Inhibition of *Trypanosoma brucei* gene expression by RNA interference using an integratable vector with opposing T7 promoters. *J Biol Chem* **275:** 40174-9.

Wasan K.M., Brocks D.R., Lee S.D., Sachs-Barrable K., and Thornton S.J. (2008) Impact of lipoproteins on the biological activity and disposition of hydrophobic drugs: Implications for drug discovery. *Nat Rev Drug Discov* **7:** 84-99.

Wheeler R.J. (2010) The trypanolytic factor-mechanism, impacts and applications. *Trends Parasitol* **26:** 457-464.

WHO W.H.O. (2010) WHO fact sheet on African trypanosomiasis.

Xiang S., Callaghan M.M., Watson K.G., and Tong L. (2009) A different mechanism for the inhibition of the carboxyltransferase domain of acetyl-coenzyme A carboxylase by tepraloxydim. *Proc Natl Acad Sci U S A* **106:** 20723-20727.

Zhang H., Tweel B., Li J., and Tong L. (2004a) Crystal structure of the carboxyltransferase domain of acetyl-coenzyme A carboxylase in complex with CP-640186. *Structure* **12:** 1683-1691.

Zhang H., Tweel B., and Tong L. (2004b) Molecular basis for the inhibition of the carboxyltransferase domain of acetyl-coenzyme-A carboxylase by haloxyfop and diclofop. *Proc Natl Acad Sci U S A* **101:** 5910-5915.

CHAPTER TWO

REQUIREMENT FOR ACETYL-COA CARBOXYLASE IN *Trypanosoma brucei* IS DEPENDENT UPON THE GROWTH ENVIRONMENT

Patrick A. Vigueira and Kimberly S. Paul

Department of Biological Sciences, Clemson University, Clemson, SC

ABSTRACT

Trypanosoma brucei, the causative agent of human African trypanosomiasis, possesses two fatty acid synthesis pathways: a major *de novo* synthesis pathway in the ER and a mitochondrial pathway. The 2-carbon donor for both pathways is malonyl-CoA, which is synthesized from acetyl-CoA by Acetyl-CoA Carboxylase (ACC). Here, we show that *T. brucei* ACC shares the same enzyme architecture and moderate ~30% identity with yeast and human ACCs. ACC is cytoplasmic and appears to be distributed throughout the cell in numerous puncta distinct from glycosomes and other organelles. ACC is active in both bloodstream and procyclic forms. Reduction of ACC activity by RNA interference (RNAi) resulted in a stage-specific phenotype. In procyclic forms, ACC RNAi resulted in 50-75% reduction in fatty acid elongation and a 64% reduction in growth in low lipid media. In bloodstream forms, ACC RNAi resulted in a minor 15% decrease in fatty acid elongation and no growth defect in culture, even in low lipid media. However, ACC RNAi did attenuate virulence in a mouse model of infection. Thus, the requirement for ACC in *T. brucei* is dependent upon the growth environment in two different life cycle stages.

Published in: *Molecular Microbiology,* **80:** 117-132.

INTRODUCTION

The deadly protozoan parasite *Trypanosoma brucei*, the causative agent of African sleeping sickness in humans and Nagana in livestock, is vectored by the bloodsucking tsetse fly and infects the blood and cerebrospinal fluid of its human and animal hosts. As it transits through its life cycle, the parasite encounters a number of different host microenvironments that differ in their availability of key nutrients such as proteins and lipids, including fatty acids. For example, there is a ~300X lower concentration of lipids in the cerebrospinal fluid compared to blood (Lentner, 1981). One important function of fatty acids in *T. brucei* is to anchor cell surface glycoproteins as part of their glycosylphosphatidylinositol (GPI) anchors. These cell surface glycoproteins play key roles in the parasite's ability to evade host defenses. For example, switching of the GPI-anchored Variant Surface Glycoprotein (VSG) surface coat via antigenic variation protects *T. brucei* against immune attack in the mammalian bloodstream (reviewed in Morrison *et al.*, 2009; Mansfield and Paulnock, 2005). Similarly, the GPI-anchored procyclin proteins may protect *T. brucei* against proteolytic attack in the tsetse midgut (Acosta-Serrano *et al.*, 2001). The parasite has two ways to supply itself with fatty acids: acquire fatty acids from the host or synthesize its own fatty acids *de novo* (Smith and Bütikofer, 2010). There is a significant difference between the energy required for fatty acid uptake and synthesis: uptake of a 16-carbon fatty acid by passive diffusion would require 1 ATP for activation to its CoA derivative, while synthesis of the same 16-carbon

fatty acyl CoA would require 6 ATPs and 12 reducing units (Lee *et al.*, 2006). Thus, fatty acid uptake is likely preferred over the more energy intensive fatty acid synthesis pathway. However, when the host fatty acid supply is insufficient, the parasite must then synthesize its own fatty acids to meet its needs.

T. brucei has two fatty acid synthesis pathways: the fatty acid elongase pathway of the endoplasmic reticulum that serves as the major pathway for synthesis (Lee *et al.*, 2006), and a minor pathway in the mitochondrion that catalyzes the synthesis of mitochondrial fatty acids (Stephens *et al.*, 2007; Guler *et al.*, 2008). *T. brucei* fatty acid elongation consists of a conserved cycle of reactions that starts with the condensation of the 2-carbon donor, malonyl-CoA, with an acyl-CoA primer (4–18 carbons long) followed by reduction, dehydration, and reduction steps to yield a fatty acyl chain that is two carbons longer. Malonyl-CoA is synthesized from acetyl-CoA by Acetyl-CoA Carboxylase (ACC), a member of the biotin-dependent carboxylase family of enzymes (Jitrapakdee and Wallace, 2003). The ACC reaction is catalyzed in two steps: first, the ATP-dependent carboxylation of the biotin prosthetic group, followed by transfer of the carboxyl group from biotin to the acceptor acetyl-CoA. Because the synthesis of malonyl-CoA requires the hydrolysis of ATP, the ACC reaction is considered the first committed step in fatty acid synthesis and is a well-documented control point for the regulation of this pathway in mammals and yeast (reviewed in Tehlivets *et al.*, 2007; Saggerson, 2008).

As *T. brucei* can acquire fatty acids from the host as well as synthesize them, the parasite likely has a mechanism to modulate its fatty acid synthesis pathway(s) in response to the environmental supply. Two published observations support this idea. First, bloodstream form *T. brucei* labeled with [^{3}H]myristate (C14:0) in whole blood showed no elongation, but cells labeled in medium with only 5% serum lipids showed efficient elongatation of [^{3}H]myristate into longer fatty acids (Doering *et al.*, 1993). Second, *T. brucei* midgut procyclic forms grown in lipid-depleted medium had up-regulated the entire fatty acid elongase pathway compared to cells grown in normal medium (Lee *et al.*, 2006). We propose that this ability to control fatty acid synthesis in response to the environment is critical to the process of host adaptation, allowing maximal usage of host resources to conserve energy that otherwise would be used for biosynthesis. To begin elucidating the mechanism(s) by which *T. brucei* fatty acid synthesis is regulated in response to the environment, we focused on ACC because it catalyzes the first committed step of fatty acid synthesis, is known to be highly regulated by multiple mechanisms in other systems, and could theoretically control flux through the fatty acid synthesis pathway via the availability of its key substrate, malonyl-CoA.

Here, we performed an initial characterization of *T. brucei* ACC. We show that ACC has a punctate cytoplasmic localization and that ACC is required by procyclic forms for growth in culture under lipid-limited conditions and by bloodstream forms for full virulence in mice.

RESULTS

Comparison of T. brucei ACC to other ACCs

Alignment analysis revealed that the overall domain structure of *T. brucei* ACC is similar to eukaryotic-type multi-domain ACCs, with an N-terminal biotin carboxylase domain, a C-terminal carboxyltransferase domain, and a biotin carboxyl carrier domain sandwiched in the middle (Barber *et al.*, 2005) (Fig. 2.1). Despite this conservation in overall enzyme architecture, *T. brucei* ACC shares limited overall identities of 31% and 33% with *S. cerevisiae* ACC and human ACC1, respectively, while human and yeast ACCs shared a slightly higher 44% identity (Fig. 2.2). Comparison of *T. brucei* ACC with ACCs from *Trypanosoma cruzi* and *Leishmania major* revealed a much higher degree of conservation among the trypanosomes, with 58% (Tb vs. Lm), 60% (Tc vs. Lm), and 66% (Tb vs. Tc) identities. As expected, overall sequence similarity was highest in the regions constituting the core of the biotin carboxylase domain, carboxyltransferase domain, and the residues surrounding the biotin attachment site (Fig. 2.2 and Fig. 2.3). Most of the residues shown by X-ray crystallography and/or mutational analysis to be involved in substrate binding and catalysis are conserved (see residues marked by asterisks in Fig. 2.2 and 2.3) (Thoden *et al.*, 2000; Zhang *et al.*, 2003; Shen *et al.*, 2004; Tong, 2005; Lee *et al.*, 2008; Chou *et al.*, 2009). In contrast, the large linker region between the biotin carboxyl carrier and the carboxyltransferase domains showed less conservation (Fig. 2.2 and 2.3), presumably reflecting its primarily structural role.

In addition, the predicted *T. brucei* ACC gene has a very short 7 amino acid N-terminal sequence prior to the first conserved residue of the biotin carboxylase domain, compared to that of *S. cerevisiae* ACC (36 amino acids) and the human ACC1 isoforms (17 - 132 amino acids) (Fig. 2.2; National Center for Biotechnology Information protein database). This short N-terminal sequence might be conserved in trypanosomatids, as the *L. major* ACC N-terminus appears to be equally truncated (Fig. 2.3). In most human ACC1 and ACC2 variants, the N-terminal leader sequence contains a conserved serine (e.g. Ser117 in ACC1 isoform 1), which is a key site of post-transcriptional regulation by AMP-activated protein kinase (AMPK) (Barber et al., 2005). In contrast, the *S. cerevisiae* ACC N-terminus lacks this phosphorylation site and is instead regulated by SNF1/AMPK phosphorylation at other serine residues within the poorly conserved linker between the BCCP and CT domains (Fig. 2.1) (Woods *et al.*, 1994; Shirra *et al.*, 2001; Ficarro *et al.*, 2002; Tehlivets et al., 2007). Like *S. cerevisiae* ACC, the *T. brucei* ACC N-terminal leader also lacks the conserved serine, and thus may be regulated at other sites or by distinct mechanisms from those controlling human ACC.

ACC is expressed in both bloodstream and procyclic forms

The TriTrypDB indicates that the *T. brucei* genome encodes a single predicted ACC isoform (Tb927.8.7100) (Aslett *et al.*, 2009), which was confirmed by Southern blotting (data not shown). Northern analysis of total mRNA revealed that the ACC mRNA is ~8.8 Kb and is transcribed in both bloodstream and

procyclic form life cycle stages (Fig. 2.4A). ACC (and other biotinylated proteins) can be detected on western blots using streptavidin conjugated to horseradish peroxidase (SA-HRP), which recognizes the biotin prosthetic group (Nikolau *et al.*, 1985, Haneji and Koide, 1989). In addition to ACC, the *T. brucei* genome contains one other biotinylated protein: the 74 kD alpha subunit of 3-methylcrotonyl-CoA carboxylase (Tb927.8.6970), which is a mitochondrial enzyme involved in amino acid degradation. SA-HRP blotting of bloodstream and procyclic form lysates revealed a predominant >200 kD band, roughly consistent with the predicted size of ACC (243 kD) (Fig. 2.4B and 2.5B) given the resolving power of the gel in this size range. The 74 kD alpha subunit of the 3-methylcronotonyl-CoA carboxylase was not readily detected in total lysates, but could be detected in partially purified mitochondrial fractions (data not shown). Although additional cross-reacting bands become evident upon longer exposures, we show that the >200 kD band is specifically depleted upon ACC RNAi, as discussed below (Fig. 2.9B). Finally, ACC enzyme activity was detected in both bloodstream and procyclic form lysates and was dependent upon the addition of ATP and acetyl-CoA (Fig. 2.4C). Taken together, these data show that ACC is expressed and active in both life cycle stages.

ACC is cytoplasmic and localized to numerous puncta

Multiple prediction algorithms (WoLF PSORT, TargetP/SignalP, and PredoTar) found no known targeting motifs in the ACC protein, predicting ACC to be cytosolic (Horton *et al.*, 2007; Emanuelsson *et al.*, 2007; Small *et al.*, 2004).

To experimentally assess the localization of ACC, we used an epitope-tagging strategy to create a procyclic form cell line (PF ACC-myc) with a c-myc tag fused to the C-terminus of ACC. To minimize the possibility of mislocalizing the tagged protein due to over-expression of an ectopic copy, we tagged the genomic locus of only one ACC allele. Using immunoprecipitation with anti-c-myc antibody covalently linked to beads, we found that ACC-myc immunoprecipitates possessed ACC activity, while control immunoprecipitates from untagged cells were inactive (Fig. 2.5). This result indicates that the myc-tagged ACC allele encoded a functional enzyme.

First, we subjected lysates of PF ACC-myc cells to sub-cellular fractionation by differential centrifugation (see Fig. 2.6A for scheme) and analyzed the fractions by SDS-PAGE and western blotting (Fig. 2.6B). ACC-myc showed a fractionation pattern similar to the cytoplasmic marker HSP70, and distinct from the markers for the glycosome and ER. Moreover, the ACC-myc fractionation pattern was the same as that of native ACC in both PF ACC-myc cells (Fig. 2.6B) and wild-type procyclic cells (data not shown), indicating that the c-myc epitope was not affecting the localization of the tagged ACC.

Next, we examined the sub-cellular localization of ACC by immunofluorescence microscopy. ACC-myc was not uniformly distributed in the cytoplasm, but instead localized to a multitude of small distinct puncta (Fig. 2.7 and 2.8, panels B, D, J, N, R, and V). Wild-type cells had no visible fluorescent signal at the same exposure time (Fig. 2.8, panels F and H) and only a faint haze

with an exposure 3.5 times longer (data not shown). A field of cells captured at a lower magnification demonstrated that specific labeling with the anti-c-myc antibody was reflected in the whole cell population (Fig. 2.8, panels C, D, G, and H). The ACC puncta did not co-localize with markers for the cytoplasm (cytoplasmic HSP70), the glycosomes (pyruvate phosphate dikinase, aldolase, and glyceraldehyde phosphate dehydrogenase), the ER (BiP), or the mitochondrion (lipoamide dehydrogenase) (Fig. 2.8, panels M-P, I-L, Q-T, and U-X, respectively). Furthermore, the distribution of ACC-myc is distinct from that of Nile Red-stained lipid droplets (Fig. 2.8, panels Y and Z), Golgi (Ho *et al.*, 2006; Ramirez *et al.*, 2008), and acidocalcisomes, which are larger and less numerous (de Jesus *et al.*, 2010; Fang *et al.*, 2007).

RNA interference of ACC is efficient in both bloodstream and procyclic forms

Because our attempts to delete both alleles of ACC were unsuccessful, we chose to assess the functional role of ACC in *T. brucei* using the pZJM RNAi vector to induce knockdown of ACC mRNA in bloodstream and procyclic cells (Wang *et al.*, 2000; Morris *et al.*, 2001). Northern analysis of total RNA showed that induction of RNAi reduced ACC mRNA by 76% in bloodstream forms and 85% in procyclic forms (Fig. 2.9A). Similar results were obtained with at least four independent clones (data not shown). Like others, we have observed that the ACC RNAi cells can undergo RNAi reversion (Chen *et al.*, 2003; Motyka and Englund, 2004). By day 25, northern analysis showed that procyclic cells had

completely recovered expression of ACC mRNA, even though ACC dsRNA was still being produced (data not shown). SA-HRP blotting revealed the loss of ACC protein over 10 days of RNAi (Fig. 2.9B). A separate analysis of 4 independent inductions showed that four days of ACC RNAi reduced ACC protein by 91 ± 7% in both bloodstream and procyclic forms. Four days of ACC RNAi also significantly reduced ACC activity in lysates (Fig. 2.9C), with an 87 ± 1% and 90 ± 1% reduction in bloodstream and procyclic cells, respectively (Fig. 2.10A and B). Finally, ACC RNAi resulted in no growth inhibition in either bloodstream and procyclic cells (Fig. 2.9D), with doubling times of 8 h and 15 h, respectively (Fig. 2.10C). Fluorescence microscopy revealed that ACC RNAi resulted in no gross defects in cell morphology, or in the structure of the mitochondrion, ER, or nuclear/mitochondrial DNA as revealed by immunostaining with specific antibodies to a mitochondrial marker (lipoamide dehydrogenase), an ER marker (BiP), or by staining with the DNA intercalating dye DAPI (data not shown).

Effect of ACC RNAi on overall lipid metabolism

To look for ACC RNAi-induced changes in fatty acid metabolism, ACC RNAi cells were incubated with [^{3}H]laurate (C12:0) or [^{3}H]myristate (C14:0), which can be elongated by the fatty acid elongase pathway and incorporated into lipids. Analysis of the labeled lipids by thin-layer chromatography (TLC) in the absence of RNAi showed labeling of neutral lipids at the top, free fatty acids co-migrating with the free fatty acid marker, myristate (Myr), and various phospholipids co-migrating above and below the phospholipid marker,

phosphatidylcholine (PtdC) (Fig. 2.11A, lanes 1, 3, 5, and 7). Migrating below the phospholipids, we also observed labeling of the bloodstream form specific lipids, Glycolipids A and C (and their intermediates) (Buxbaum *et al.*, 1994), which are precursors to the VSG GPI-anchor (Fig. 2.11A, lanes 5 and 7). In procyclic forms, ACC RNAi resulted in little change in the overall labeling patterns of [^{3}H]laurate or [^{3}H]myristate, except for an accumulation of free fatty acids and one of the phospholipids (indicated by asterisk; likely phosphatidylethanolamine based on its migration) (Fig. 2.11A, lanes 2 and 4). In bloodstream forms, ACC RNAi labeling resulted in no change in the species labeled by [^{3}H]laurate (Fig. 2.11A, lanes 5 and 6). In contrast, ACC RNAi reduced incorporation of [^{3}H]myristate into phospholipids (Fig. 2.11A, lanes 7 and 8), while no loss of labeling was observed in the bloodstream-specific Glycolipids A and C.

ACC is required for elongation of fatty acids

We next examined the effect of ACC RNAi on the major pathway for fatty acid synthesis in *T. brucei*. Because the cell-free fatty acid elongation assay bypasses the ACC step (Morita *et al.*, 2000b), we examined fatty acid elongation *in vivo.* Cells labeled with [^{3}H]laurate (C12:0) and [^{3}H]myristate (C14:0), which should be converted to longer fatty acids if the elongase pathway is functioning (Lee *et al.*, 2006), were analyzed for elongation products using reverse-phase TLC. In uninduced procyclic forms, both [^{3}H]laurate and [^{3}H]myristate were elongated to products up to 18 carbons (Fig. 2.11B, lanes 1 and 3). ACC RNAi in procyclics resulted in a 74 ± 6% and 53 ± 5% inhibition of [^{3}H]laurate and

[^{3}H]myristate elongation, respectively (Fig. 2.11B, lanes 2 and 4). Uninduced bloodstream forms readily elongated [^{3}H]laurate (Fig. 2.11B, lane 5), but little [^{3}H]myristate elongation occurred (Fig. 2.11B, lane 7). ACC RNAi in bloodstream forms resulted in a 15 ± 5% inhibition of [^{3}H]laurate elongation (Fig. 2.11B, lane 6), and completely abolished the minor elongation that occurred with [^{3}H]myristate (Fig. 2.11B, lane 8).

Effect of ACC RNAi on growth in low-lipid media

Even though ACC RNAi reduced elongase activity, the cells were still able to grow normally in culture (Fig. 2.9D). Because *T. brucei* can also readily acquire fatty acids from the medium (Dixon *et al.*, 1971; Voorheis, 1980; Bowes *et al.*, 1993; Lee *et al.*, 1999; Coppens *et al.*, 1995), we assessed the growth of ACC RNAi cells in low lipid media. ACC RNAi in bloodstream forms still showed no effect on growth in two different formulations of low lipid medium compared to the uninduced control (Fig. 2.12A). In contrast, ACC RNAi in procyclic forms reduced growth by 64% in low lipid medium (Fig. 2.12B). Furthermore, 68% of this growth defect could be reversed by the addition of 35 μM stearate (C18:0), suggesting that the growth defect arose from a lack of fatty acids rather than some other limiting factor in the medium. Finally, pre-adaptation of bloodstream and procyclic cells by growth in low lipid media for 10 days prior to induction of ACC RNAi did not enhance the effect of ACC RNAi on growth (Fig. 2.13).

ACC is required for full virulence in mice

To assess the virulence of ACC RNAi cells, NIH Swiss mice (n=10 per group) were either left untreated (uninduced control) or treated with doxycycline (a bioavailable tetracycline analog) in their drinking water to induce ACC RNAi. Mice were then infected intra-peritoneally with 1 x 10^5 freshly thawed bloodstream form ACC RNAi trypanosomes. The uninduced control infection resulted in a mean time-to-death of 12.7 days by Kaplan-Meier survival analysis (Fig. 2.14). However, when ACC RNAi was induced in the doxycycline-treated mice, the mean time-to-death was significantly increased to 22.3 days (p = 0.0021, Wilcoxon test).

DISCUSSION

Among the protozoa, only the ACCs of the Apicomplexan parasites *Toxoplasma gondii* and *Plasmodium falciparum* have been characterized. These Apicomplexans possess two eukaryotic-type multi-domain ACC isozymes: a plastid ACC1 that functions in plastid *de novo* fatty acid synthesis and a cytosolic ACC2, with proposed functions in fatty acid elongation, polyketide synthesis, and mitochondrial fatty acid synthesis (Zuther *et al.*, 1999; Jelenska *et al.*, 2001; Gardner *et al.*, 2002; Waller *et al.*, 2003; Mazumdar and Striepen, 2007). Here, we have performed the first characterization of the sole trypanosome ACC isozyme in bloodstream and procyclic forms and explored its role in fatty acid metabolism.

The cytosolic punctate distribution of ACC-myc in *T. brucei* has not been observed previously in other eukaryotes and thus, appears to be novel. What are these puncta? They could represent a fixation artifact from the paraformaldehye. However, ACC-myc showed the same punctate pattern when cells were fixed in cold methanol, suggesting this is not the case (data not shown). The puncta could also represent non-specific aggregation due to the c-myc epitope tag. Four reasons argue against this: first, ACC-myc showed the same fractionation pattern as native ACC, suggesting that the myc tag has no significant effect upon the sub-cellular distribution of ACC; second, ACC-myc immunoprecipitates possess ACC activity, suggesting that the myc tag did not affect enzyme function; third, because the myc tag was incorporated into the genomic locus, ACC-myc is likely

expressed at endogenous levels rather than at the high levels associated with epitope-tag artifacts; fourth, one previous report of a cytosolic myc-tagged protein showed diffuse staining in *T. brucei* rather than the puncta we observe for ACC (Peterson *et al.*, 1997).

An intriguing alternative is that these puncta might represent polymerization of ACC in *T. brucei*. Mammalian and avian ACCs polymerize into filaments (Kleinschmidt *et al.*, 1969; Mackall *et al.*, 1978), and there is evidence suggesting yeast ACC may also polymerize (Schneiter *et al.*, 1996). In birds and mammals, ACC polymerization is dynamic and the polymer form is the active form (Ashcraft *et al.*, 1980; Beaty and Lane, 1983; Beaty and Lane, 1985; Thampy and Wakil, 1988; Kim et al., 2010). Whether they are non-specific aggregates or polymers, the nature of the ACC puncta must be independently confirmed using an alternative epitope tag or an antibody to native *T. brucei* ACC before their function can begin to be explored.

Among unicellular eukaryotes, ACC has been most extensively characterized in the yeasts. In both *S. cerevisiae* and *Schizosaccharomyces pombe*, deletion of ACC is lethal (Hasslacher *et al.*, 1993; Saitoh *et al.*, 1996), while a reduction in ACC activity leads to growth inhibition and a range of defects in nuclear and vacuolar membrane function (Saitoh *et al.*, 1996; Schneiter *et al.*, 1996; Schneiter *et al.*, 2000). Thus, we predicted that ACC RNAi would reduce overall lipid biosynthesis activity, resulting in growth inhibition in *T. brucei*. Instead, we found that bloodstream form and procyclic cells differed in the effect

of ACC RNAi upon fatty acid elongation and growth in culture. We also found that the effect of ACC RNAi was dependent upon the growth environment.

Based on our results, we propose that procyclic form *T. brucei* is dependent upon ACC only when environmental lipids are limiting. It is well known that *T. brucei* can readily take up and use lipids from their environment (Dixon *et al.*, 1971; Voorheis, 1980; Bowes *et al.*, 1993; Lee *et al.*, 1999; Coppens *et al.*, 1995). Thus, in normal medium, procyclic cells primarily rely on fatty acid uptake to satisfy their needs, rather than *de novo* synthesis. Therefore, reduction of fatty acid elongation upon ACC RNAi had a limited effect on overall lipid metabolism because the cells were already relying upon exogenous lipids. In low lipid medium, however, the procyclics require ACC and fatty acid elongation to compensate for the fatty acid deficit. Under these conditions, reduction of ACC activity and fatty acid elongation rendered the cells unable to grow efficiently. This growth defect of procyclic ACC RNAi cells in low lipid conditions is very similar to that seen with RNAi of the enoyl-CoA reductase in the fatty acid elongation pathway *(Lee et al.*, 2006), consistent with the coupling of these enzymes into the same metabolic pathway.

In bloodstream forms, the response to ACC RNAi differed significantly from procyclic forms. Despite efficient knockdown of ACC activity, fatty acid elongation was only moderately reduced, and the cells exhibited no growth defect in either normal or low lipid media. This suggests that in cultured bloodstream forms, the fatty acid elongation pathway may not be very dependent

upon ACC. This result was unexpected for two reasons: first, in all other eukaryotes examined to date, fatty acid synthesis and elongation are dependent upon malonyl-CoA supplied by ACC; second, bloodstream form cells have a high demand for myristate to anchor their VSG surface coat, which is a relatively scarce fatty acid in serum and scarcer still in standard culture medium (Paul *et al.*, 2001). One possible explanation is that the residual ~10% ACC activity supports sufficient fatty acid elongation. If true, this suggests that the level of ACC expression in bloodstream forms is at >10-fold excess over what is required for growth in culture. Other metabolic enzymes, such as trypanothione reductase (Krieger *et al.*, 2000) and several glycolytic enzymes (Albert *et al.*, 2005; Caceres *et al.*, 2010), have been reported to be present in excess, though a 75-90% knockdown of these enzymes did cause an observable growth defect.

In contrast to procyclics, loss of ACC had little apparent impact upon bloodstream forms in culture, except one notable effect upon the metabolism of [^{3}H]myristate. As previously reported (Doering *et al.*, 1993; Morita *et al.*, 2000b), very little elongation of [^{3}H]myristate occurs in bloodstream forms, likely resulting from the exclusive use of myristate as the fatty acid moiety in the VSG GPI-anchors (Ferguson *et al.*, 1988). However, under ACC RNAi conditions, we observed a general loss in the incorporation of [^{3}H]myristate into phospholipids, while incorporation into the VSG GPI anchor precursors, Glycolipids A and C was preserved. Thus, ACC RNAi revealed a partitioning of the myristate pool, where the myristoylation of the GPI anchors takes priority over incorporation into

phospholipids. This phenomenon has been observed previously (Doering *et al.*, 1993; Morita *et al.*, 2000b), and highlights the special importance of myristate in bloodstream form *T. brucei*. Morita *et al*. reported that myristate produced by the ELO pathway was preferentially incorporated into the VSG GPI anchors. Here, we show that exogenous myristate is likewise preferentially incorporated into the VSG GPI anchors, perhaps by special delivery from acyl-CoA binding protein (Milne and Ferguson, 2000), or by one or more acyl-CoA synthetases, four of which can efficiently activate myristate to myristoyl-CoA (Jiang and Englund, 2001).

Low levels of ACC were sufficient for growth of bloodstream forms in culture, even in low lipid media where the fatty acid elongase pathway is known to be up-regulated (Lee *et al.*, 2006). Yet ACC RNAi led to decreased virulence in a mouse model of infection. One major difference between *in vitro* culture and growth in the animal host is the presence of the host's immune system. Thus, one likely explanation for the reduced virulence is that ACC RNAi reduced the ability of the parasite to evade the immune system. The primary means of *T. brucei* to avoid the host's adaptive immune system is antigenic variation, in which a "new" VSG variant is trafficked to the surface while the "old" VSG variant is either shed from the cell surface or internalized and degraded (Seyfang *et al.*, 1990; Mansfield and Paulnock, 2005). Furthermore, VSG itself is constantly recycling off and back on to the cell surface via coupled endocytosis/exocytosis (Engstler *et al.*, 2004). Perhaps the ACC RNAi cells are compromised in their

ability to maintain their VSG coat due to problems in trafficking and/or recycling. This phenomenon has been observed previously for conditional knockouts of phosphatidylinositol synthase and neutral sphingomyelinase (Young and Smith, 2010; Martin and Smith, 2006).

Another important immune evasion strategy of *T. brucei* is the endocytosis-mediated clearance of antibodies bound to the surface of the parasite (Schwede and Carrington, 2010). Under immune pressure, *T. brucei* dramatically increases its endocytic activity in order to clear complement-activating surface immune complexes (Balber *et al.*, 1979; Russo *et al.*, 1993; O'Beirne *et al.*, 1998; Engstler *et al.*, 2007; Natesan *et al.*, 2007). Thus, the ACC RNAi cells may be unable to meet the increased demand in lipid synthesis arising from the dramatic upregulation in membrane turnover in the animal host. The resulting failure to adequately clear surface antibody complexes would then lead to reduced virulence.

Although the survival of the mice was increased under ACC RNAi induction, the mice were unable to clear the infection and ultimately, nearly all succumbed. The mice's inability to clear the infection is likely due to the emergence of RNAi revertants through positive selection and the fact that antibiotic selection of the transgenes necessary for RNAi (T7 polymerase and *Tet* repressor) was not maintained during infection to avoid drug toxicity (Lecordier *et al.*, 2005; Jetton *et al.*, 2009). Supporting this idea, trypanosomes isolated from an induced mouse late in infection (~10^7 parasites/ml) were shown to be

expressing ACC protein by SA-HRP blotting, though the level of ACC detected was less than that in trypanosomes isolated from a control uninduced mouse (data not shown).

This work extends our understanding of fatty acid synthesis in *T. brucei* and points to the importance of exogenous sources of fatty acids in the overall lipid metabolism of these parasites. Finally our data raise key questions about how *T. brucei* senses environmental fatty acids and transduces this information into regulatory decisions governing its fatty acid metabolism. Such processes are key to survival, enabling the parasite to adapt its fatty acid metabolism to each host environment to satisfy its lipid needs while minimizing wasteful energy expenditure.

MATERIALS AND METHODS

Reagents

All chemicals and reagents were purchased from Thermo Fisher Scientific and Sigma except: Minimum Essential Medium Eagle (MEM), Iscove's Modified Dulbecco's Medium (IMDM), 4'-6-diamidino-2-phenylindole (DAPI) (Invitrogen), Serum Plus (JRH Biosciences), delipidated fetal bovine serum (FBS) (Cocalico Biologicals), poly-L-lysine solution and normal goat serum (Electron Microscopy Sciences). [α-^{32}P]dATP (Perkin-Elmer), and [^{14}C]$NaHCO_3$, and [^{3}H]-labeled fatty acids (American Radiolabeled Chemicals). The mouse monoclonal 9E10 anti-c-myc antibody was from Santa Cruz Biotechnology. The rabbit polyclonal antibodies to BiP and cytoplasmic HSP70 were generously provided by Dr. Jay Bangs (University of Wisconsin-Madison) (Bangs *et al.*, 1993; McDowell *et al.*, 1998). The rabbit polyclonal anti-lipoamide dehydrogenase antibody was a kind gift of Dr. Luise Krauth-Siegel (University of Heidelberg) (Schoneck *et al.*, 1997). The rabbit polyclonal 2841D anti-glycosome antibody was a generous gift from Dr. Marilyn Parsons (Seattle Biomedical Research Institute) (Parker *et al.*, 1995) and recognizes three glycosomal enzymes: Pyruvate Phosphate Dikinase (PPDK) (~100 kD), Aldolase (~41 kD), and Glyceraldehyde Phosphate Dehydrogenase (GAPDH) (~39 kD).

Trypanosome Strains and Cell Lines

Wild-type procyclic and bloodstream form *T. brucei* strain 427 were provided by Dr. Paul Englund (Johns Hopkins School of Medicine). Procyclic and bloodstream form *T. brucei* transgenic cell lines containing genomically-integrated Tet repressor and T7 polymerase (29-13 and 90-13 respectively (Wirtz *et al.*, 1999; Hirumi and Hirumi, 1989)) were generously provided by Dr. George Cross (Rockefeller University). Bloodstream form parasites were grown in HMI-9 medium (Hirumi and Hirumi, 1989) containing 10% heat-inactivated FBS/10% Serum Plus and supplemented with 2.5 µg/ml G418, 5 µg/ml hygromycin, and 2.5 µg/ml phleomycin, as needed. Procyclic form parasites were grown in SDM-79 medium (Brun and Shonenberger, 1979) containing 10% heat-inactivated FBS and supplemented with 15 µg/ml G418, 50 µg/ml hygromycin, and 2.5 µg/ml phleomycin, as needed.

Preparation of Low-Lipid Media

The only source of lipids in media comes from the serum additives. According to the manufacturers, both Serum Plus and delipidated FBS contain ~20% serum lipids. Two types of low-lipid HMI-9 media were prepared. Delipidated medium (DL) was prepared with 10% Serum Plus and 10% delipidated FBS. Serum Plus only medium (SP) was prepared with 10% Serum Plus only. Thus, the DL and SP media contain serum lipids equivalent to 4% and 2% FBS, respectively, compared to 12% for normal HMI-9 medium. For procyclic cells, low-lipid DL medium was prepared with 10% delipidated FBS, and

contained serum lipids equivalent to 2% FBS, compared to 10% for normal SDM-79. For fatty acid rescue experiments, a final concentration of 35 μM stearate (C18:0) was added to the medium.

RNA Purification and Northern Analysis

Total RNA was purified and northern analysis was performed as previously described (Wang *et al.*, 2000), except 1 x 10^7 cell equivalents or 10-15 μg of total RNA was loaded per lane and blots probed with a ^{32}P-labeled DNA probe corresponding to the same ACC sequence used for ACC RNAi (see below).

Preparation of Cell Lysates

Hypotonic lysates were prepared as described (Morita *et al.*, 2000b). We also prepared lysates using an alternative method developed for radioimmunoprecipitation assays (RIPA): 1 x 10^8 cells were washed twice in BBSG (50 mM Bicine-Na^+ pH 8, 50 mM NaCl, 5 mM KCl, 70 mM glucose) and the final cell pellet frozen on dry ice. The frozen pellet was overlaid with 100 μl TBS-RIPA buffer (1X Tris-Buffered Saline (TBS), 2 mM EDTA, 0.5 mM DTT, 1% (v/v) nonidet P-40, 0.5% (w/v) sodium deoxycholate, 0.1% (w/v) SDS) supplemented with 0.5 μg/ml leupeptin, 1 mM phenylmethanesulfonyl fluoride (PMSF), 0.1 mM Nα-*p*-tosyl-L-lysine chloromethyl ketone hydrochloride (TLCK), 2 μM pepstatin A and allowed to thaw on ice for 10 min. Cells were vortexed every 5 min for 30 min, with 20 sec of resting on ice between vortexing. Cell

lysates were centrifuged for 30 min at 4°C at 16,000 x g to remove cell debris. Supernatant was removed, aliquotted, snap frozen in liquid nitrogen, and stored at -80°C.

Streptavidin Blotting

For streptavidin-blotting, lysates were fractionated on 8% SDS-PAGE gels, transferred to nitrocellulose, and blocked in Wash Buffer (1% dry milk, 1X TBS, 0.05% Tween-20). Blots were probed for ACC with streptavidin-horseradish peroxidase conjugate (SA-HRP) (Pierce) diluted 1:200 in Streptavidin Wash Buffer (0.2% dry milk, 1X TBS, 0.05% Tween-20). Blots were washed 4X in Streptavidin Wash Buffer, followed by 2 washes in 1X TBS/0.05% Tween-20. The blots were developed using the Pico SuperSignal Enhanced Chemiluminescence kit (Pierce), and exposed to HyBlot CL film (Denville). For some experiments the blot was cut, and the top half probed for ACC with SA-HRP as above, while the bottom half was probed for tubulin as follows. Blot was incubated with a mouse anti-tubulin antibody (clone B-5-1-2 ; Sigma) diluted 1:500,000 in Wash Buffer, washed 4X in Wash Buffer, and probed with HRP-conjugated goat anti-mouse IgG antibody (Invitrogen) diluted 1:20,000 in Wash Buffer. After 4 washes in Wash Buffer and 2 washes in 1X TBS, 0.05% Tween-20, blots were developed for ECL. Semi-quantitative analysis of blots was performed using densitometry (NIH Image J software) of appropriately exposed films (unsaturated signal within the linear range of the film).

ACC Enzyme Activity

To assay ACC activity, we modified a biotin carboxylase assay described previously (Wurtele and Nikolau, 1990). To remove endogenous CoA substrates, lysates were either dialyzed into BC Buffer (50 mM Tris-Cl pH 8, 5 mM $MgCl_2$, 2 mM DTT) for 4-12h at 4°C or alternatively, were desalted on a G50-80 sephadex column (Sigma) equilibrated in BC Buffer. Treated lysates were then incubated in a final volume of 100 µl BC Buffer supplemented with 5 mM ATP, 0.6 mM acetyl-CoA, 1 mg/ml fatty acid free bovine serum albumin (BSA) (Sigma), and 2 mM [^{14}C]$NaHCO_3$ (14.9 mCi/mmol) for 30 min at 30°C, mixing every 10 min. Reactions were stopped by transferring tubes to ice for 5 min. Unreacted [^{14}C]$NaHCO_3$ was released as [^{14}C]CO_2 by the addition of 50 µl 6N HCl. Acid-precipitated [^{14}C]malonyl-CoA product was collected on Whatman #1 filter circles, air-dried, and quantified by scintillation counting. Linear regressions and Student *t*-Test analyses were performed using Microsoft Excel.

Generation of ACC-myc Cell Line

We used an *in situ* epitope-tagging strategy to generate a procyclic cell line with the C-terminus of one ACC allele fused to the c-myc epitope. We used PCR with bipartite primers and the appropriate plasmid template to generate a 936 bp linear tagging construct (ACC-MYC/Phleo/ACC 3'-UTR) with the following features (in 5'-3' order): 3' end of ACC gene fused in-frame with c-myc epitope ending with stop codon, α/β tubulin intergenic region, phleomycin resistance gene, 5' end of ACC 3' UTR sequence. To make this construct we used a 2-step

PCR procedure. First, we used a forward primer comprised of the last 54 bp of the ACC gene (without stop codon) followed by 6 bp of the c-myc epitope (5'-GACGAAAGGATGCGGCGTGCGGCCATGCAGGCGCTGGAACGTACAACC GCGAAGGGCCGCTCTGAGCAA-3'). The reverse primer sequence is comprised of 21 bp of the phleomycin resistance gene followed by the first 44 bp of the ACC 3'-UTR (5'-TAATTCTCATTCCTTGCCTCCAGTGGCGCCGCATCCCACGCCATGTCAG TCCTGCTCCTCGGCCAC-3). For template DNA, we used the mycPHLEO plasmid (a generous gift of Dr. Meredith Morris, Clemson University), which contains the c-myc sequence, α/β tubulin intergenic region, and phleomycin resistance gene. The resulting amplicon encoding the linear tagging construct was cloned into the pCR 2.1-TOPO vector and sequenced. For the second PCR step, we used shorter forward and reverse primers that flank the linear tagging construct (5'-GACGAAAGGATGCGGCGT-3', and 5'-TAATTCTCATTCCTTGCCTCC-3', respectively) to perform a large-scale PCR. The resulting amplicon (ACC-MYC/Phleo/ACC 3'-UTR) was purified using a MinElute column (Qiagen), and 15 µg of purified targeting construct was electroporated into 1 x 10^8 procyclic form 427 cells and selected in 2.5 µg/ml phleomycin. Integration of the tagging construct into the genomic locus via homologous recombination generated an in-frame fusion of the c-myc epitope to the 3' end of one allele of ACC. Correct integration was confirmed by diagnostic PCR and western blotting.

Sub-Cellular Fractionation

Hypotonic lysates of wild-type and ACC-myc-expressing procyclic form cells were subjected to differential centrifugation (Bangs *et al.*, 1993; Roggy and Bangs, 1999). Briefly, lysate and then supernatants were fractionated by three successive centrifugation steps: a 1,000 x g step yielding P1 (cell fragments, nuclei, mitochondria) and S1 fractions; a 100,000 x g step yielding P2 (microsomes) and S2 fractions; and a second 100,000 x g step yielding P3 (residual microsomes) and S3 (cytosol) fractions (Fig. 2.6A). Samples of each sub-cellular fraction (1.5 x 10^6 cell equivalents) were separated by 10% SDS-PAGE and transferred to nitrocellulose. Membranes were processed for streptavidin blotting as described above. To probe for ACC-myc or sub-cellular markers, membranes were blocked ≥ 1 h in 5% milk/1X TBS and probed with primary antibodies diluted in 5% milk/1X TBS/0.5% Tween-20 as follows: anti-c-myc (clone 9E10), 1:250; anti-glycosome, 1:7,500; anti-cytosolic HSP70, 1:4000; anti-BiP, 1:2000. HRP-conjugated goat anti-mouse or goat anti-rabbit secondary antibodies (Pierce) were diluted 1:10,000 in 5% milk/1X TBS/0.5% Tween-20. After washing, blots were developed using ECL and exposed to film as described above.

Microscopy

Microscopy was performed essentially as described in (Field *et al.*, 2004). Briefly, wild-type and ACC-myc procyclic cells were harvested by centrifugation (800 x g, 10 min), washed once with ice-cold Voorheis's modified PBS (vPBS)

(Nolan *et al.*, 2000), and fixed on ice in 3% paraformaldehyde (w/v) in vPBS for 1 h. Fixed parasites were adhered to poly-L-lysine treated glass slides and permeabilized for 10 min in 0.1% Triton X-100 (v/v) in vPBS. Slides were incubated in microscopy blocking solution (MBS: 0.5% bovine serum albumin (BSA) (w/v), 5% normal goat serum (v/v), 20% FBS (v/v) in vPBS) for ≥ 1 h. Primary antibodies were used at the following dilutions in MBS: 9E10 anti-C-myc, 1:100; anti-glycosome, 1:100; anti-cytoplasmic HSP70, 1:1000; anti-BiP 1:1000 (ER marker); and anti-lipoamide dehydrogenase 1:500 (mitochondrial marker). Secondary antibodies were goat anti-mouse and goat anti-rabbit conjugated to Alexa Fluor 488 (green) or Alexa Fluor 594 (red) (Invitrogen) diluted 1:750 in MBS. To stain lipid droplets, cells were incubated with 0.005% Nile Red diluted in vPBS (Greenspan *et al.*, 1985; Robibaro *et al.*, 2002). The broad emission spectra of Nile Red prevents the co-staining of lipid droplets and ACC-myc in the same cells (Wolinski and Kohlwein, 2008). Immediately prior to imaging, the nucleus and kinetoplast were stained with 4',6-diamidino-2-phenylindole (DAPI) (1 mg/mL in vPBS) (Invitrogen) (Field *et al.*, 2004). Images were collected using a Nikon TE2000 widefield epifluorescence microscope and image acquisition was performed using the Nikon NIS Elements software package.

RNA Interference

To make the ACC RNAi construct, a fragment bracketing the start codon of ACC (-110 to +467 nt) was amplified by PCR (Roche Expand High Fidelity) from wild-type procyclic form 427 genomic DNA using a forward primer

containing a 5' Xho I site (5'-CCGctcgagTCCGAGCTCGCAAAGTG-3') and a reverse primer containing a 5' Hind III site (5'-CCCaagcttGTCGCCCAAAGCAAACATC-3'). This 572 bp amplicon was cloned first into pCR2.1 TOPO prior to sub-cloning into the tetracycline-inducible RNAi vector pZJM (Wang *et al.*, 2000). The pZJM.ACC plasmid was confirmed by sequencing (one T-to-C difference from 927 sequence at nt -55).

Bloodstream and procyclic form RNAi cell lines were generated as described previously (Wang *et al.*, 2000; Morris *et al.*, 2001), with modifications suggested by J. Roper and M. Ferguson (pers. comm.). pZJM.ACC plasmid was linearized by Not I digestion and precipitated in ethanol to a final concentration of 10 mg/ml. Prior to transfection, cells were washed twice in Cytomix (van den Hoff *et al.*, 1992). For transfection into 29-13 procyclic cells, 100 µg of linearized pZJM.ACC was electroporated into 1 x 10^8 washed cells in a final volume of 0.5 ml. A stable non-clonal procyclic ACC RNAi population was established first, followed by isolation of clonal cell lines by limiting dilution. For transfection into 90-13 bloodstream form cells, 5 replicate transfections were prepared, each containing 100 µg linearized pZJM.ACC and 3 x 10^7 washed cells in a final volume of 0.5 ml. After electroporation, the 5 transfections were pooled and dispensed into 24 well plates, resulting in clonal cell lines.

For growth curves, ACC RNAi cells were diluted into normal or low-lipid media, induced for RNAi by the addition of tetracycline (1 µg/ml final) (Wang *et al.*, 2000) and cell density monitored using either a Z1 dual-threshold Coulter

Counter (Beckman) or a FACScan flow cytometer (Becton Dickinson). For comparison purposes, the slopes of the growth curves (linear correlation coefficients) were derived from linear regressions performed using Microsoft Excel. Doubling times were calculated from the slopes. Student *t*-Test analysis was performed using Microsoft Excel.

Metabolic Labeling and Lipid Analysis

Metabolic labeling was performed essentially as described (Paul *et al.*, 2004). Briefly, after 7 days of RNAi induction, 1 x 10^8 cells were washed 3X in BBSG and resuspended in 1 ml of either HMI-9 (for bloodstream forms) or SDM-79 (for procyclics). The 1 ml of cell suspension was then added to tubes containing 50 µCi of dried down [11,12-^{3}H]laurate (C12:0; 50-60 mCi/mmol) or [9,10-^{3}H]myristate (C14:0; 50-60 Ci/mmol) and incubated for 2 h in a 37°C (bloodstream forms) or 28°C (procyclic forms) CO_2 incubator. Total lipids were extracted using a modified Folch method, equal DPMs were loaded per lane (4,000-10,000), and analyzed by normal phase thin-layer chromatography (TLC) on Kieselgel 60 plates as described previously (Morita *et al.*, 2000a; Morita *et al.*, 2000b; Paul *et al.*, 2004). Labeled lipid species were identified based on known migration patterns in this TLC system (Doering *et al.*, 1993) or co-migration with the following markers: [^{3}H]myristate for all free fatty acids, [1-^{14}C]dimyristoyl phosphatidylcholine (American Radiolabeled Chemicals) for the various phospholipid species, and the bloodstream-specific VSG anchor precursors, Glycolipids A and C, which were generated using a cell-free

glycosylphosphatidylinositol anchor biosynthesis reaction (Morita *et al.*, 2000a; Paul *et al.*, 2004). To analyze the fatty acids by chain length, total lipid extracts were converted to fatty acid methyl esters (FAMEs), extracted in hexane, equal DPMs were loaded per lane (4,000-10,000), and analyzed by C18 reverse-phase TLC (Morita *et al.*, 2000b; Paul *et al.*, 2004). For chain length markers, FAMEs were prepared in parallel from [11,12-^{3}H]laurate (C12), [9,10-^{3}H]myristate (C14), [9,10-^{3}H]palmitate (C16), and [9,10-^{3}H]stearate (C18). Semi-quantitative analysis of TLCs was performed using densitometry (NIH Image J software) of appropriately exposed autoradiographic films with an unsaturated signal within the linear range of the film. To determine fatty acid elongation, each FAME spot was quantified and then calculated as follows: total C12 elongation = 100 x ([C14 + C16 + C18]/[C12 + C14 + C16 + C18]); total C14 elongation = 100 x ([C16 + C18]/[C14 + C16 + C18]).

Mouse Infections

Analysis of ACC RNAi in mice was performed essentially as described (Lecordier *et al.*, 2005). 20 Female NIH Swiss mice (10-12 weeks) were divided into 2 groups of 10 and pre-treated via their drinking water for 2 days with either 1 mg/ml doxycycline/ 5% sucrose (+ RNAi group) or 5% sucrose alone (no RNAi group). Doxycycline is a bioavailable tetracycline analog that will induce RNAi *in vivo* (Lecordier *et al.*, 2005) and does not itself affect the course of infection (Rothberg *et al.*, 2006; Abdulla *et al.*, 2008). Mice were then infected by intraperitoneal injection with 1 x 10^{5} bloodstream form ACC RNAi cells freshly

thawed from frozen stabilates. Mice were maintained on treated water for the duration of the experiment, with fresh changes every 2 days. Course of infection was monitored and time to death was recorded. Parasitemias were monitored periodically in a randomly selected sub-set of mice by tail stick and examination of blood smears. Mice were monitored daily for general appearance, behavior, and weight loss. If a mouse reached a humane endpoint (parasitemia ≥ 10^8, >20% weight loss, or obvious distress) the mouse was euthanized and time of death marked as the following day. Trypanosomes were purified from blood by DE52 anion exchange chromatography (Lonsdale-Eccles and Grab, 1987) and equal cell equivalents were assessed for ACC protein by SA-HRP blotting as described above. Kaplan-Meier analysis was performed using JMP software. Experiments were carried out in accordance with protocols approved by the Institutional Animal Care and Use Committee (IACUC) of Clemson University.

ClustalW Alignment of ACCs

Full-length sequence of the TREU 927 *T. brucei* ACC gene (Tb927.8.7100) and the *Leishmania major* ACC gene (LmjF31.2970) were downloaded from the TriTrypDB genome database (www.TriTrypDB.org (Aslett *et al.*, 2009)). The *Trypanosoma cruzi* ACC gene was reconstructed from two unlinked DNA sequence fragments (TcChr31-S nt 149040-152627 (+2) and TcChr31-S nt 152824-155282 (+3)) downloaded from TriTrypDB. ACC gene sequences for *Saccharomyces cerevisiae* ACC (Accession # AAA20073) and human ACC1 (Isoform 1, Accession # NP_942131) were downloaded from

National Center for Biotechnology Information (NCBI). Alignments were performed using ClustalW (Larkin *et al.*, 2007) followed by some manual adjustments.

ACC-MYC Immunoprecipitation and ACC Assay

Lysates from 2.5 x 10^8 cells were created by addition of 600 µl of hypotonic buffer and vigorous shearing through a 27.5 gauge needle. Lysates were then centrifuged for 10 min at 1000 x g to remove cellular debris. Following centrifugation, a 500 µl sample of cleared lysate was aspirated and added to 10 µl of immobilized anti-C-myc agarose beads (5 µg of anti-C-myc antibody in 2.5 µL settled agarose beads) (Thermo Scientific) and incubated end-over-end at 4°C for 1 h. The beads were then centrifuged, washed twice, and resuspended in 150 µl of BC buffer. Two-fold serial dilutions were made in BC buffer and assayed for ACC enzymatic activity as described in Experimental Procedures. Total activity was normalized to the “no lysate” control.

ACKNOWLEDGEMENTS

This work was supported in part by the National Institutes of Health 1R15AI081207 (KP) and Clemson University Funds (KP). We thank Jay Bangs, George Cross, Paul Englund, Luise Krauth-Siegel, Jim Morris, Meredith Morris, and Marilyn Parsons for their generous donation of antibodies, plasmids, and cell lines. We thank the staff of the Godley-Snell Research Center for their assistance with the mouse studies. We thank Maurizio del Poeta, Jim Morris, Meredith Morris, Kerry Smith, Lesly Temesvari, and Marilyn Parsons, and members of our laboratory for their helpful suggestions. We also thank Paul Englund, Jenny Guler, Soo Hee Lee, Yasu Morita, Sunayan Ray, and Jamie Wood for critical reading of the manuscript. We are indebted to Paul Englund in whose laboratory this work was initiated.

FIGURES

Figure 2.1: *T. brucei* Acetyl-CoA Carboxylase (TbACC) Gene Structure. A. Cartoon showing comparative enzyme architectures of *T. brucei* ACC (TbACC), *Saccharomyces cerevisiae* ACC1 (ScACC1), and human ACC1 (HsACC1). Entire protein sequence (black line) with Biotin carboxylase (BC) domains (hatched boxes), Biotin Carboxyl Carrier Protein (BCCP) Domains (black boxes), and Carboxyltransferase (CT) domains (white boxes) are drawn to scale. Conserved phosphorylation sites are indicated by capital Ps above the line. **B.** Alignment of the N-terminal sequences of TbACC, ScACC1, and HsACC1. The two conserved N-terminal serine phosphorylation sites in HsACC1 are indicated by shadowboxing. The first part of the conserved Biotin Carboxylase (BC) domain is in bold text and indicated by black bar underneath the text.

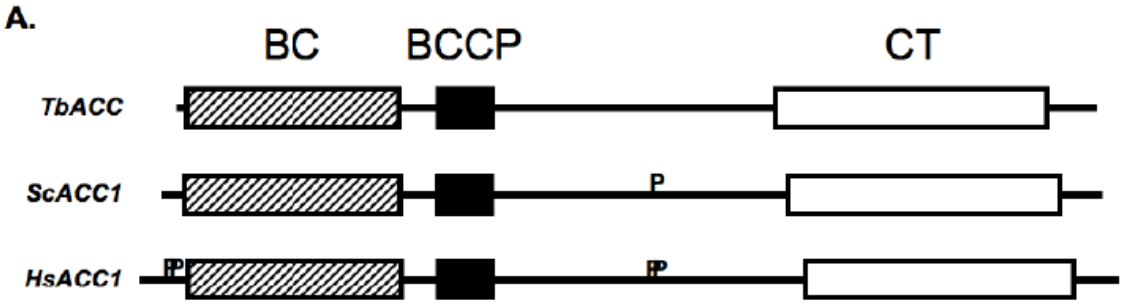

B.

```
TbACC              ------------------------------------------------------------
ScACC1             ------------------------------------------------------------
HsACC1           1 MDEPSPLAQPLELNQHSRFIIGSVSEDNSEDEISNLVKLDLLEEKEGSLSPASVGSDTL

TbACC    1 ----------------------------MSLSSPVTTMRPQLHGMKELCRFLGGKRPIERLLIANNGL
ScACC1   1 MSEESLFESSPQKMEYEITNYSERHTELPGHFIGLNTVDKLEESPLRDFVKSHGGHTVISKILIANNGI
HsACC1  60 SDLGISSLQDGLALHIRSSMSGLHLVKQGRDRKKIDSQRDFTVASPAEFVTRFGGNKVIEKVLIANNGI
```

Figure 2.2: ClustalW alignment of ACC genes from *T. brucei*, *S. cerevisiae* ACC1, and human ACC1. Identical residues are shaded in black, conserved residues are shaded in gray. ATP-binding motif (ATP) and biotinylation site (biotin) are boxed. Asterisks mark residues important for binding and/or catalysis as indicated by the crystal structure and/or mutational analyses.

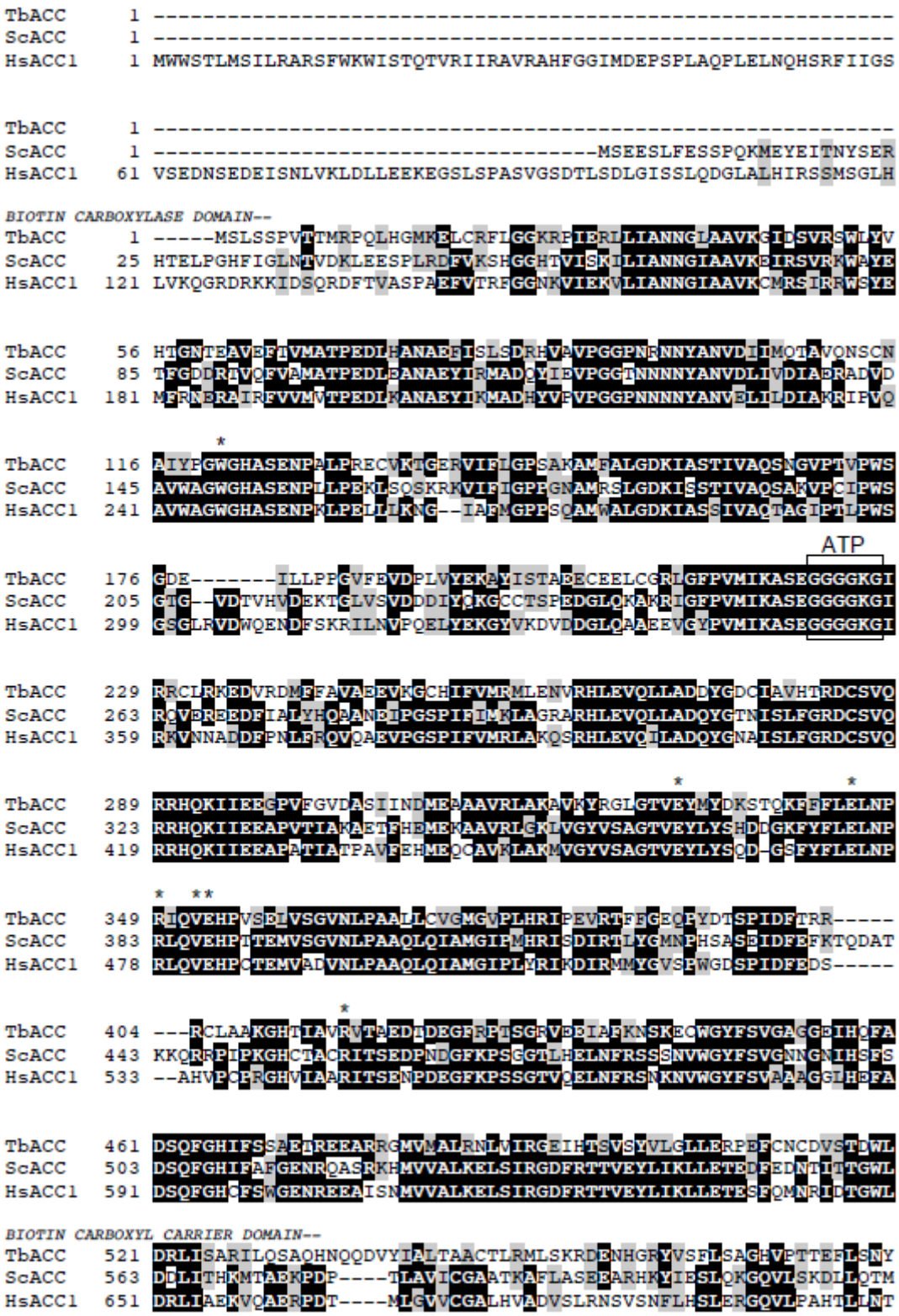
BIOTIN CARBOXYLASE DOMAIN--
ATP
BIOTIN CARBOXYL CARRIER DOMAIN--

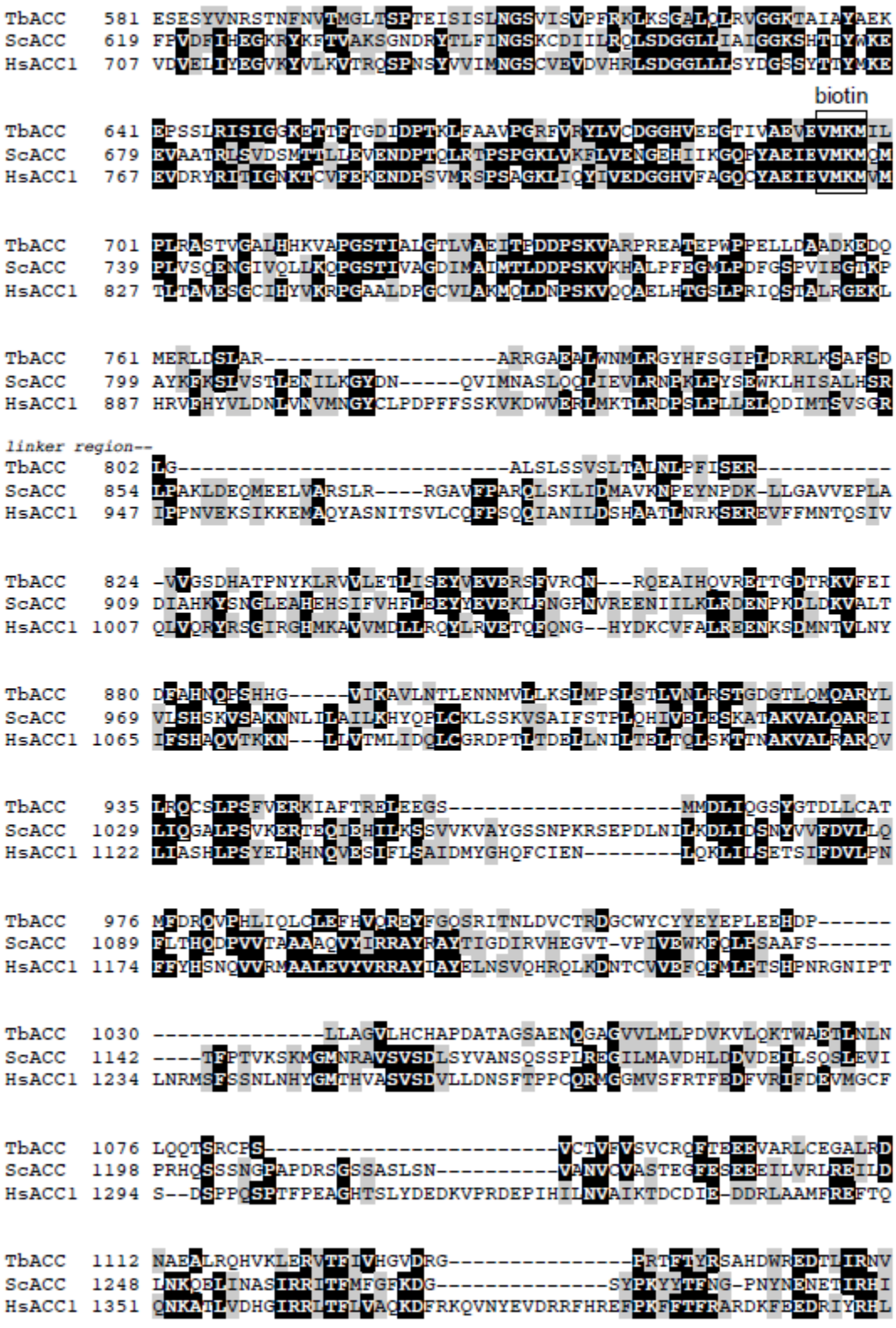
biotin
linker region--

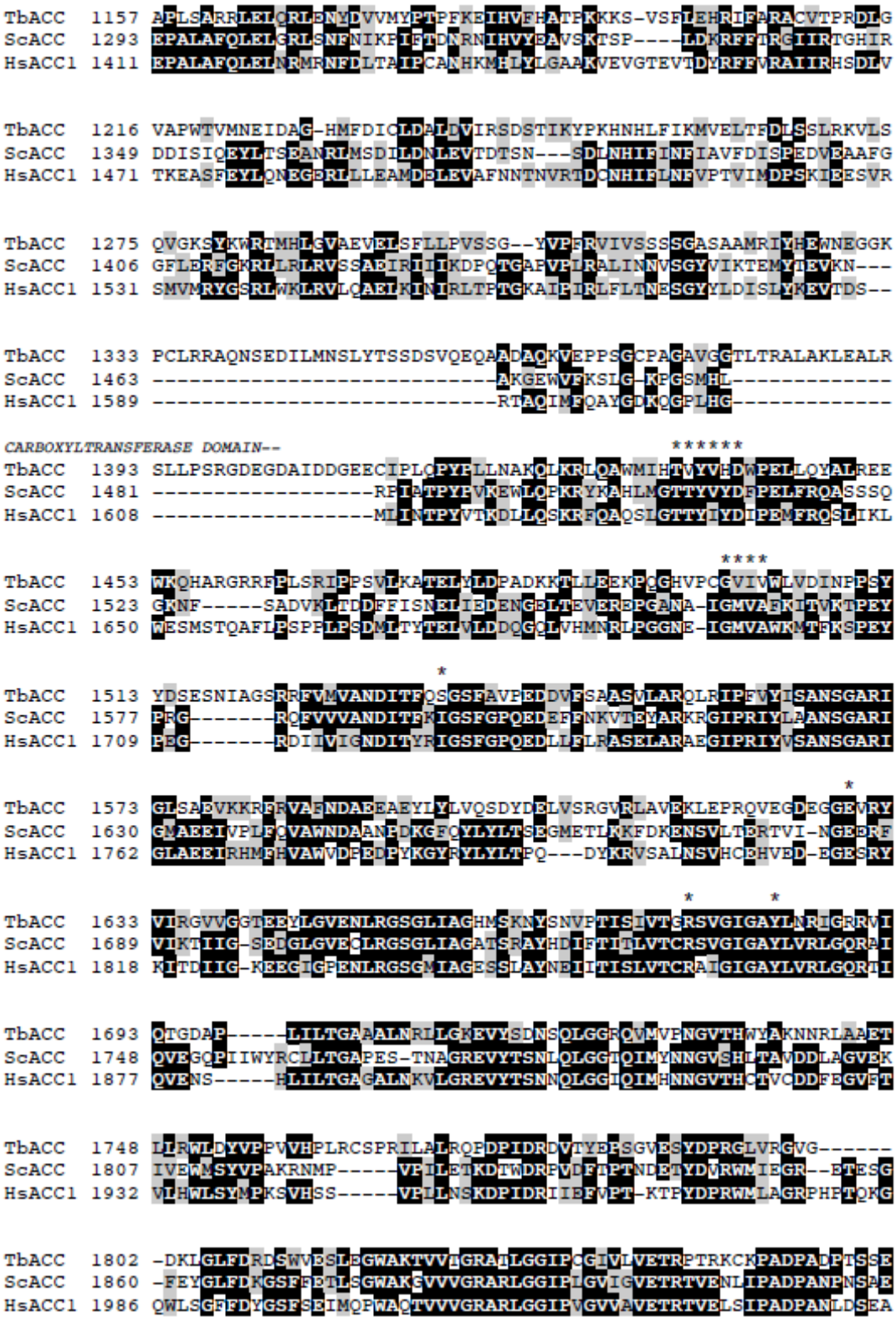
TbACC 1157
ScACC 1293
HsACC1 1411
TbACC 1216
ScACC 1349
HsACC1 1471
TbACC 1275
ScACC 1406
HsACC1 1531
TbACC 1333
ScACC 1463
HsACC1 1589
CARBOXYLTRANSFERASE DOMAIN--
TbACC 1393
ScACC 1481
HsACC1 1608
TbACC 1453
ScACC 1523
HsACC1 1650
TbACC 1513
ScACC 1577
HsACC1 1709
TbACC 1573
ScACC 1630
HsACC1 1762
TbACC 1633
ScACC 1689
HsACC1 1818
TbACC 1693
ScACC 1748
HsACC1 1877
TbACC 1748
ScACC 1807
HsACC1 1932
TbACC 1802
ScACC 1860
HsACC1 1986

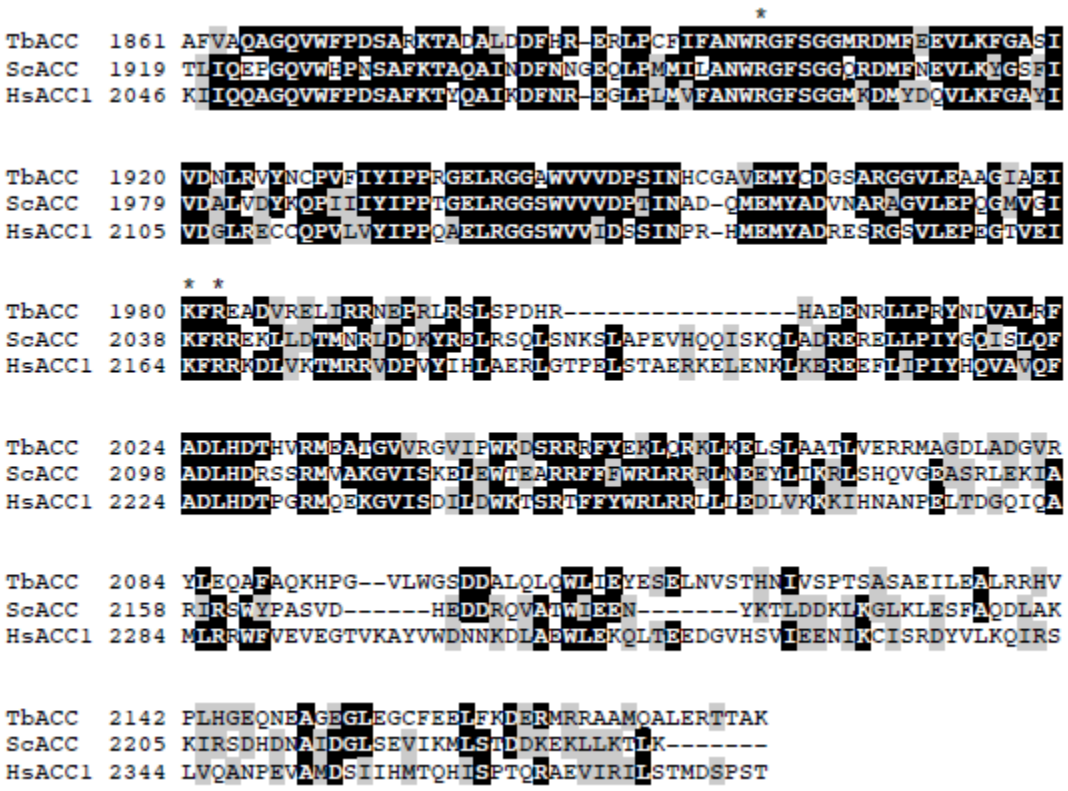
TbACC 1861
ScACC 1919
HsACC1 2046
TbACC 1920
ScACC 1979
HsACC1 2105
TbACC 1980
ScACC 2038
HsACC1 2164
TbACC 2024
ScACC 2098
HsACC1 2224
TbACC 2084
ScACC 2158
HsACC1 2284
TbACC 2142
ScACC 2205
HsACC1 2344

Figure 2.3: ClustalW alignment of ACC genes from three trypanosomatids: *T. brucei*, *T. cruzi*, *and L. major*. Identical residues are shaded in black, conserved residues are shaded in gray. ATP-binding motif (ATP) and biotinylation site (biotin) are boxed. Asterisks mark residues important for binding and/or catalysis as indicated by the crystal structure and/or mutational analyses.

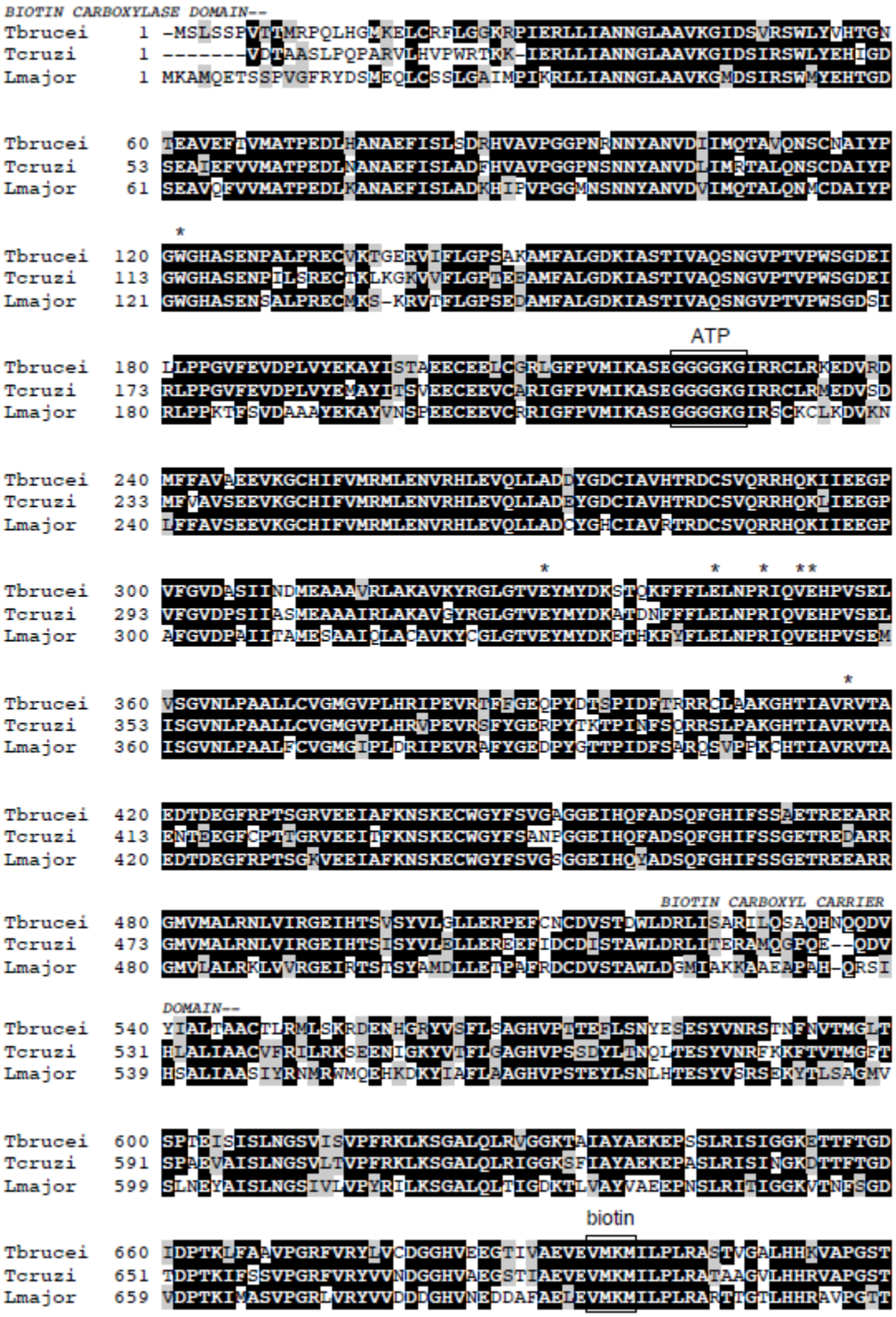
BIOTIN CARBOXYLASE DOMAIN--
ATP
BIOTIN CARBOXYL CARRIER
DOMAIN--
biotin

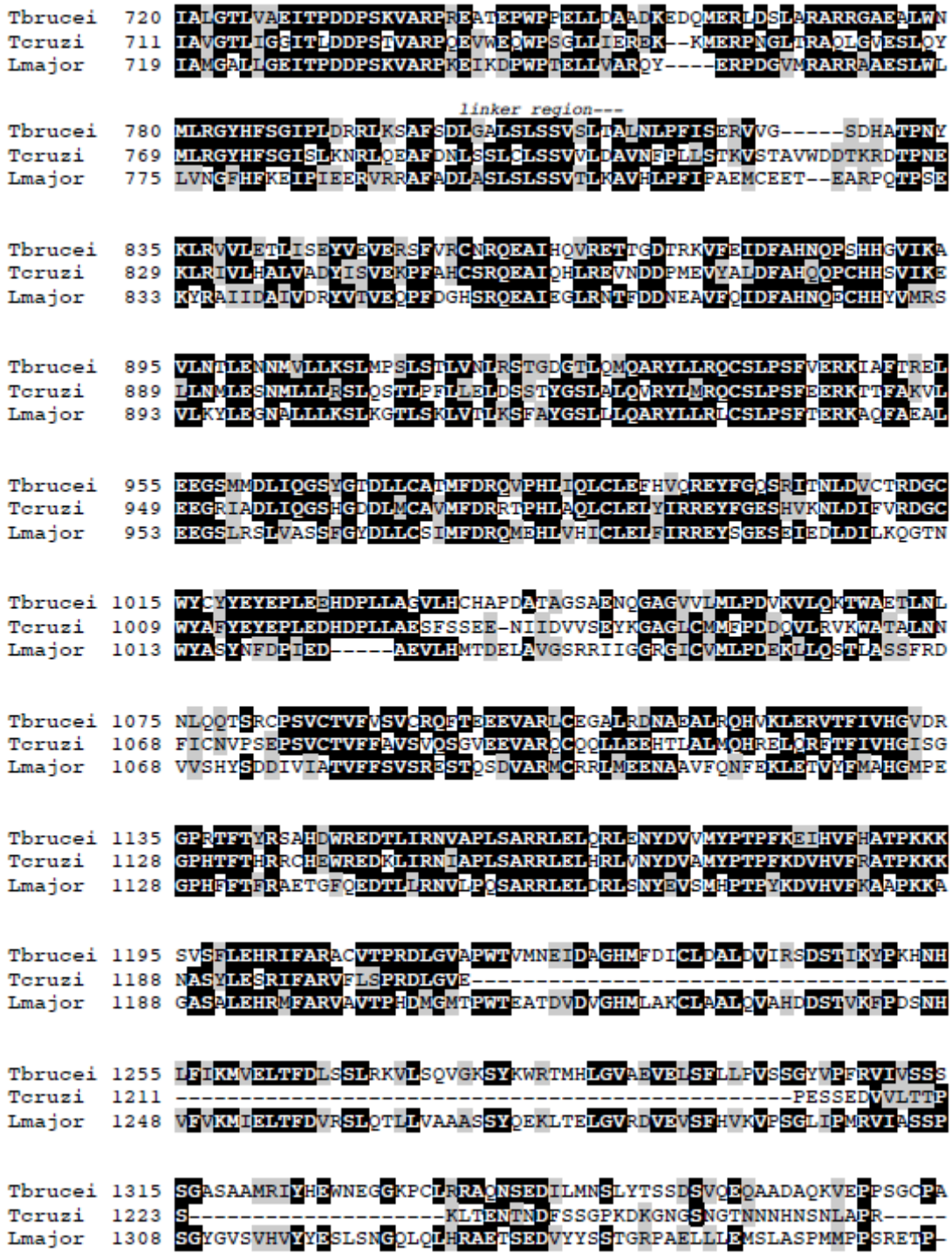
linker region

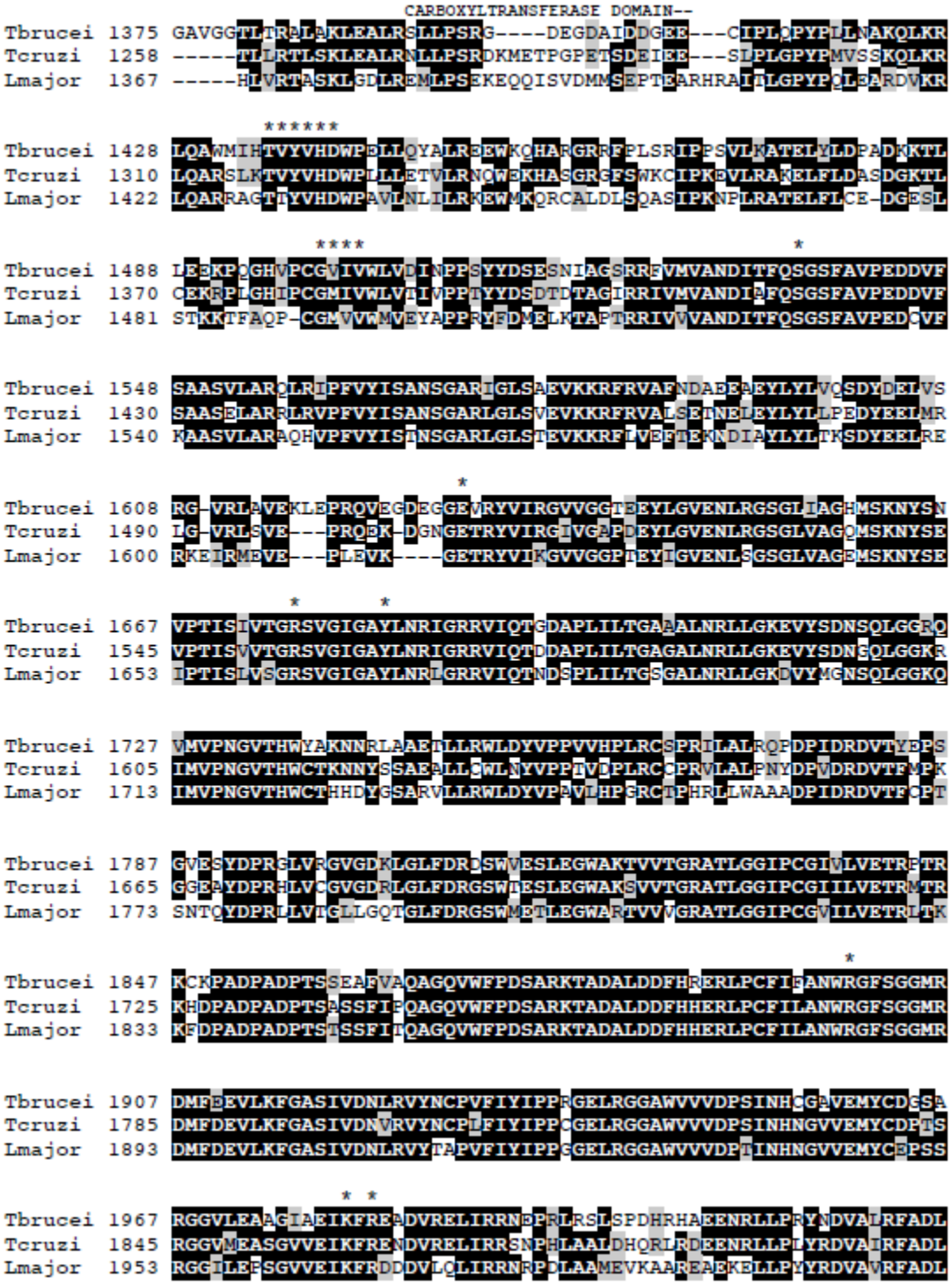
CARBOXYLTRANSFERASE DOMAIN--
Tbrucei 1375 GAVGGTLTRALAKLEALRSLLPSRG----DEGDAIDDGEE---CIPLQPYPLLNAKQLKR
Tcruzi 1258 -----TLLRTLSKLEALRNLLPSRDKMETPGPETSDEIEE---SLPLGPYPMVSSKQLKR
Lmajor 1367 -----HLVRTASKLGDLREMLPSEKEQQISVDMMSEPTEARHRAIALGPYPQLEARDVKR
Tbrucei 1428 LQAWMIHTVYVHDWPELLQYALRDEWKQHARGRRFPLSRIPPSVLKATELYLDPADKKTL
Tcruzi 1310 LQARSLKTVYVHDWPLLLETVLRNCWEKHASGRGFSWKCIPKEVLRAKELFLDASDGKTL
Lmajor 1422 LQARRAGTIYVHDWPAVLNLILRKEWMKQRCALDLSQASIPKNPLRATELFLCE-DGESL
Tbrucei 1488 LEEKPQGHVPCGVIVWLVDINPPSYYDSESNIAGSRREVMVANDITFQSGSFAVPEDDVF
Tcruzi 1370 GEKRPLGHIPCGMIVWLVTIVPPTYYDSDTDTAGIRRIVMVANDIAFQSGSFAVPEDDVF
Lmajor 1481 STKKTFAQP-CGLVVWMVEYAPPRYFDMELKTAPTRRIVVVANDITFQSGSFAVPEDCVF
Tbrucei 1548 SAASVLARQLRIPFVYISANSGARIGLSAEVKKRFRVAFNDAEDAEYLYLVQSDYDELVS
Tcruzi 1430 SAASELARRLRVPFVYISANSGARLGLSVEVKKRFRVALSETNELEYLYLLPEDYEELMR
Lmajor 1540 KAASVLARAQHVPFVYISTNSGARLGLSTEVKKRFLVEFTEKNDIAYLYLTKSDYEELRE
Tbrucei 1608 RG-VRLAVEKLEPRQVEGDEGGEVRYVIRGVVGGTEEYLGVENLRGSGLIAGHMSKNYSN
Tcruzi 1490 IG-VRLSVE---PRQEK-DGNGETRYVIRGIVGAPDEYLGVENLRGSGLVAGQMSKNYSE
Lmajor 1600 RKEIRMEVE---PLEVK----GETRYVIKGVVGGPTEYIGVENLSGSGLVAGEMSKNYSE
Tbrucei 1667 VPTISIVTGRSVGIGAYLNRIGRRVIQTGDAPLILTGAAALNRLLGKEVYSDNSQLGGRQ
Tcruzi 1545 VPTISVVTGRSVGIGAYLNRIGRRVIQTDDAPLILTGAGALNRLLGKEVYSDNSQLGGKR
Lmajor 1653 IPTISLVSGRSVGIGAYLNRLGRRVIQTNDSPLILTGSGALNRLLGKDVYMGNSQLGGKQ
Tbrucei 1727 VMVPNGVTHWYAKNNRLAAETLLRWLDYVPPVVHPLRCSPRILALRQPDPIDRDVTYEPS
Tcruzi 1605 IMVPNGVTHWCTKNNYSSAEALLQWLNYVPPTVDPLRCCPRVLALPNYDPVDRDVTFMPK
Lmajor 1713 IMVPNGVTHWCTHHDYGSARVLLRWLDYVPAVLHPGRCTPHRLLWAAADPIDRDVTFCPT
Tbrucei 1787 GVESYDPRGLVRGVGDKLGLFDRQSWVESLEGWAKTVVTGRATLGGIPCGIVLVETRFTR
Tcruzi 1665 GGEAYDPRHLVCGVGDRLGLFDRGSWTESLEGWAKSVVTGRATLGGIPCGIILVETRMTR
Lmajor 1773 SNTQYDPRLLVTGLLGQTGLFDRGSWMETLEGWARTVVVGRATLGGIPCGVILVETRLTK
Tbrucei 1847 KCKPADPADPTSSEAFVAQAGQVWFPDSARKTADALDDFHRERLPCFIFANWRGFSGGMR
Tcruzi 1725 KHDPADPADPTSASSFIPQAGQVWFPDSARKTADALDDFHHERLPCFILANWRGFSGGMR
Lmajor 1833 KFDPADPADPTSTSSFITQAGQVWFPDSARKTADALDDFHHERLPCFILANWRGFSGGMR
Tbrucei 1907 DMFDEVLKFGASIVDNLRVYNCPVFIYIPPRGELRGGAWVVVDPSINHCGAVEMYCDGSA
Tcruzi 1785 DMFDEVLKFGASIVDNVRVYNCPLFIYIPPCGELRGGAWVVVDPSINHNGVVEMYCDPTS
Lmajor 1893 DMFDEVLKFGASIVDNLRVYTAPVFIYIPPGGELRGGAWVVVDPTINHNGVVEMYCEPSS
Tbrucei 1967 RGGVLEAAGIAEIKFREADVRELIRRNDPRLRSLSPDHRHAEENRLLPRYNDVALRFADL
Tcruzi 1845 RGGVMEASGVVEIKFRENDVRELIRRSNPHLAALDHQRLRDEENRLLPLYRDVAIRFADL
Lmajor 1953 RGGILEPSGVVEIKFRDDDVLQLIRRNRPDLAAMEVKAAREAGKELLPVYRDVAVRFADL

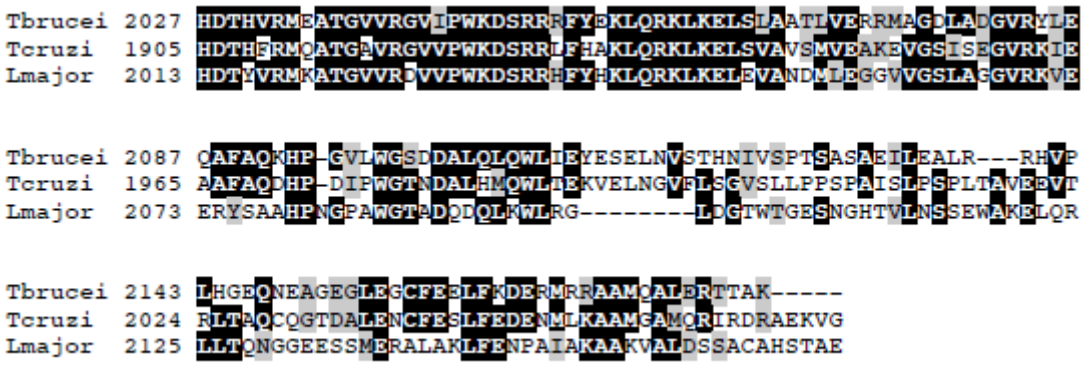
Tbrucei 2027
Tcruzi 1905
Lmajor 2013
Tbrucei 2087
Tcruzi 1965
Lmajor 2073
Tbrucei 2143
Tcruzi 2024
Lmajor 2125

Figure 2.4: ACC Transcribed in Both Bloodstream and Procyclic Forms. A. Total RNA (~1 x 10^7 cell equivalents) was probed for ACC by northern blotting with a ^{32}P-labelled DNA probe. Loading control is ethidium bromide stained ribosomal RNAs (EtBr rRNAs). gDNA, genomic DNA. **B.** Total lysates (20 µg protein) were probed for ACC by blotting with SA-HRP, which recognizes the ACC biotin prosthetic group. Loading control is lower half of blot probed for tubulin. **C.** ACC activity was measured in lysates (100 µg of protein) of bloodstream forms (BF; gray bars) and procyclic forms (PF; white bars) by assaying the conversion of [^{14}C]sodium bicarbonate into the acid-resistant [^{14}C]malonyl-CoA product, which was dried onto filters and measured by scintillation counting. Lysate concentration was within linear range for the assay. Values were normalized to no lysate controls before averaging. Mean of 6 experiments is shown. Error bars indicate the SEM (p >0.5 for difference between bloodstream and procyclic form activity, Student's t-Test).

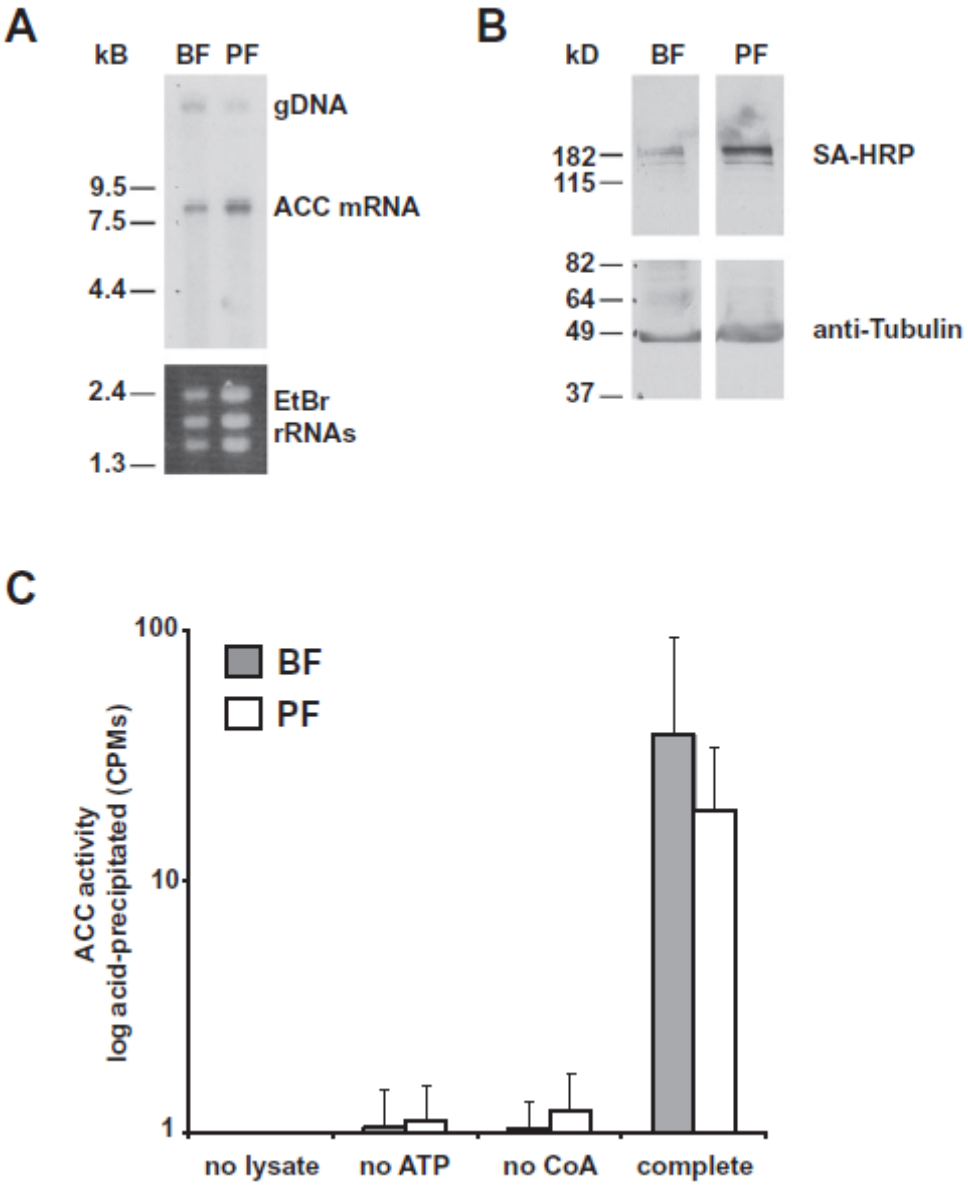
A
kB
BF PF
gDNA
9.5
7.5
ACC mRNA
4.4
2.4
EtBr
rRNAs
1.3
B
kD
BF
PF
182
115
SA-HRP
82
64
49
anti-Tubulin
37
C
100
BF
PF
ACC activity
log acid-precipitated (CPMs)
10
1
no lysate
no ATP
no CoA
complete

Figure 2.5: ACC Activity is evident in anti-C-myc immunoprecipitation from ACC-MYC cell lysate. Lysate from procyclic form ACC-myc cells (light gray bars) and control 29-13 cells (black bars) were subjected to immunoprecipitation with anti-c-myc coated latex beads. Washed beads containing bound proteins were serially-diluted and assayed for ACC activity by measuring the conversion of [^{14}C]sodium bicarbonate to [^{14}C]malonyl-CoA by scintillation counting of the acid-resistant product. Total activity of each sample was normalized to the "no lysate" control.

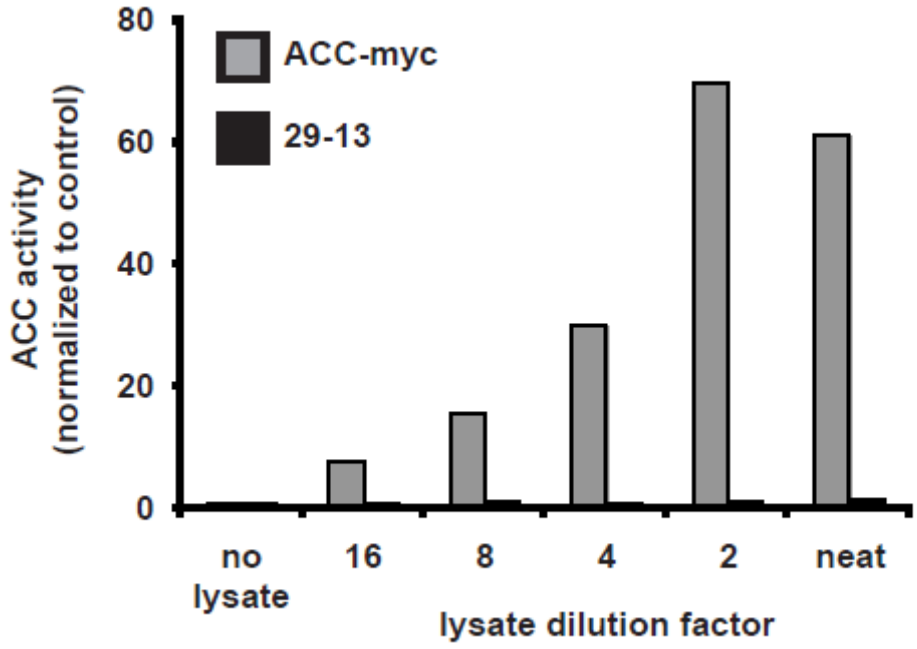

Figure 2.6: Sub-Cellular Fractionation Shows ACC to be Cytosolic. A. Scheme for sub-cellular fractionation by differential centrifugation of lysates prepared from procyclic form ACC-myc cells. **B.** Starting lysate (L) and sub-cellular pellet (P) and supernatant (S) fractions were probed by western blotting for ACC-myc (c-myc), total ACC (SA-HRP), cytoplasmic HSP70 (cytoplasmic marker), glycosomes, and BiP (ER marker). The anti-glycosome antibody recognizes three glycosomal enzymes: pyruvate phosphate dikinase (PPDK) (~100 kD), aldolase (~41 kD), and glyceraldehyde phosphate dehydrogenase (GAPDH) (~39 kD). The identity of the ~50 kD band is not known. Example shown is representative of two independent fractionations.

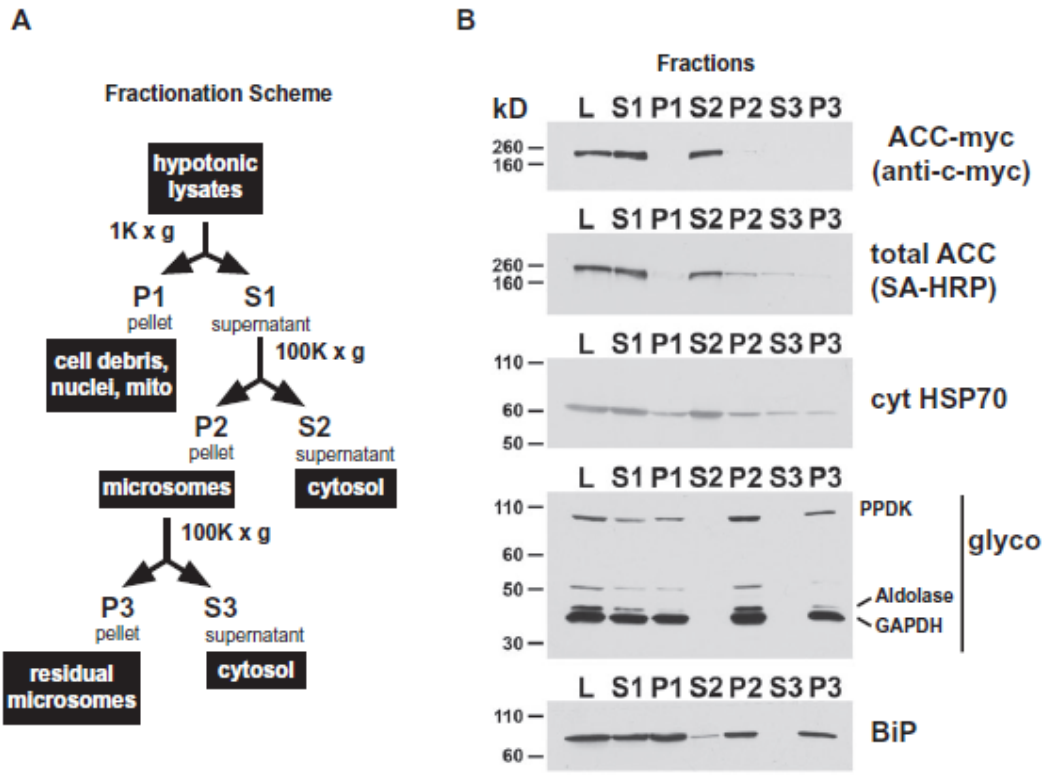

Figure 2.7: Immunofluorescence microscopy shows ACC distribution is distinct from glycosomes. Procyclic form ACC-myc cells were fixed permeabilized, and ACC-myc (green) localized with mouse anti-c-myc primary antibody and Alexa-Fluor 488 conjugated goat anti-mouse secondary antibody (B, F). Glycosomes (red) were localized with rabbit anti-glycosome primary antibody and Alex-Fluor 594 conjugated goat-anti-rabbit secondary antibody (C, G). Merged views show the red and green channels (D, H). Cells were co-stained with DAPI (blue) to indicate nuclear and mitochondrial DNA (A, E). Cells were imaged at 100X. Scale bars = 10 μm.

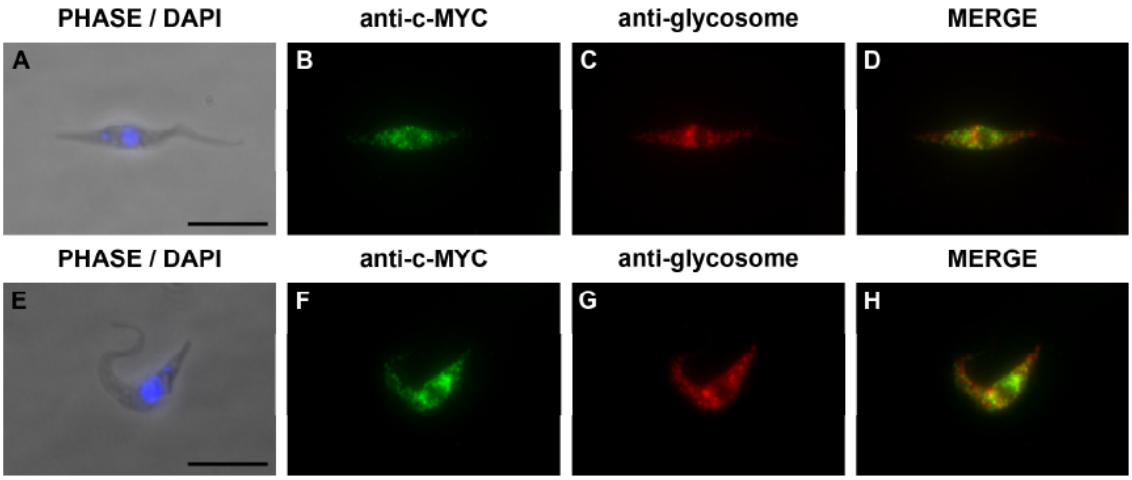

Figure 2.8: Immunofluorescence Microscopy Shows ACC is Localized to Cytoplasmic Puncta. A–H. Procyclic form ACC-myc cells (A–D) and wild-type procyclic cells (E–H) were fixed, permeabilized, and ACC-myc localized by staining with mouse anti-c-myc primary antibody and Alexa-Fluor 488 conjugated goat anti-mouse secondary antibody (green). **I–X.** Procyclic form ACC-myc cells were co-localized for ACC-myc as above (green) along with rabbit antibodies for various sub-cellular markers: I–L, glycosome (anti-glycosomal); M–P, cytoplasm (anti-cytoplasmic HSP70); Q–T, ER (anti-BiP); and U–X, mitochondrion (anti-lipoamide dehydrogenase (LipDH)). Secondary antibody was goat-anti-rabbit conjugated to Alex-Fluor 594 (red). **Y–Z.** Wild-type procyclic cells were stained with Nile red to show lipid droplets. All cells were co-stained with DAPI (blue) to indicate nuclear and mitochondrial DNA. Cells were imaged at 100X (A, B, E, F, I–Z) and 60X (C,D,G,H). Scale bars = 10 μm.

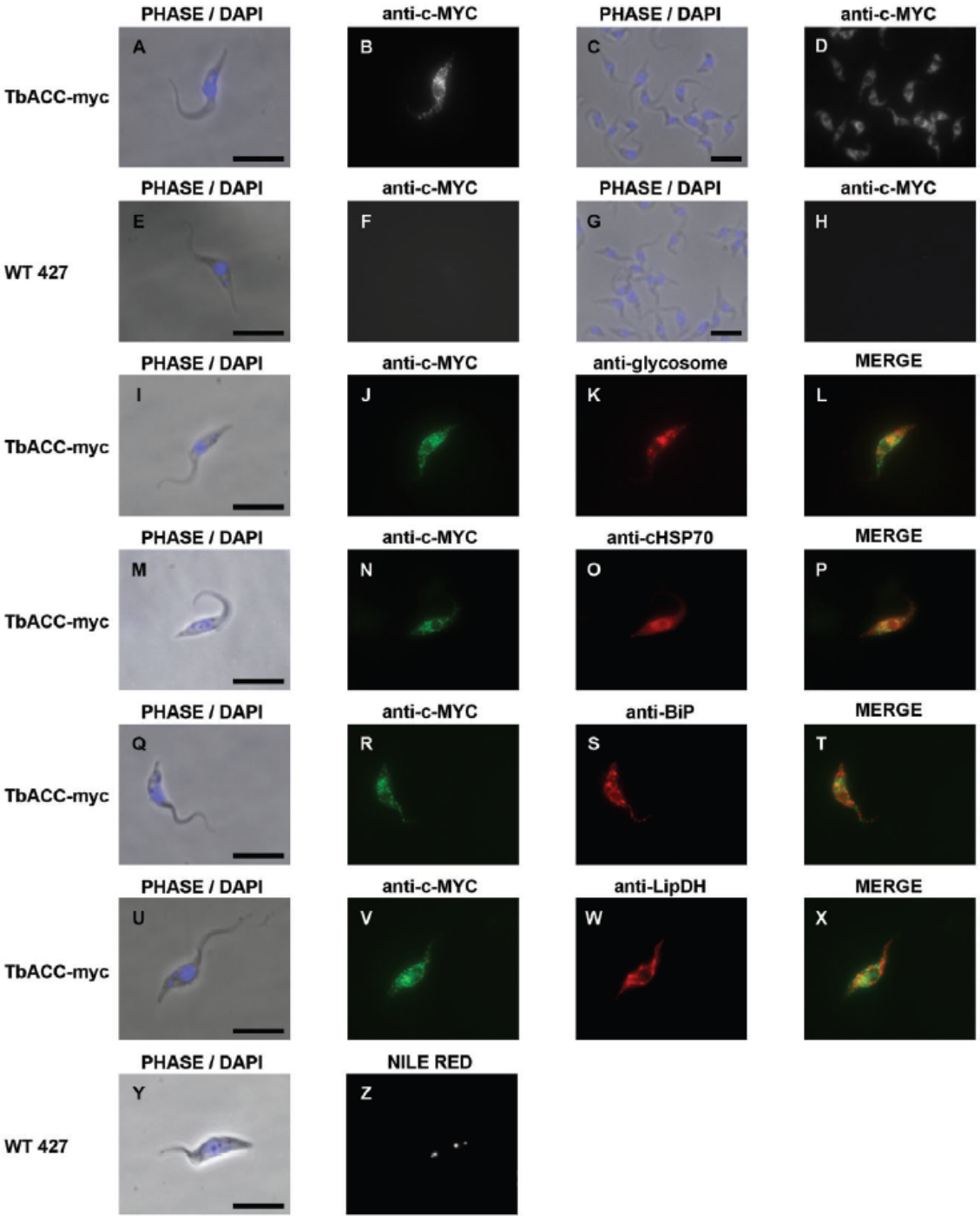
PHASE / DAPI
anti-c-MYC
PHASE / DAPI
anti-c-MYC
TbACC-myc
A
B
C
D
PHASE / DAPI
anti-c-MYC
PHASE / DAPI
anti-c-MYC
WT 427
E
F
G
H
PHASE / DAPI
anti-c-MYC
anti-glycosome
MERGE
TbACC-myc
I
J
K
L
PHASE / DAPI
anti-c-MYC
anti-cHSP70
MERGE
TbACC-myc
M
N
O
P
PHASE / DAPI
anti-c-MYC
anti-BiP
MERGE
TbACC-myc
Q
R
S
T
PHASE / DAPI
anti-c-MYC
anti-LipDH
MERGE
TbACC-myc
U
V
W
X
PHASE / DAPI
NILE RED
WT 427
Y
Z

Figure 2.9: RNA interference of ACC in Bloodstream and Procyclic Forms. **A.** Total RNA (10-15 µg) was isolated from ACC RNAi cells after 2 days of RNAi induction (+ RNAi) or from uninduced controls (– RNAi) and probed for ACC by northern blotting with a ^{32}P-labelled DNA probe corresponding to the ACC RNAi target sequence. ACC mRNA, the Tet-induced double-stranded RNA (dsRNA), and contaminating genomic DNA (gDNA) are indicated at the right. Loading control is ethidium bromide stained ribosomal RNAs (rRNAs). One of 4 independent clones with similar results is shown. **B.** ACC RNAi cells were induced for 0–10 days. Total cell lysates (20 µg) from each time point were probed for ACC by SA-HRP blotting. Blot is over-exposed to show non-specific cross-reacting bands. A representative of 2 independent experiments is shown. **C.** ACC RNAi cells were induced for 4 days and hypotonic lysates from induced (+ RNAi) and uninduced control cells (no RNAi) were assayed for ACC activity by measuring the conversion of [^{14}C]sodium bicarbonate to [^{14}C]malonyl-CoA by scintillation counting of the acid-resistant product. Inset shows SA-HRP blotting of the same lysates to indicate extent of ACC RNAi. A representative of 2 independent experiments is shown. **D.** ACC RNAi cells were induced and cell growth was monitored for 14 days (+ RNAi) in comparison to control uninduced cultures (no RNAi). Asterisk indicates when RNA was isolated for the northern blot. A representative of 4 independent experiments is shown.

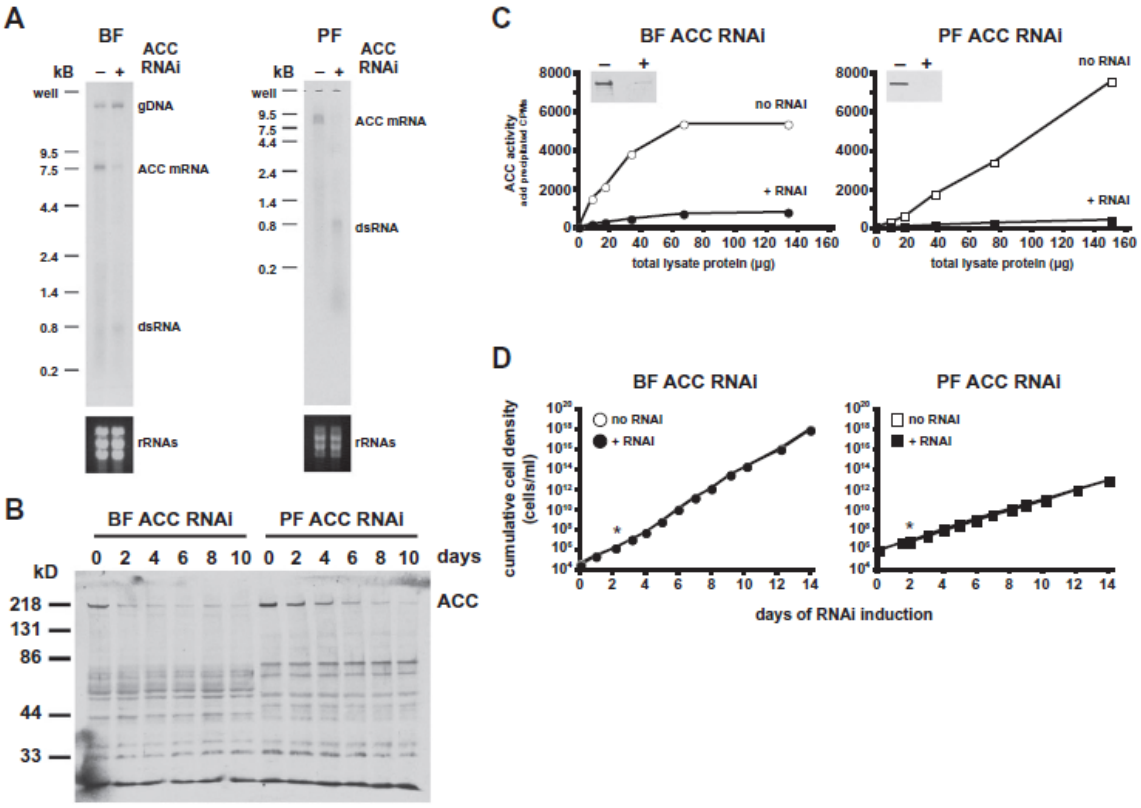
A
BF
ACC RNAi
kB
– +
well
gDNA
9.5
7.5
ACC mRNA
4.4
2.4
1.4
0.8
dsRNA
0.2
rRNAs
PF
ACC RNAi
kB
– +
well
9.5
7.5
4.4
ACC mRNA
2.4
1.4
0.8
dsRNA
0.2
rRNAs
B
BF ACC RNAi
PF ACC RNAi
0 2 4 6 8 10 0 2 4 6 8 10 days
kD
218
131
86
44
33
ACC
C
BF ACC RNAi
PF ACC RNAi
– +
no RNAi
+ RNAi
ACC activity
total lysate protein (µg)
D
BF ACC RNAi
PF ACC RNAi
cumulative cell density (cells/ml)
no RNAi
+ RNAi
days of RNAi induction

Figure 2.10: ACC RNAi reduces ACC activity, but has no effect on growth in normal media. A. ACC RNAi cells were induced for 4 days and hypotonic lysates from induced (+ RNAi; closed symbols) and uninduced control cells (no RNAi; open symbols) were assayed for ACC activity by measuring the conversion of [^{14}C]sodium bicarbonate to [^{14}C]malonyl-CoA by scintillation counting of the acid-resistant product. Total activity was normalized to "no lysate" control. Linear regression of pooled data from all independent experiments is shown (n=2 for bloodstream (left panel); n=3 for procyclic (right panel)). **B.** Linear regression correlation coefficients of ACC activity data in panel A. ACC RNAi reduced ACC activity by 87 ± 1% and 90 ±1% in bloodstream (gray bars) and procyclic cells (open bars), respectively. Error bars indicate SEM (p <0.0005 for difference between No RNAi and +RNAi, Student's t-Test). **C.** ACC RNAi cells were induced (+RNAi) or left uninduced (No RNAi), and cell growth monitored for up to 14 days. Doubling times for bloodstream (gray bars) and procyclic (open bars) trypanosomes were determined from 4 independent growth curves. Error bars indicate SEM (p >0.1 for difference between No RNAi and +RNAi, Student's t-Test).

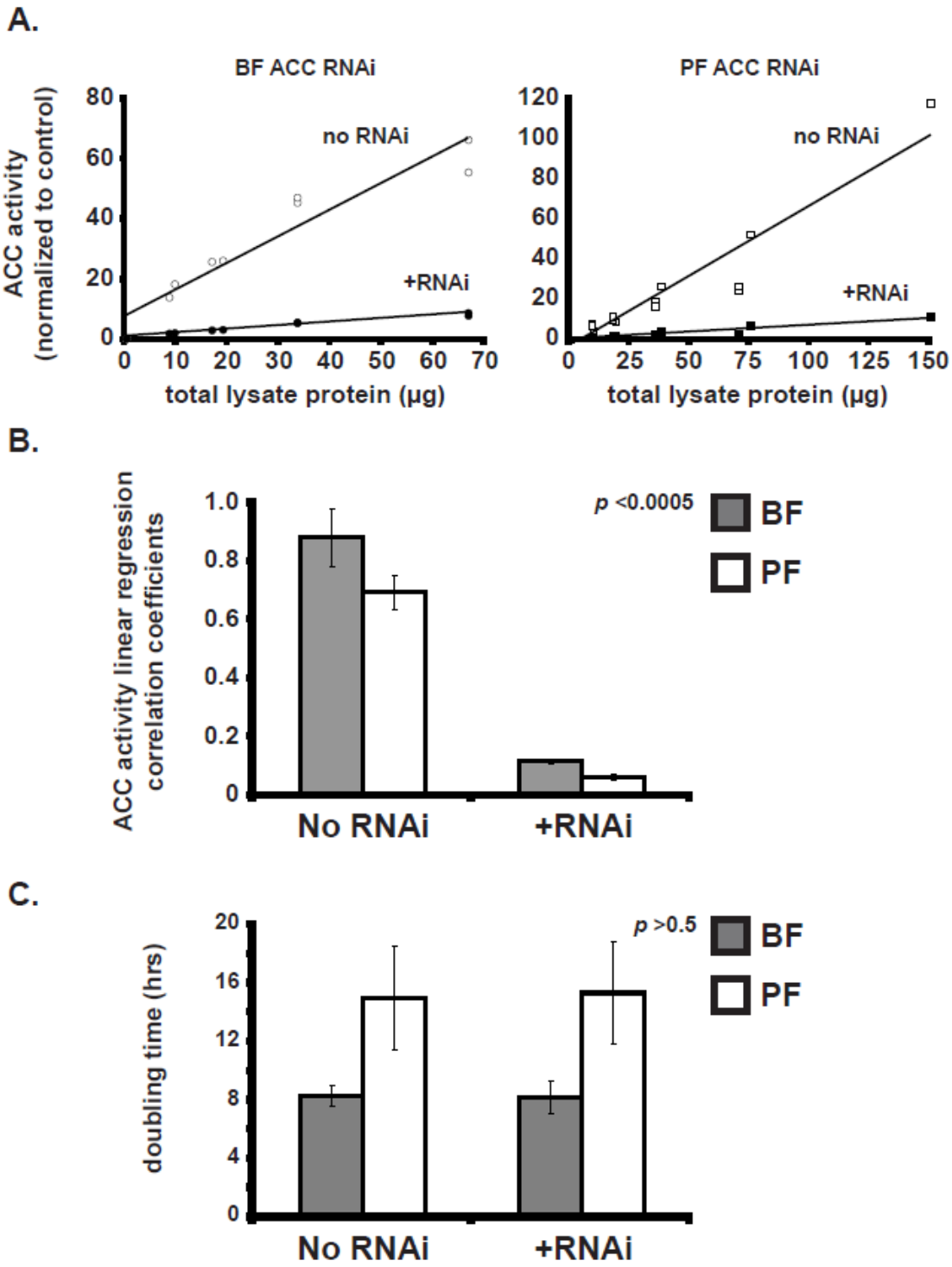
A.
BF ACC RNAi
PF ACC RNAi
ACC activity
(normalized to control)
no RNAi
+RNAi
total lysate protein (µg)
B.
ACC activity linear regression
correlation coefficients
p <0.0005
BF
PF
No RNAi
+RNAi
C.
doubling time (hrs)
p >0.5
BF
PF
No RNAi
+RNAi

Figure 2.11: ACC RNAi Reduces Fatty Acid Elongation. A. ACC RNAi cells were induced for 7 days. Induced (+ RNAi) and uninduced (– RNAi) cells were then incubated with 50 µCi of [^{3}H]laurate (C12) or [^{3}H]myristate (C14) for 2 h. Total lipids were extracted in chloroform/methanol (final chloroform/methanol/water ratio of 10:10:3) and equal DPMS per lane were loaded and resolved on Kieselgel 60 plates with chloroform/methanol/water (10:10:3) as the mobile phase. Plates were sprayed with En3Hance, dried, and exposed to film. Cell type, RNAi conditions, and type of [^{3}H]fatty acid label are indicated at the top. The origin (O) and lipid markers (M) (myristate (Myr), phosphatidylcholine (PtdC), and VSG GPI anchor precursors glycolipid C (C) and A (A)) are indicated at the right. Relative migration of neutral lipids (NL), free fatty acids (FFA), phospholipids (PL), and VSG GPI synthesis pathway products are indicated on left. Asterisk indicates putative phosphatidylethanolamine species. Lane numbers and marker lane (M) are indicated at the bottom. A representative of two independent experiments is shown. **B.** The fatty acids in the total lipid extracts in panel A were converted to FAMEs, extracted in hexane, and equal DPMs per lane were loaded and resolved by C18 reverse-phase high-performance TLC using chloroform/methanol/water (5:15:3) as the mobile phase. Plates were sprayed with En3Hance, dried, and exposed to film. RNAi conditions and type of label are indicated at the top. The origin (O) and lipid markers for C12, C14, C16, and C18 FAMEs are indicated at the right. Lane numbers and

marker lane (M) are indicated at the bottom. A representative of two independent experiments is shown.

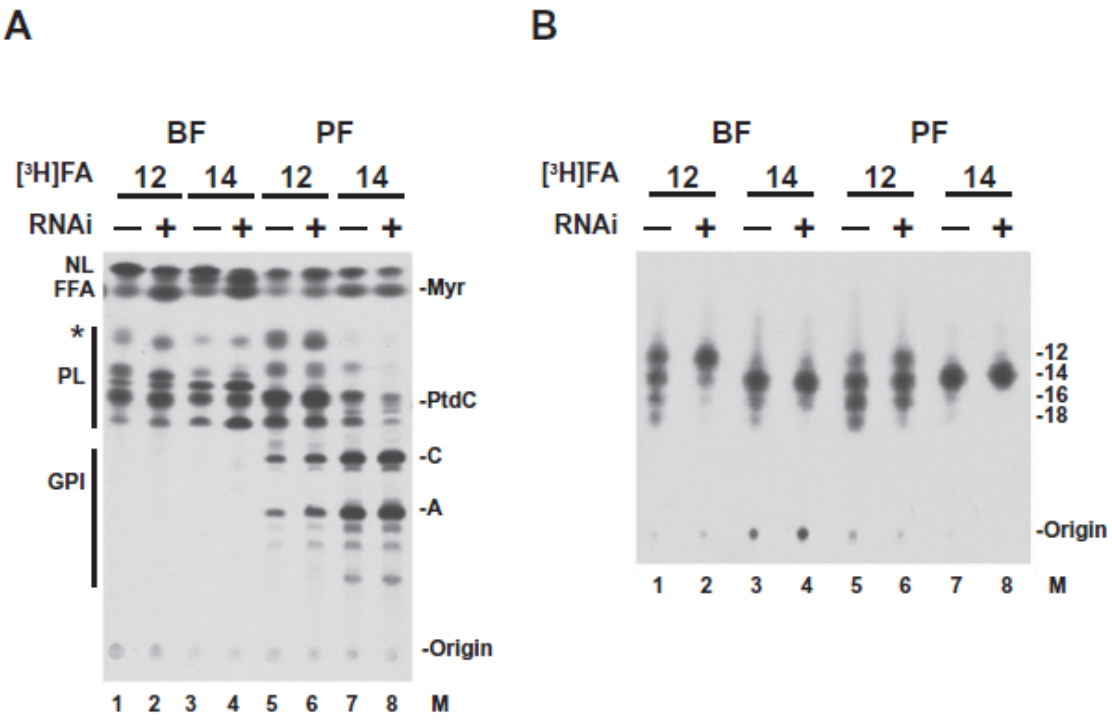
A
BF
PF
[3H]FA
12
14
12
14
RNAi
— + — + — + — +
NL
FFA
*
PL
GPI
-Myr
-PtdC
-C
-A
-Origin
1 2 3 4 5 6 7 8 M
B
BF
PF
[3H]FA
12
14
12
14
RNAi
— + — + — + — +
-12
-14
-16
-18
-Origin
1 2 3 4 5 6 7 8 M

Figure 2.12: Growth of ACC RNAi Cells in Low Lipid Conditions. ACC RNAi cells were seeded into normal or low-lipid media, induced for ACC RNAi for 10 days, and the cell densities of induced (+RNAi) and uninduced control (No RNAi) cultures were recorded every other day. **A.** Bloodstream form ACC RNAi cells in normal medium (NM), or two types of low-lipid media: medium made with delipidated FBS (DL) and medium made with only Serum Plus (SP). **B.** Procyclic form ACC RNAi in normal medium (NM) or low-lipid medium made with delipidated FBS (DL). **C.** Procyclic form ACC RNAi in DL medium or DL medium supplemented with 35 μM stearate (DL + C18). For all panels, average of three replicates is shown. Error bars show SEM, but are smaller than the data symbols.

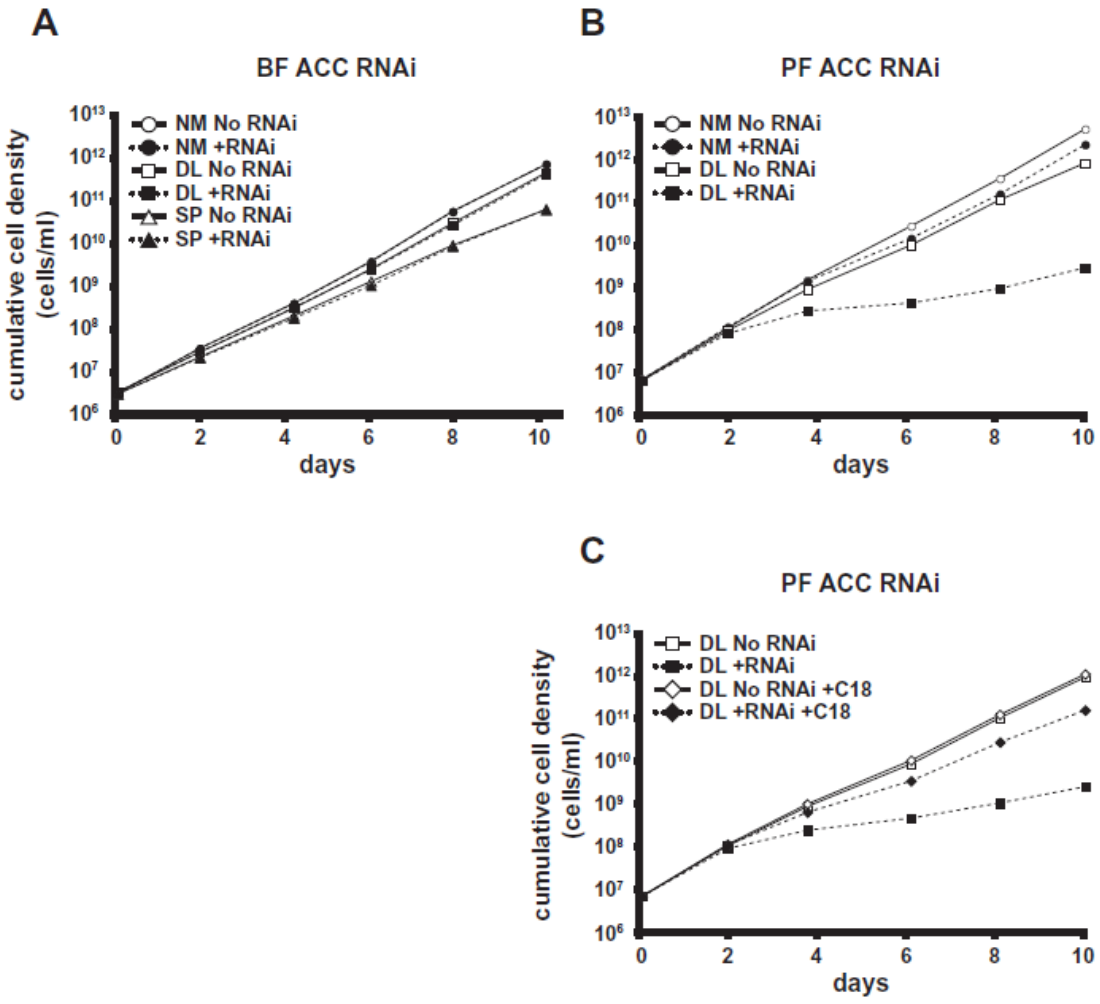
A
BF ACC RNAi
NM No RNAi
NM +RNAi
DL No RNAi
DL +RNAi
SP No RNAi
SP +RNAi
cumulative cell density (cells/ml)
days
B
PF ACC RNAi
NM No RNAi
NM +RNAi
DL No RNAi
DL +RNAi
days
C
PF ACC RNAi
DL No RNAi
DL +RNAi
DL No RNAi +C18
DL +RNAi +C18
cumulative cell density (cells/ml)
days

Figure 2.13: Pre-adaptation in low lipid media does not alter effect of ACC RNAi on growth. A. ACC RNAi cells were seeded into normal or low-lipid media, grown for 10 days (pre-adaptation), then induced for ACC RNAi for an additional 10 days. Cell densities of induced (+RNAi, closed symbols) and uninduced control (No RNAi; open symbols) cultures were recorded every other day during the RNAi induction. For each sample, the first medium listed is the pre-adaptation medium and the second medium listed is the induction medium (e.g. NM/NM means pre-adapted in NM and induced NM). **A.** Bloodstream form ACC RNAi cells in normal medium (NM), or two types of low-lipid media: medium made with delipidated FBS (DL) and medium made with only Serum Plus (SP). **B.** Procyclic form ACC RNAi in normal medium (NM) or low-lipid medium made with delipidated FBS (DL). Experiment was performed in duplicate.

A.

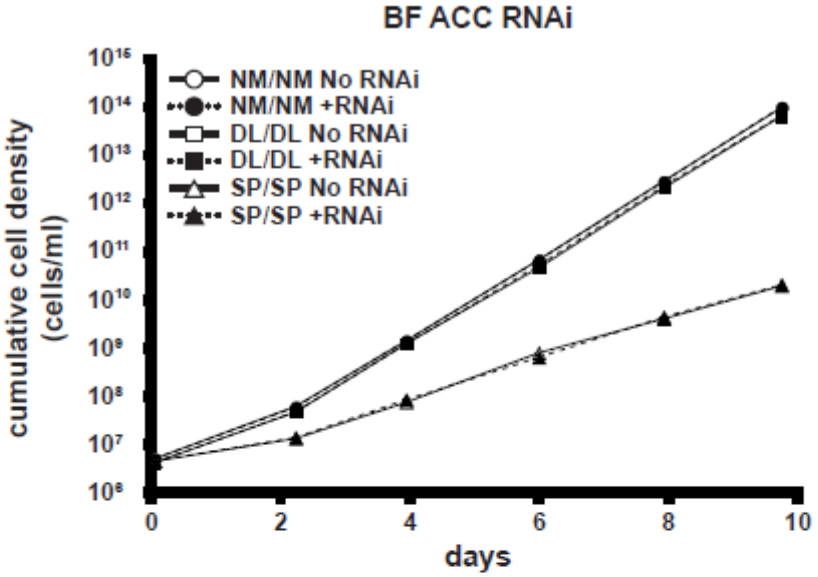
BF ACC RNAi
NM/NM No RNAi
NM/NM +RNAi
DL/DL No RNAi
DL/DL +RNAi
SP/SP No RNAi
SP/SP +RNAi
cumulative cell density (cells/ml)
days

B.

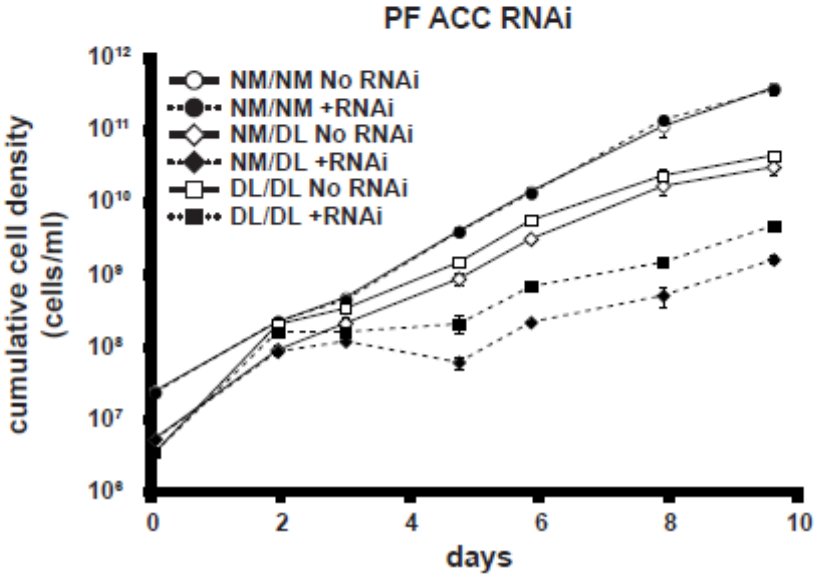
PF ACC RNAi
NM/NM No RNAi
NM/NM +RNAi
NM/DL No RNAi
NM/DL +RNAi
DL/DL No RNAi
DL/DL +RNAi
cumulative cell density (cells/ml)
days

Figure 2.14: ACC RNAi Cells Show Reduced Virulence in a Mouse Model of Infection. Kaplan-Meier survival analysis of mice infected with bloodstream form ACC RNAi trypanosomes. NIH Swiss mice (10 per group) were pre-dosed in their drinking water for 48 h with 1 mg/ml doxycycline in 5% sucrose water (+ RNAi) or 5% sucrose water as a control (No RNAi). At 48 h, mice were infected by intra-peritoneal injection of 1 x 10^5 ACC RNAi trypanosomes and monitored for time of death for 30 days. Mice were maintained on the doxycycline/sucrose or sucrose water for the duration. Significance was determined by Wilcoxon Test.

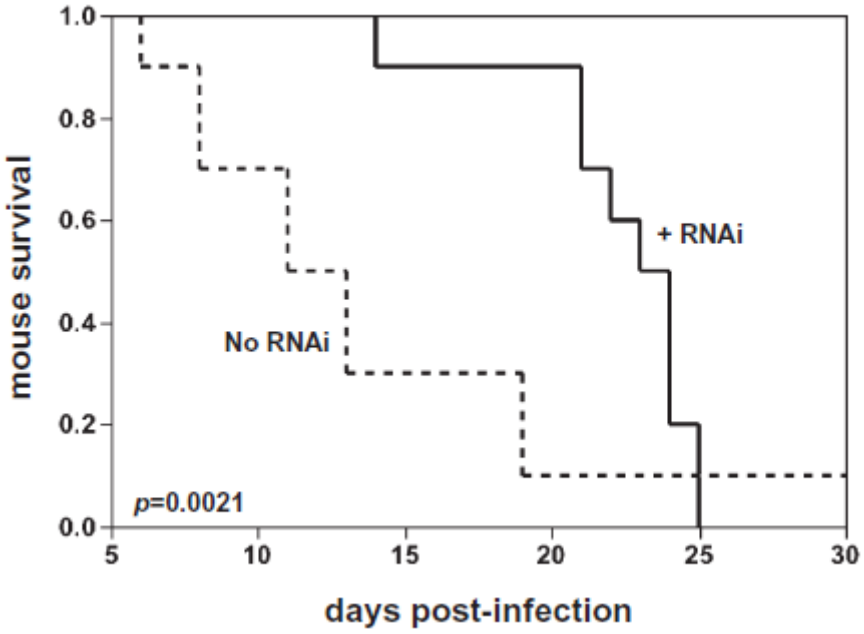

REFERENCES

Abdulla, M. H., T. O'Brien, Z. B. Mackey, M. Sajid, D. J. Grab and McKerrow, J. H. (2008) RNA interference of *Trypanosoma brucei* cathepsin B and L affects disease progression in a mouse model. *PLoS Negl Trop Dis* **2**: e298.

Acosta-Serrano, A., E. Vassella, M. Liniger, C. Kunz Renggli, R. Brun, I. Roditi and Englund, P. T. (2001) The surface coat of procyclic *Trypanosoma brucei*: programmed expression and proteolytic cleavage of procyclin in the tsetse fly. *Proc Natl Acad Sci U S A* **98**: 1513-1518.

Albert, M. A., J. R. Haanstra, V. Hannaert, J. Van Roy, F. R. Opperdoes, B. M. Bakker and Michels, P. A. (2005) Experimental and *in silico* analyses of glycolytic flux control in bloodstream form *Trypanosoma brucei*. *J Biol Chem* **280**: 28306-28315.

Ashcraft, B. A., W. S. Fillers, S. L. Augustine and S. D. Clarke, S. D. (1980) Polymer-protomer transition of acetyl-CoA carboxylase occurs *in vivo* and varies with nutritional conditions. *J Biol Chem* **255**: 10033-10035.

Aslett, M., C. Aurrecoechea, M. Berriman, J. Brestelli, B. P. Brunk, M. Carrington, D. P. Depledge, S. Fischer, B. Gajria, X. Gao, M. J. Gardner, A. Gingle, G. Grant, O. S. Harb, M. Heiges, C. Hertz-Fowler, R. Houston, F. Innamorato, J. Iodice, J. C. Kissinger, E. Kraemer, W. Li, F. J. Logan, J. A. Miller, S. Mitra, P. J. Myler, V. Nayak, C. Pennington, I. Phan, D. F. Pinney, G. Ramasamy, M. B. Rogers, D. S. Roos, C. Ross, D. Sivam, D. F. Smith, G. Srinivasamoorthy, C. J. Stoeckert, Jr., S. Subramanian, R. Thibodeau, A. Tivey, C. Treatman, G. Velarde and H. Wang, H. (2009) TriTrypDB: a functional genomic resource for the Trypanosomatidae. *Nucleic Acids Res* **38**: D457-462.

Balber, A. E., J. D. Bangs, S. M. Jones and Proia, R. L. (1979) Inactivation or elimination of potentially trypanolytic, complement-activating immune complexes by pathogenic trypanosomes. *Infect Immun* **24**: 617-627.

Bangs, J. D., L. Uyetake, M. J. Brickman, A. E. Balber and J. C. Boothroyd, J. C. (1993) Molecular cloning and cellular localization of a BiP homologue in *Trypanosoma brucei*. Divergent ER retention signals in a lower eukaryote. *J Cell Sci* **105**: 1101-1113.

Barber, M. C., N. T. Price and Travers, M. T. (2005) Structure and regulation of acetyl-CoA carboxylase genes of metazoa. *Biochim Biophys Acta* **1733**: 1-28.

Beaty, N. B. and Lane, M. D. (1983) The polymerization of acetyl-CoA carboxylase. *J Biol Chem* **258**: 13051-13055.

Beaty, N. B. and Lane, M. D. (1985) Kinetics of citrate-induced activation and polymerization of chick liver acetyl-CoA carboxylase. *Ann N Y Acad Sci* **447**: 23-37.

Bowes, A. E., A. H. Samad, P. Jiang, B. Weaver and Mellors, A. (1993) The acquisition of lysophosphatidylcholine by African trypanosomes. *J.Biol.Chem.* **268**: 13885-13892.

Brun, R. and Shonenberger, M. (1979) Cultivation and *in vitro* cloning of procyclic culture forms of *Trypanosoma brucei* in a semi-defined medium. *Acta Tropica* **36**: 289-292.

Buxbaum, L. U., J. Raper, F. R. Opperdoes and Englund, P. T. (1994) Myristate exchange: a second glycosyl phosphatidylinositol myristoylation reaction in African trypanosomes. *J.Biol.Chem.* **269**: 30212-30220.

Caceres, A. J., P. A. Michels and Hannaert, V. (2010) Genetic validation of aldolase and glyceraldehyde-3-phosphate dehydrogenase as drug targets in *Trypanosoma brucei*. *Mol Biochem Parasitol* **169**: 50-54.

Chen, Y., C. H. Hung, T. Burderer and Lee, G. S. (2003) Development of RNA interference revertants in *Trypanosoma brucei* cell lines generated with a double stranded RNA expression construct driven by two opposing promoters. *Mol Biochem Parasitol* **126**: 275-279.

Chou, C. Y., L. P. Yu and Tong, L. (2009) Crystal structure of biotin carboxylase in complex with substrates and implications for its catalytic mechanism. *J Biol Chem* **284**: 11690-11697.

Coppens, I., T. Levade and Courtoy, P. J. (1995) Host plasma low density lipoprotein particles as an essential source of lipids for the bloodstream forms of *Trypanosoma brucei*. *J.Biol.Chem.* **270**: 5736-5741.

de Jesus, T. C., R. R. Tonelli, S. C. Nardelli, L. da Silva Augusto, M. C. Motta, W. Girard-Dias, K. Miranda, P. Ulrich, V. Jimenez, A. Barquilla, M. Navarro, R. Docampo and Schenkman, S. (2010) Target of rapamycin (TOR)-like 1 kinase is involved in the control of polyphosphate levels and acidocalcisome maintenance in *Trypanosoma brucei*. *J Biol Chem* **285**: 24131-24140.

Dixon, H., C. D. Ginger and Williamson, J. (1971) The lipid metabolism of blood and culture forms of *Trypanosoma lewisi* and *Trypanosoma rhodesiense*. *Comp.Biochem.Physiol.[B]* **39**: 247-266.

Doering, T. L., M. S. Pessin, E. F. Hoff, G. W. Hart, D. M. Raben and Englund, P. T. (1993) Trypanosome metabolism of myristate, the fatty acid required for the variant surface glycoprotein membrane anchor. *J.Biol.Chem.* **268**: 9215-9222.

Emanuelsson, O., S. Brunak, G. von Heijne and Nielsen, H. (2007) Locating proteins in the cell using TargetP, SignalP and related tools. *Nat Protoc* **2**: 953-971.

Engstler, M., T. Pfohl, S. Herminghaus, M. Boshart, G. Wiegertjes, N. Heddergott and Overath, P. (2007) Hydrodynamic flow-mediated protein sorting on the cell surface of trypanosomes. *Cell* **131**: 505-515.

Engstler, M., L. Thilo, F. Weise, C. G. Grunfelder, H. Schwarz, M. Boshart and Overath, P. (2004) Kinetics of endocytosis and recycling of the GPI-anchored variant surface glycoprotein in *Trypanosoma brucei*. *J Cell Sci* **117**: 1105-1115.

Fang, J., P. Rohloff, K. Miranda and Docampo, R. (2007) Ablation of a small transmembrane protein of *Trypanosoma brucei* (TbVTC1) involved in the synthesis of polyphosphate alters acidocalcisome biogenesis and function, and leads to a cytokinesis defect. *Biochem J* **407**: 161-170.

Ferguson, M. A., S. W. Homans, R. A. Dwek and Rademacher, T. W. (1988) Glycosyl-phosphatidylinositol moiety that anchors *Trypanosoma brucei* variant surface glycoprotein to the membrane. *Science* **239**: 753-759.

Ficarro, S. B., M. L. McCleland, P. T. Stukenberg, D. J. Burke, M. M. Ross, J. Shabanowitz, D. F. Hunt and White, F. M. (2002) Phosphoproteome analysis by mass spectrometry and its application to *Saccharomyces cerevisiae*. *Nat Biotechnol* **20**: 301-305.

Field, M. C., C. L. Allen, V. Dhir, D. Goulding, B. S. Hall, G. W. Morgan, P. Veazey and Engstler, M. (2004) New approaches to the microscopic imaging of *Trypanosoma brucei*. *Microsc Microanal* **10**: 621-636.

Gardner, M. J., N. Hall, E. Fung, O. White, M. Berriman, R. W. Hyman, J. M. Carlton, A. Pain, K. E. Nelson, S. Bowman, I. T. Paulsen, K. James, J. A. Eisen, K. Rutherford, S. L. Salzberg, A. Craig, S. Kyes, M. S. Chan, V. Nene, S. J. Shallom, B. Suh, J. Peterson, S. Angiuoli, M. Pertea, J. Allen, J. Selengut, D. Haft, M. W. Mather, A. B. Vaidya, D. M. Martin, A. H. Fairlamb, M. J. Fraunholz, D. S. Roos, S. A. Ralph, G. I. McFadden, L. M. Cummings, G. M. Subramanian, C. Mungall, J. C. Venter, D. J. Carucci, S. L. Hoffman, C. Newbold, R. W. Davis, C. M. Fraser and Barrell, B. (2002) Genome sequence of the human malaria parasite *Plasmodium falciparum*. *Nature* **419**: 498-511.

Greenspan, P., E. P. Mayer and Fowler, S. D. (1985) Nile red: a selective fluorescent stain for intracellular lipid droplets. *J Cell Biol* **100**: 965-973.

Guler, J. L., E. Kriegova, T. K. Smith, J. Lukes and Englund, P. T. (2008) Mitochondrial fatty acid synthesis is required for normal mitochondrial morphology and function in *Trypanosoma brucei*. *Mol Microbiol* **67**: 1125-1142.

Haneji, T. and Koide, S. S. (1989) Transblot identification of biotin-containing proteins in rat liver. *Anal Biochem* **177**: 57-61.

Hasslacher, M., A. S. Ivessa, F. Paltauf and Kohlwein, S. D. (1993) Acetyl-CoA carboxylase from yeast is an essential enzyme and is regulated by factors that control phospholipid metabolism. *J Biol Chem* **268**: 10946-10952.

Hirumi, H. and Hirumi, K. (1989) Continuous cultivation of *Trypanosoma brucei* blood stream forms in a medium containing a low concentration of serum protein without feeder cell layers. *J.Parasitol.* **75**: 985-989.

Ho, H. H., C. Y. He, C. L. de Graffenried, L. J. Murrells and Warren, G. (2006) Ordered assembly of the duplicating Golgi in *Trypanosoma brucei*. *Proc Natl Acad Sci U S A* **103**: 7676-7681.

Horton, P., K. J. Park, T. Obayashi, N. Fujita, H. Harada, C. J. Adams-Collier and Nakai, K. (2007) WoLF PSORT: protein localization predictor. *Nucleic Acids Res* **35**: W585-587.

Jelenska, J., M. J. Crawford, O. S. Harb, E. Zuther, R. Haselkorn, D. S. Roos and Gornicki, P. (2001) Subcellular localization of acetyl-CoA carboxylase in the apicomplexan parasite *Toxoplasma gondii*. *Proc Natl Acad Sci U S A* **98**: 2723-2728.

Jetton, N., K. G. Rothberg, J. G. Hubbard, J. Wise, Y. Li, H. L. Ball and Ruben, L. (2009) The cell cycle as a therapeutic target against *Trypanosoma brucei*: Hesperadin inhibits Aurora kinase-1 and blocks mitotic progression in bloodstream forms. *Mol Microbiol* **72**: 442-458.

Jiang, D. W. and Englund, P. T. (2001) Four *Trypanosoma brucei* fatty acyl-CoA synthetases: fatty acid specificity of the recombinant proteins. *Biochem J* **358**: 757-761.

Jitrapakdee, S. and Wallace, J. C. (2003) The biotin enzyme family: conserved structural motifs and domain rearrangements. *Curr Protein Pept Sci* **4**: 217-229.

Kim, C. W., Y. A. Moon, S. W. Park, D. Cheng, H. J. Kwon and Horton, J. D. (2010) Induced polymerization of mammalian acetyl-CoA carboxylase by MIG12 provides a tertiary level of regulation of fatty acid synthesis. *Proc Natl Acad Sci U S A* **107**: 9626-9631.

Kleinschmidt, A. K., J. Moss and Lane, D. M. (1969) Acetyl coenzyme A carboxylase: filamentous nature of the animal enzymes. *Science* **166**: 1276-1278.

Krieger, S., W. Schwarz, M. R. Ariyanayagam, A. H. Fairlamb, R. L. Krauth-Siegel and Clayton, C. (2000) Trypanosomes lacking trypanothione reductase are avirulent and show increased sensitivity to oxidative stress. *Mol Microbiol* **35**: 542-552.

Larkin, M. A., G. Blackshields, N. P. Brown, R. Chenna, P. A. McGettigan, H. McWilliam, F. Valentin, I. M. Wallace, A. Wilm, R. Lopez, J. D. Thompson, T. J. Gibson and Higgins, D. G. (2007) Clustal W and Clustal X version 2.0. *Bioinformatics* **23**: 2947-2948.

Lecordier, L., D. Walgraffe, S. Devaux, P. Poelvoorde, E. Pays and Vanhamme, L. (2005) *Trypanosoma brucei* RNA interference in the mammalian host. *Mol Biochem Parasitol* **140**: 127-131.

Lee, C. K., H. K. Cheong, K. S. Ryu, J. I. Lee, W. Lee, Y. H. Jeon and Cheong, C. (2008) Biotinoyl domain of human acetyl-CoA carboxylase: Structural insights into the carboxyl transfer mechanism. *Proteins* **72**: 613-624.

Lee, M. G., F. T. Yen, Y. Zhang and Bihain, B. E. (1999) Acquisition of lipoproteins in the procyclic form of *Trypanosoma brucei*. *Mol Biochem Parasitol* **100**: 153-162.

Lee, S. H., J. L. Stephens, K. S. Paul and Englund, P. T. (2006) Fatty acid synthesis by elongases in trypanosomes. *Cell* **126**: 691-699.

Lentner, C., (1981) *Units of Measurement, Body Fluids, Composition of the Body, Nutrition*. Ciba-Geigy Ltd., Basel, Switzerland.

Lonsdale-Eccles, J. D. and Grab, D. J. (1987) Purification of African trypanosomes can cause biochemical changes in the parasites. *J.Protozool.* **34**: 405-408.

Mackall, J. C., M. D. Lane, K. R. Leonard, M. Pendergast and Kleinschmidt, A. K. (1978) Subunit size and paracrystal structure of avian liver acetyl-CoA carboxylase. *J Mol Biol* **123**: 595-606.

Mansfield, J. M. and Paulnock, D. M. (2005) Regulation of innate and acquired immunity in African trypanosomiasis. *Parasite Immunol* **27**: 361-371.

Martin, K. L. and Smith, T. K. (2006) Phosphatidylinositol synthesis is essential in bloodstream form *Trypanosoma brucei*. *Biochem J* **396**: 287-295.

Mazumdar, J. and Striepen, B. (2007) Make it or take it: fatty acid metabolism of apicomplexan parasites. *Eukaryot Cell* **6**: 1727-1735.

McDowell, M. A., D. M. Ransom and Bangs, J. D. (1998) Glycosylphosphatidylinositol-dependent secretory transport in *Trypanosoma brucei*. *Biochem J* **335**: 681-689.

Milne, K. G. and Ferguson, M. A. (2000) Cloning, expression, and characterization of the acyl-CoA-binding protein in African trypanosomes. *J Biol Chem* **275**: 12503-12508.

Morita, Y. S., A. Acosta-Serrano, L. U. Buxbaum and Englund, P. T. (2000a) Glycosyl phosphatidylinositol myristoylation in African trypanosomes. New intermediates in the pathway for fatty acid remodeling. *J Biol Chem* **275**: 14147-14154.

Morita, Y. S., K. S. Paul and Englund, P. T. (2000b) Specialized fatty acid synthesis in African trypanosomes: myristate for GPI anchors. *Science* **288**: 140-143.

Morris, J. C., Z. Wang, M. E. Drew, K. S. Paul and Englund, P. T. (2001) Inhibition of bloodstream form *Trypanosoma brucei* gene expression by RNA interference using the pZJM dual T7 vector. *Mol Biochem Parasitol* **117**: 111-113.

Morrison, L. J., L. Marcello and McCulloch, R. (2009) Antigenic variation in the African trypanosome: molecular mechanisms and phenotypic complexity. *Cell Microbiol* **11**: 1724-1734.

Motyka, S. A. and Englund, P. T. (2004) RNA interference for analysis of gene function in trypanosomatids. *Curr Opin Microbiol* **7**: 362-368.

Natesan, S. K., L. Peacock, K. Matthews, W. Gibson and Field, M. C. (2007) Activation of endocytosis as an adaptation to the mammalian host by trypanosomes. *Eukaryot Cell* **6**: 2029-2037.

Nikolau, B. J., E. S. Wurtele and Stumpf, P. K. (1985) Use of streptavidin to detect biotin-containing proteins in plants. *Anal Biochem* **149**: 448-453.

Nolan, D. P., D. G. Jackson, M. J. Biggs, E. D. Brabazon, A. Pays, F. Van Laethem, F. Paturiaux-Hanocq, J. F. Elliott, H. P. Voorheis and Pays, E. (2000) Characterization of a novel alanine-rich protein located in surface microdomains in *Trypanosoma brucei*. *J Biol Chem* **275**: 4072-4080.

O'Beirne, C., C. M. Lowry and Voorheis, H. P. (1998) Both IgM and IgG anti-VSG antibodies initiate a cycle of aggregation-disaggregation of bloodstream forms of *Trypanosoma brucei* without damage to the parasite. *Mol Biochem Parasitol* **91**: 165-193.

Parker, H. L., T. Hill, K. Alexander, N. B. Murphy, W. R. Fish and Parsons, M. (1995) Three genes and two isozymes: gene conversion and the compartmentalization and expression of the phosphoglycerate kinases of *Trypanosoma (Nannomonas) congolense*. *Mol Biochem Parasitol* **69**: 269-279.

Paul, K. S., C. J. Bacchi and Englund, P. T. (2004) Multiple triclosan targets in *Trypanosoma brucei*. *Eukaryot Cell* **3**: 855-861.

Paul, K. S., D. Jiang, Y. S. Morita and Englund, P. T. (2001) Fatty acid synthesis in African trypanosomes: a solution to the myristate mystery. *Trends Parasitol* **17**: 381-387.

Peterson, G. C., J. M. Sommer, S. Klosterman, C. C. Wang and Parsons, M. (1997) *Trypanosoma brucei*: identification of an internal region of phosphoglycerate kinase required for targeting to glycosomal microbodies. *Exp Parasitol* **85**: 16-23.

Ramirez, I. B., C. L. de Graffenried, I. Ebersberger, J. Yelinek, C. Y. He, A. Price and Warren, G. (2008) TbG63, a golgin involved in Golgi architecture in *Trypanosoma brucei*. *J Cell Sci* **121**: 1538-1546.

Robibaro, B., T. T. Stedman, I. Coppens, H. M. Ngo, M. Pypaert, T. Bivona, H. W. Nam and Joiner, K. A. (2002) *Toxoplasma gondii* Rab5 enhances cholesterol acquisition from host cells. *Cell Microbiol* **4**: 139-152.

Roggy, J. L. and Bangs, J. D. (1999) Molecular cloning and biochemical characterization of a VCP homolog in African trypanosomes. *Mol Biochem Parasitol* **98**: 1-15.

Rothberg, K. G., D. L. Burdette, J. Pfannstiel, N. Jetton, R. Singh and Ruben, L. (2006) The RACK1 homologue from *Trypanosoma brucei* is required for the onset and progression of cytokinesis. *J Biol Chem* **281**: 9781-9790.

Russo, D. C., D. J. Grab, J. D. Lonsdale-Eccles, M. K. Shaw and Williams, D. J. (1993) Directional movement of variable surface glycoprotein-antibody complexes in *Trypanosoma brucei*. *Eur J Cell Biol* **62**: 432-441.

Saggerson, D., (2008) Malonyl-CoA, a key signaling molecule in mammalian cells. *Annu Rev Nutr* **28**: 253-272.

Saitoh, S., K. Takahashi, K. Nabeshima, Y. Yamashita, Y. Nakaseko, A. Hirata and Yanagida, M. (1996) Aberrant mitosis in fission yeast mutants defective in fatty acid synthetase and acetyl CoA carboxylase. *J Cell Biol* **134**: 949-961.

Schneiter, R., C. E. Guerra, M. Lampl, V. Tatzer, G. Zellnig, H. L. Klein and Kohlwein, S. D. (2000) A novel cold-sensitive allele of the rate-limiting enzyme of fatty acid synthesis, acetyl coenzyme A carboxylase, affects the morphology of the yeast vacuole through acylation of Vac8p. *Mol Cell Biol* **20**: 2984-2995.

Schneiter, R., M. Hitomi, A. S. Ivessa, E. V. Fasch, S. D. Kohlwein and Tartakoff, A. M. (1996) A yeast acetyl coenzyme A carboxylase mutant links very-long-chain fatty acid synthesis to the structure and function of the nuclear membrane-pore complex. *Mol Cell Biol* **16**: 7161-7172.

Schoneck, R., O. Billaut-Mulot, P. Numrich, M. A. Ouaissi and Krauth-Siegel, R. L. (1997) Cloning, sequencing and functional expression of dihydrolipoamide dehydrogenase from the human pathogen *Trypanosoma cruzi*. *Eur J Biochem* **243**: 739-747.

Schwede, A. and Carrington, M. (2010) Bloodstream form trypanosome plasma membrane proteins: antigenic variation and invariant antigens. *Parasitology*: 1-11.

Seyfang, A., D. Mecke and Duszenko, M. (1990) Degradation, recycling, and shedding of *Trypanosoma brucei* variant surface glycoprotein. *J Protozool* **37**: 546-552.

Shen, Y., S. L. Volrath, S. C. Weatherly, T. D. Elich and Tong, L. (2004) A mechanism for the potent inhibition of eukaryotic acetyl-coenzyme A carboxylase by soraphen A, a macrocyclic polyketide natural product. *Mol Cell* **16**: 881-891.

Shirra, M. K., J. Patton-Vogt, A. Ulrich, O. Liuta-Tehlivets, S. D. Kohlwein, S. A. Henry and Arndt, K. M. (2001) Inhibition of acetyl coenzyme A carboxylase activity restores expression of the INO1 gene in a snf1 mutant strain of *Saccharomyces cerevisiae*. *Mol Cell Biol* **21**: 5710-5722.

Small, I., N. Peeters, F. Legeai and Lurin, C. (2004) Predotar: A tool for rapidly screening proteomes for N-terminal targeting sequences. *Proteomics* **4**: 1581-1590.

Smith, T. K. and Bütikofer, P. (2010) Lipid metabolism in *Trypanosoma brucei*. *Mol Biochem Parasitol* **172**: 66-79.

Stephens, J. L., S. H. Lee, K. S. Paul and Englund, P. T. (2007) Mitochondrial fatty acid synthesis in *Trypanosoma brucei*. *J Biol Chem* **282**: 4427-4436.

Tehlivets, O., K. Scheuringer and Kohlwein, S. D. (2007) Fatty acid synthesis and elongation in yeast. *Biochim Biophys Acta* **1771**: 255-270.

Thampy, K. G. and Wakil, S. J. (1988) Regulation of acetyl-coenzyme A carboxylase. II. Effect of fasting and refeeding on the activity, phosphate content, and aggregation state of the enzyme. *J Biol Chem* **263**: 6454-6458.

Thoden, J. B., C. Z. Blanchard, H. M. Holden and Waldrop, G. L. (2000) Movement of the biotin carboxylase B-domain as a result of ATP binding. *J Biol Chem* **275**: 16183-16190.

Tong, L., (2005) Acetyl-coenzyme A carboxylase: crucial metabolic enzyme and attractive target for drug discovery. *Cell Mol Life Sci* **62**: 1784-1803.

van den Hoff, M. J., A. F. Moorman and Lamers, W. H. (1992) Electroporation in 'intracellular' buffer increases cell survival. *Nucleic Acids Res* **20**: 2902.

Voorheis, H. P., (1980) Fatty acid uptake by bloodstream forms of *Trypanosoma brucei* and other species of the kinetoplastida. *Mol Biochem Parasitol* **1**: 177-186.

Waller, R. F., S. A. Ralph, M. B. Reed, V. Su, J. D. Douglas, D. E. Minnikin, A. F. Cowman, G. S. Besra and McFadden, G. I. (2003) A type II pathway for fatty acid biosynthesis presents drug targets in *Plasmodium falciparum. Antimicrob Agents Chemother* **47**: 297-301.

Wang, Z., J. C. Morris, M. E. Drew and Englund, P. T. (2000) Inhibition of *Trypanosoma brucei* gene expression by RNA interference using an integratable vector with opposing T7 promoters. *J Biol Chem* **275**: 40174-40179.

Wirtz, E., S. Leal, C. Ochatt and Cross, G. A. (1999) A tightly regulated inducible expression system for conditional gene knock-outs and dominant-negative genetics in *Trypanosoma brucei*. *Mol Biochem Parasitol* **99**: 89-101.

Wolinski, H. and Kohlwein, S. D. (2008) Microscopic analysis of lipid droplet metabolism and dynamics in yeast. *Methods Mol Biol* **457**: 151-163.

Woods, A., M. R. Munday, J. Scott, X. Yang, M. Carlson and Carling, D. (1994) Yeast SNF1 is functionally related to mammalian AMP-activated protein kinase and regulates acetyl-CoA carboxylase *in vivo*. *J Biol Chem* **269**: 19509-19515.

Wurtele, E. S. and Nikolau, B. J. (1990) Plants contain multiple biotin enzymes: discovery of 3-methylcrotonyl-CoA carboxylase, propionyl-CoA carboxylase and pyruvate carboxylase in the plant kingdom. *Arch Biochem Biophys* **278**: 179-186.

Young, S. A. and Smith, T. K. (2010) The essential neutral sphingomyelinase is involved in the trafficking of the variant surface glycoprotein in the bloodstream form of *Trypanosoma brucei*. *Mol Microbiol* **76**: 1461-1482.

Zhang, H., Z. Yang, Y. Shen and Tong, L. (2003) Crystal structure of the carboxyltransferase domain of acetyl-coenzyme A carboxylase. *Science* **299**: 2064-2067.

Zuther, E., J. J. Johnson, R. Haselkorn, R. McLeod and Gornicki, P. (1999) Growth of *Toxoplasma gondii* is inhibited by aryloxyphenoxypropionate herbicides targeting acetyl-CoA carboxylase. *Proc Natl Acad Sci U S A* **96**: 13387-13392.

CHAPTER THREE

INHIBITION OF *Trypanosoma brucei* ACETYL-COA CARBOXYLASE BY HALOXYFOP

Patrick A. Vigueira and Kimberly S. Paul

Department of Biological Sciences, Clemson University, Clemson, SC

ABSTRACT

Trypanosoma brucei, a eukaryotic pathogen that causes African sleeping sickness in humans and nagana in cattle, depends on the enzyme acetyl-CoA carboxylase (ACC) for full virulence in mice. ACC produces malonyl-CoA, the two carbon donor for fatty acid synthesis. We assessed the effect of haloxyfop, an aryloxyphenoxypropionate herbicide inhibitor of plastid ACCs in many plants as well as *Toxoplasma gondii*, on *T. brucei* ACC activity and growth in culture. Haloxyfop inhibited TbACC in cell lysate (EC_{50} 67 μM), despite the presence of an amino acid motif typically associated with resistance. Haloxyfop also reduced growth of bloodstream and procyclic form parasites (EC_{50} of 0.8 mM and 1.2 mM). However, the effect on growth was likely due to off-target effects because haloxyfop treatment had no effect on fatty acid elongation or incorporation into complex lipids *in vivo*.

INTRODUCTION

Trypanosoma brucei is a protozoan parasite and the etiological agent of human African trypanosomiasis, also known as African sleeping sickness. The disease causes significant morbidity and mortality across its range in sub-Saharan Africa. The World Health Organization estimates that 60 million people are at risk of contracting sleeping sickness (WHO, 2010). Livestock and working animals are also susceptible to infection, and the resulting disease, nagana, is estimated to cause 4.5 billion dollars in trypanosome-related agricultural losses each year (FAO, Food and Agricultural Organization of the United Nations, 2007).

The public health consequences and enormous economic burden caused by *T. brucei* highlight the desperate need for new chemotherapeutic treatments for these diseases. Currently, available drugs have substantial negative side effects, and parasite drug resistance is an ever-present concern (Burri, 2010). Vaccine development is not a viable option. This strategy is confounded by the parasite's ability to change its glycoprotein surface coat through a process called antigenic variation (Horn *et al.*, 2010).

Previously, we reported that *T. brucei* acetyl-CoA carboxylase (TbACC) is required to efficiently establish and maintain an infection in a mouse model (Vigueira *et al.*, 2011). Knockdown of TbACC by RNA interference (RNAi) nearly doubled the mean time until death, suggesting TbACC is a suitable candidate for investigation as a drug target. In *T. brucei*, TbACC exists as a single

cytoplasmically-disposed isoform. TbACC is a large multidomain enzyme, consisting of biotin carboxylase, biotin-carboxyl carrier protein (BCCP), and carboxyl-transferase (CT) domains. ACC catalyzes the first committed step in fatty acid synthesis (FAS): the ATP-dependent carboxylation of acetyl-CoA to make malonyl-CoA, the two-carbon donor for FAS (Vigueira *et al.*, 2011). In lieu of a conventional fatty acid synthase, the parasite utilizes a series of microsomal elongases (ELO) for the bulk of FAS (Lee *et al.*, 2006). See (Lee *et al.*, 2007) for review of *T. brucei* FAS.

ACC has long been recognized as a useful target for chemical intervention in crop management. The aryloxyphenoxypropionates (FOPs) and the cyclohexanediones (DIMs) are ACC inhibitors commonly used to control grass weeds affecting a number of agricultural crops (e.g. leaf vegetables, onion, strawberry). The FOPs and DIMs target the plastid ACCs of grasses by binding the CT domain and causing conformational changes that prevent transfer of the carboxyl group from the BCCP domain to the acetyl-CoA substrate (Delye *et al.*, 2003; Zhang *et al.*, 2004; Xiang *et al.*, 2009).

Research into weed FOP- and DIM-resistance mechanisms has identified two amino acid residues in ACC that appear important in determining resistance status. In the yeast, *Saccharomyces cerevisiae*, these residues are L1705 and V1967, and according to the crystal structure, these residues lie in the haloxyfop binding pocket of the CT domain (Zhang *et al.*, 2004). In rye grass, *Lolium rigidum*, a single change from the native I at either of these important residues is

sufficient to confer resistance to FOPs, specifically haloxyfop (Zagnitko *et al.*, 2001; Delye *et al.*, 2003). However, a growing body of evidence suggests that these residues are likely just two of multiple potential residues in the highly conserved CT domain capable of influencing FOP sensitivity (Zhang *et al.*, 2004; Zhang *et al.*, 2006a; Zhang *et al.*, 2006b; Liu *et al.*, 2007).

ACC and lipid metabolism have also been identified as potential drug targets for treating parasitic protozoan infections (Surolia *et al.*, 2001; Roberts *et al.*, 2003; Paul *et al.*, 2004; Singh *et al.*, 2009). In particular, haloxyfop has been demonstrated to inhibit the apicoplast-localized ACC of the apicomplexan parasite *Toxoplasma gondii* (Zuther *et al.*, 1999). Here, we report the sensitivity of a second protozoan ACC to haloxyfop. Despite possessing the amino acid sequence motif typically associated with haloxyfop resistance, TbACC is inhibited by haloxyfop. We demonstrate that haloxyfop kills insect midgut stage, procyclic form (PF) and mammalian bloodstream form (BF) parasites *in vitro*. However, *in vivo* lipid metabolism is not detectably influenced upon treatment, suggesting that the toxicity of haloxyfop to *T. brucei* cannot be entirely attributed to TbACC inhibition.

RESULTS

Effect of FOPs and sethoxydim on TbACC activity

We tested 4 compounds from the FOP family and a single representative from the DIM family of herbicides for their effect on TbACC enzymatic activity in PF lysate. TbACC activity is assayed in desalted cell lysate by measuring the incorporation of the [^{14}C]CO_2 from [^{14}C]$NaHCO_3$ into the acid-resistant [^{14}C]malonyl-CoA product (Vigueira *et al.*, 2011). Haloxyfop was the most potent inhibitor of the assay with an EC_{50} of 67 µM, and EC_{90} of 400 µM (Fig. 3.1E). The other tested FOPs (clodinafop, fluazifop, quizalifop) and the DIM compound (sethoxydim) had either no inhibitory activity or had EC_{50} values >400 µM (Fig. 3.1A-D). As haloxyfop showed promising activity, we used this compound in our subsequent studies.

TbACC contains residues that confer resistance in other ACCs

Previous work on FOPS has revealed that resistance can be traced to two key amino acid residues in the haloxyfop binding pocket of the ACC CT domain, L1705 and V1967 in *Saccharomyces cerevisiae* (Zhang *et al.*, 2004). In ACCs that have been experimentally determined to be resistant to inhibition by haloxyfop, the proteins possess the L/V motif at equivalent positions (Fig. 3.2). However, in sensitive ACCs, there are typically deviations from this pattern at either or both positions: L-1705-I or V-1967-I variants. TbACC has an L/V pair (L1650 and V1912) identical to the yeast L/V pair and would therefore be predicted to be resistant to haloxyfop.

Effect of haloxyfop on growth in culture

We have previously demonstrated that RNAi of ACC causes little reduction in parasite growth rate when cells are cultured in normal media (Vigueira *et al.*, 2011). Therefore, we sought to determine the maximum concentration of haloxyfop that could be tolerated by the parasites without having a major impact on growth rate. For growth of PF cells, haloxyfop concentrations up to 100 μM had no significant effect on doubling time, though 250 μM haloxyfop caused a slight, statistically significant increase (Fig. 3.3B). For BF cells, growth remained unchanged in the presence of up to 250 μM haloxyfop (Fig. 3.3E). The overall effect on growth rate over ten days was minimal in both PF and BF parasites (Fig. 3.3A, D), suggesting that potentially lethal, off-target effects are kept to a minimum at haloxyfop concentrations ≤250 μM. At higher haloxyfop concentrations (250 μM to 2 mM), we observed a statistically significant reduction in cell growth over 48 h (Fig. 3.3C, F) with an EC_{50} of 1.2 mM for PF parasites and an EC_{50} of 0.8 mM for BF parasites.

We detected a slight effect of the DMSO solvent on growth, with a 9% and 17% reduction in PF and BF parasites, respectively. The effect of 1% v/v DMSO on BF parasite viability has been quantified previously and is consistent with our observations (Sharlow *et al.*, 2010).

Effect of haloxyfop on fatty acid elongation

To determine whether haloxyfop treatment targets TbACC in intact cells, we assessed FA elongation *in vivo* as *T. brucei* will readily take up, elongate and

incorporate exogenous fatty acids into more complex lipids. We used haloxyfop concentrations that did not exhibit a major growth defect in PF parasites, as our previous work showed that ACC RNAi inhibited *in vivo* fatty acid elongation while showing no growth defect in normal media (Vigueira *et al.*, 2011). After a 4 day treatment with 10–250 μM haloxyfop, we incubated PF cells with [^{3}H]laurate (C12:0) and assessed its elongation by the ELO pathway. A chain length analysis of FAMEs by reverse-phase TLC demonstrated no reduction in the ability of the parasite to elongate [^{3}H]laurate (C12:0) to longer fatty acids (C14:0, C16:0, C18:0) upon haloxyfop treatment (Fig. 3.4B). Additionally, normal phase TLC of bulk lipids revealed no gross differences between haloxyfop-treated and untreated parasites in the level of incorporation of [^{3}H]laurate into phospholipids, free fatty acids, or neutral lipids (Fig. 3.4A).

Effect of haloxyfop on ACC protein levels

We next examined the possibility that the parasite compensated for haloxyfop inhibition by increasing ACC protein expression. ACC protein can be detected by western blotting with SA-HRP, which recognizes the biotin prosthetic group of ACC (Nikolau *et al.*, 1985; Haneji *et al.*, 1989; Vigueira *et al.*, 2011). After 4 days of haloxyfop treatment (10-250 μM), we observed no statistically significant changes ($p > 0.01$) in ACC protein levels when normalized to β-tubulin protein levels (Fig. 3.5).

DISCUSSION

Of the FOP and DIM compounds we tested, haloxyfop had the greatest inhibitory effect on TbACC activity in lysate (EC_{50} of 67 μM) (Fig. 3.1). The EC_{50} for haloxyfop on TbACC was determined with lysate rather than with purified protein, thus it is difficult to directly compare to other IC_{50}s reported for purified ACCs. Direct comparison of TbACC to other ACCs is also problematic because of the lab-to-lab variation in experimental procedure reported in the literature. With these limitations in mind, the sensitivity of TbACC in cell lysate is most similar to the moderate sensitivity described for that of the protozoan parasite *T. gondii* (IC_{50} 20 μM) (Zuther *et al.*, 1999) and the Norway rat, *R. norvegicus* (IC_{50} 120 μM), (Kemal *et al.*, 1992). Our data also suggests TbACC is less sensitive to haloxyfop than the plastid ACCs of ryegrass, corn, and blackgrass (IC_{50} 1-3 μM) (Secor *et al.*, 1988; De Prado *et al.*, 2000; Delye *et al.*, 2003) and more sensitive than the ACC CT domain of the yeast, *S. cerevisiae* (IC_{50} ~1.1 mM) (Zhang *et al.*, 2004).

The moderate sensitivity of TbACC to haloxyfop is somewhat surprising based on the presence of the L/V variant previously determined to confer resistance to this compound. Amino acid changes at these two positions cause sensitive plant ACCs to become resistant to FOPS and DIMS (Zagnitko *et al.*, 2001; Brown *et al.*, 2002; Christoffers *et al.*, 2002; Delye *et al.*, 2003; White *et al.*, 2005; Zhang *et al.*, 2006a). With the exception of the Norway rat, organisms

containing native ACCs with L/V variants are comparatively resistant to haloxyfop (Fig. 3.2).

The finding that TbACC possess the L/V variant and exhibits moderate sensitivity supports previous work indicating that although these residues appear important for conferring resistance, they alone are not necessarily predictive of sensitivity. Other residues in and around the haloxyfop binding pocket are likely to affect sensitivity and may moderate the effects of any single residue (Zhang *et al.*, 2004; Zhang *et al.*, 2006a; Liu *et al.*, 2007). Evidently, the sensitivity of ACCs to haloxyfop lies on a continuum, making it difficult to classify the ACC of any one organism as either “sensitive” or “resistant”.

Treatment of PF and BF parasites with haloxyfop concentrations up to 250 μM had a minimal effect on parasite growth and doubling time (Fig. 3.3A-B, D-E). However, this effect was minor compared to the dramatic effect of higher haloxyfop concentrations on PF and BF parasite growth over 48 h (Fig. 3.3C, F). BF parasites were slightly more sensitive to haloxyfop treatment than PF parasites. However, both PF and BF *T. brucei* were remarkably less sensitive to haloxyfop than *T. gondii* (EC_{50} ~100 μM) (Zuther *et al.*, 1999). We have previously demonstrated through RNAi experiments that TbACC is largely expendable in BF parasites *in vitro* and is only required when PF parasites are cultured in low-lipid media (Vigueira *et al.*, 2011). Thus, we contend that inhibition of TbACC by haloxyfop should have little to no consequence on the growth rate of the parasite *in vitro*. Consequently, the reduction in growth we observed with

haloxyfop concentrations >250 μM can be attributed to off-target effects rather than inhibition of TbACC.

Our previous work demonstrated that reduction of TbACC by RNAi causes a robust reduction in elongation of fatty acids in PF parasites (Vigueira *et al.*, 2011). Given that haloxyfop treatment inhibited TbACC activity in lysate, the inability of haloxyfop to affect FAS *in vivo* was unexpected (Fig. 3.4). Assessing the effect of haloxyfop concentrations >250 μM on fatty elongation *in vivo* was not feasible, because any observed effects could not be separated from those resulting from the profound effect of the compound on parasite growth due to likely off-target effects (Fig. 3.3C, F).

One possible explanation for this disparity between haloxyfop's effect in lysate and intact cells could be a compensatory increase in TbACC protein expression, a possibility that we ruled out (Fig. 3.5). It is also possible that incomplete inhibition of TbACC allowed available malonyl-CoA pools to remain high enough that ELO activity appeared unaffected. Alternatively, the apparent insensitivity of TbACC to haloxyfop in intact cells may be due to the fact that the compound does not efficiently enter the cell or is partitioned into a cellular compartment not accessible to TbACC. Haloxyfop's effect on growth at higher concentrations (Fig. 3.3C, F) does not negate poor membrane permeability as a possible explanation because haloxyfop could be acting at the cellular surface to cause a reduction in growth. Depolarization of the cellular membrane has been described in plants and is considered a secondary mechanism for the

graminicide activity of FOPs (Hausler *et al.*, 1991; Shimabukuro *et al.*, 1992; Ditomaso,1994; Holtum *et al.*, 1994; Wright,1994).

Another possible explanation is that haloxyfop is modified in intact *T. brucei*, rendering it unable to bind and inhibit TbACC. Because the haloxyfop binding pocket lies in a tight space on the face of the ACC protein dimer, any small modification of the compound could reduce the ability of haloxyfop to bind and inhibit enzymatic activity (Zhang *et al.*, 2003). Stereochemical inversion of haloxyfop has been observed previously in rats (Bartels *et al.*, 1989), however the inhibitory activity of the resulting enantiomer has not been determined.

In summary, we have demonstrated that haloxyfop inhibits TbACC *in vitro*, but has no detectable effect on *in vivo* lipid metabolism, suggesting that the toxicity of haloxyfop to *T. brucei* cannot be entirely attributed to TbACC inhibition. To our knowledge, this is the first report of potential off-target effects of this class of inhibitors in protozoan parasites. Furthermore, this study highlights the need for careful characterization of the mechanisms of action of small molecule inhibitors in lysates as well as in intact cells.

MATERIALS AND METHODS

Reagents

All chemicals and reagents were purchased from Thermo Fisher Scientific and Sigma, except: Serum Plus (JRH Biosciences) and streptavidin conjugated horseradish peroxidase (SA-HRP) (Pierce). Minimum Essential Medium, Iscove's Modified Dulbecco's Medium, and goat anti-mouse-HRP IgG antibody were from Invitrogen. [^{14}C]$NaHCO_3$ and ^{3}H-labeled fatty acids were from American Radiolabeled Chemicals. Silica Gel 60 and C18 reverse phase thin layer chromatography (TLC) plates were from Analtech. The mouse anti-tubulin antibody (clone B-5-1-2) was from Sigma. Clodinafop (CAS-No: 105512-06-9), haloxyfop (CAS-No: 74051-80-2), quizalifop (CAS-No: 94051-08-8) and sethoxydim (CAS-No: 74051-80-2) were from Sigma. Fluazifop (CAS-No: 69335-91-7) was from Wako.

Trypanosome strains and media

Wild-type (WT) strain 427 PF and BF *T. brucei* were provided by Dr. Paul Englund (Johns Hopkins School of Medicine). BF parasites were grown in HMI-9 medium (Hirumi *et al.*, 1989) containing 10% heat-inactivated FBS/10% Serum Plus. PF parasites were grown in SDM-79 medium (Brun *et al.*, 1979) containing 10% heat inactivated FBS.

ACC enzyme activity

To assay ACC activity, we modified a biotin carboxylase assay described previously (Wurtele *et al.*, 1990; Vigueira *et al.*, 2011). Inhibitors were prepared in

filter-sterilized dimethyl sulfoxide (DMSO) and used as 100X stocks. Lysates were incubated with inhibitors for 30 min on ice prior to the addition of reaction components. The final reaction volume of 100 µl contained 5 mM ATP, 1 mM acetyl-CoA, 1% v/v DMSO and 5 mM [^{14}C]$NaHCO_3$ (14.9 mCi/mmol), and was incubated for 30 min at 30°C with constant mixing at 500 RPM. A 50 µl sample of acid-precipitated [^{14}C]malonyl-CoA product was collected on Whatman #1 filters, air-dried, and quantified by scintillation counting.

Growth experiments

For growth curves, WT cells were diluted into fresh media containing inhibitors or DMSO solvent control and cell density was monitored every 48 h for up to 10 days using a FACScan flow cytometer (Becton Dickinson). Inhibitors were prepared in filter-sterilized DMSO and used as 100X stocks, resulting in final DMSO concentration of 1% v/v. Following each cell count, cultures were diluted to maintain logarithmic phase growth, and inhibitors or DMSO was added to maintain experimental concentrations.

Metabolic labeling and lipid analysis

Metabolic labeling was performed essentially as described (Paul *et al.*, 2004; Vigueira *et al.*, 2011). Briefly, after 4 days of haloxyfop treatment, ~1 x 10^8 PF cells were labeled with 25 µCi of [11,12-^{3}H]laurate (C12:0; 60 mCi/mmol) for 2 h in a 28°C CO_2 incubator. Total lipids were extracted in chloroform/methanol/water (10:10:3 v/v/v) and equal CPMs/lane were analyzed by normal phase TLC using chloroform/methanol/water (10:10:3 v/v/v) as the

mobile phase. Labeled lipid species were identified based on known migration patterns in this TLC system (Doering *et al.*, 1993). To analyze the fatty acids by chain length, total lipid extracts were converted to fatty acid methyl esters (FAMEs), extracted in hexane, and equal CPMs/lane were analyzed by C18 reverse-phase TLC using chloroform/methanol/water (5:15:3 v/v/v) as the mobile phase. TLCs were sprayed with En3Hance (Perkin-Elmer) and exposed to x-ray film at -80°C. For chain length markers, FAMEs were prepared in parallel from 30 µCi of [^{3}H]fatty acids: [11,12-^{3}H]laurate (C12; 60 mCi/mmol), [9,10-^{3}H]myristate (C14; 60 mCi/mmol), [9,10-^{3}H(N)]palmitate (C16; 60 mCi/mmol), and [9,10-^{3}H]stearate (C18; 60 mCi/mmol).

Streptavidin blotting

Streptavidin blotting can detect the biotin prosthetic group on ACC and was performed essentially as described (Vigueira *et al.*, 2011). Briefly, PF parasites were treated for 4 days with haloxyfop. 20 µg of whole cell lysate were fractionated on 8% SDS-PAGE gels and transferred to nitrocellulose. The blot was cut, and the top half was probed for ACC with SA-HRP (1:400 in 0.2% dry milk, 1X Tris-buffered saline (TBS), 0.05% Tween-20). The bottom was probed with a mouse anti-tubulin (clone B-5-1-2), diluted 1:50,000 in Wash Buffer (5% dry milk, 1X TBS, 0.05% Tween-20) followed by HRP-conjugated goat anti-mouse IgG secondary antibody diluted 1:10,000 in Wash Buffer. Semi-quantitative analysis of blots was performed using densitometry (NIH Image J

software) of appropriately exposed films (unsaturated signal within the linear range of the film).

Statistics

One-tailed Student's t-test analyses between control and treatments were performed using Microsoft Excel. We judged statistical significance to be $p < 0.01$. Error bars represent standard deviation from the mean.

Genetic sequence acquisition

ACC protein sequences were acquired from the genetic sequence database at the National Center for Biotechnical Information. The accession numbers for each sequence are listed: *Trypanosoma brucei* (GenBank ID: XM_842447), *Saccharomyces cerevisiae* (GenBank ID: NM_001183193), *Homo sapiens* ACC1 (GenBank ID: U19822), *Homo sapiens* ACC2 (GenBank ID: U89344), *Rattus norvegicus* (GenBank ID: J03808), *Toxoplasma gondii* (GenBank ID: AF157612), *Lolium rigidum* (GenBank ID: AY995232), *Zea mays* (GenBank ID: U19183), and *Alopecurus myosuroides* (GenBank ID: AJ310767).

ACKNOWLEDGEMENTS

This work was supported in part by the National Institutes of Health 1R15AI081207 (K.P.) and Clemson University Funds (K.P.). We thank members of the Clemson University Parasite Club for their helpful suggestions. We also thank Marianne Ligon, Ben Martin, and Ciara McKnight for experimental assistance and Jim Morris for critical reading of the manuscript.

FIGURES

Figure 3.1: Effect of FOP and DIM herbicides on TbACC activity in PF lysate. ACC activity in PF cell lysates was measured after a 30 min incubation with 20-400 μM clodinafop (A), fluazifop (B), quizalifop (C), sethoxydim (D), or haloxyfop (E). Values are expressed as a percentage of the DMSO control. DMSO concentrations were maintained at 1% v/v for all conditions. The mean of 3 experiments is shown. Error bars indicate the SD. The * indicates $p < 0.01$ for the difference between DMSO control and herbicide-treated conditions, Student's t-test.

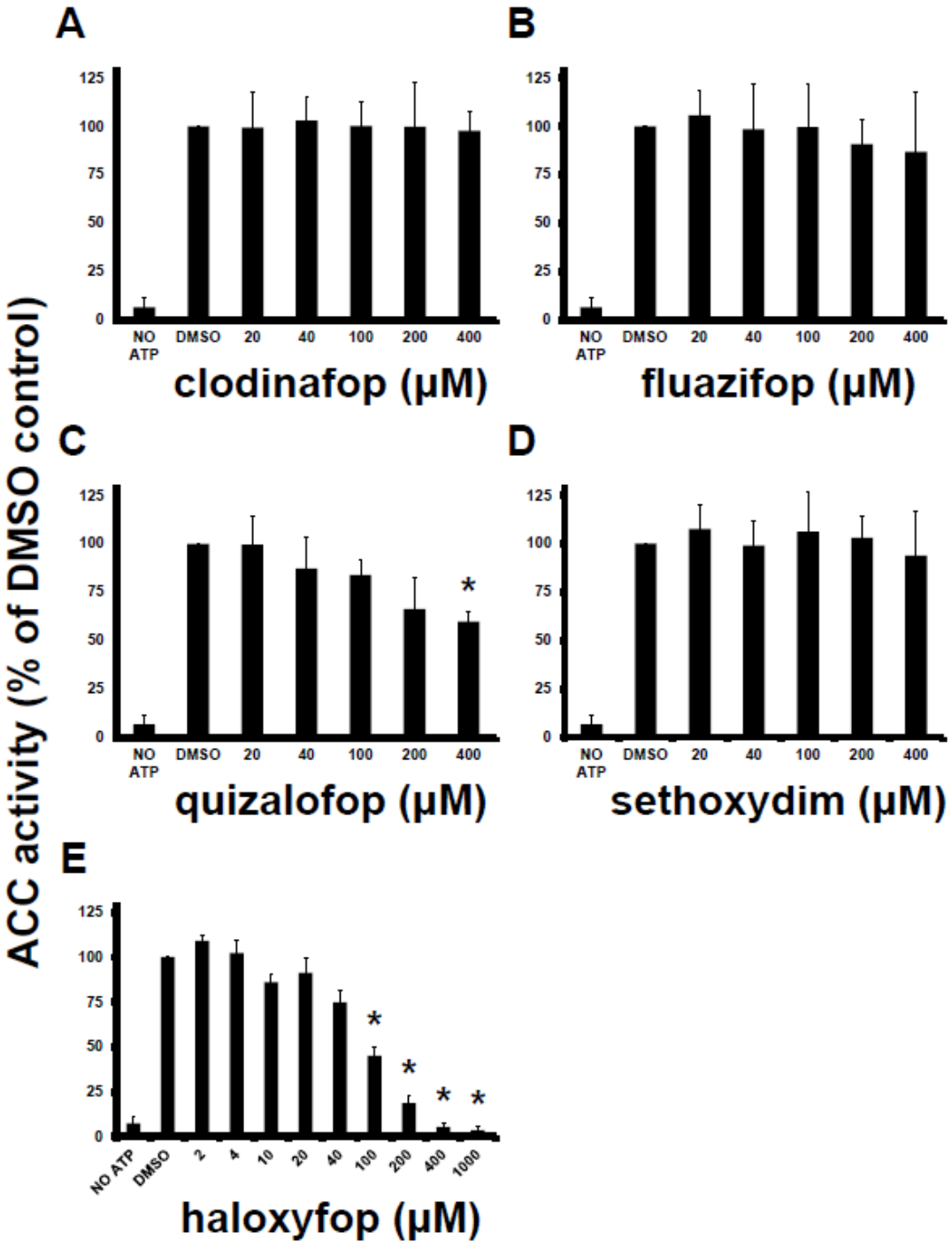
A
B
C
D
E
ACC activity (% of DMSO control)
125
100
75
50
25
0
NO ATP
DMSO
20
40
100
200
400
clodinafop (μM)
fluazifop (μM)
quizalofop (μM)
sethoxydim (μM)
*
2
4
10
1000
haloxyfop (μM)

Figure 3.2: Alignment of multidomain ACC amino acid sequences surrounding the resistance-conferring residues in the CT domain. The organism and ACC protein resistance status are indicated in the far left column (sensitive (S), moderately sensitive (MS), resistant (R)). The resistance-conferring residues, equivalent to *S. cerevisiae* L1705 and V1967, are highlighted and the highlighted numbers represent the equivalent amino acid positions in each sequence. Dashes indicate residues identical to those in *T. brucei*. Accession numbers are provided in the far right column. The *L. rigidum* sequence is a partial cDNA sequence, thus the highlighted numbers refer to the amino acid positions in the partial gene product.

ORGANISIM					ACCESSION No.
T. brucei	(MS)	LGVENLRGSGL	1650	DMFEEVLKFGA 1912	[Tb927.8.7100]
S. cerevisiae	(R)	----CL-----	1705	---N-V--Y-S 1967	[NM_001183193.1]
H. sapiens ACC1	(R)	I-P--L----M	1797	--YHQV----- 2060	[U19822]
H. sapiens ACC2	(R)	-----L----M	1933	--YDQV----- 2196	[U89344]
R. norvegicus	(MS)	--A--L----M	1793	--YDQV----- 2059	[J03808]
T. gondii ACC1	(MS)	I----L----T	2093	-----I----S 2357	[AF157612]
L. rigidum	(S)	-----IH--AA	176	-L-XGI-QA-S 436	[AY995232.1]
Z. mays	(S)	-----IH--AA	1784	-L--GI-QA-S 2044	[U19183]
A. myosuroides	(S)	-----IH--AA	1830	-L--GI-QA-S 2090	[AJ310767.1]

Figure 3.3: Effect of haloxyfop on *in vitro* growth of *T. brucei*. A,B,D,E. WT PF (A,B) and BF (D,E) cells were diluted into media containing 5–250 μM haloxyfop or DMSO control, and the cell densities of the cultures were recorded every other day for 8 days. Cumulative culture density is shown in A and D, and culture doubling times are shown in B and E. **C,F.** WT PF (C) and BF cells (F) were diluted into media containing 250 μM–2 mM haloxyfop or DMSO control, and the cell densities of the culture were determined after 48 h. Values are expressed as a percentage of DMSO control. For all panels, the mean of three replicates is shown. Error bars show SD. The * indicates $p < 0.01$ for the difference between DMSO and haloxyfop-treated conditions, Student's t-test.

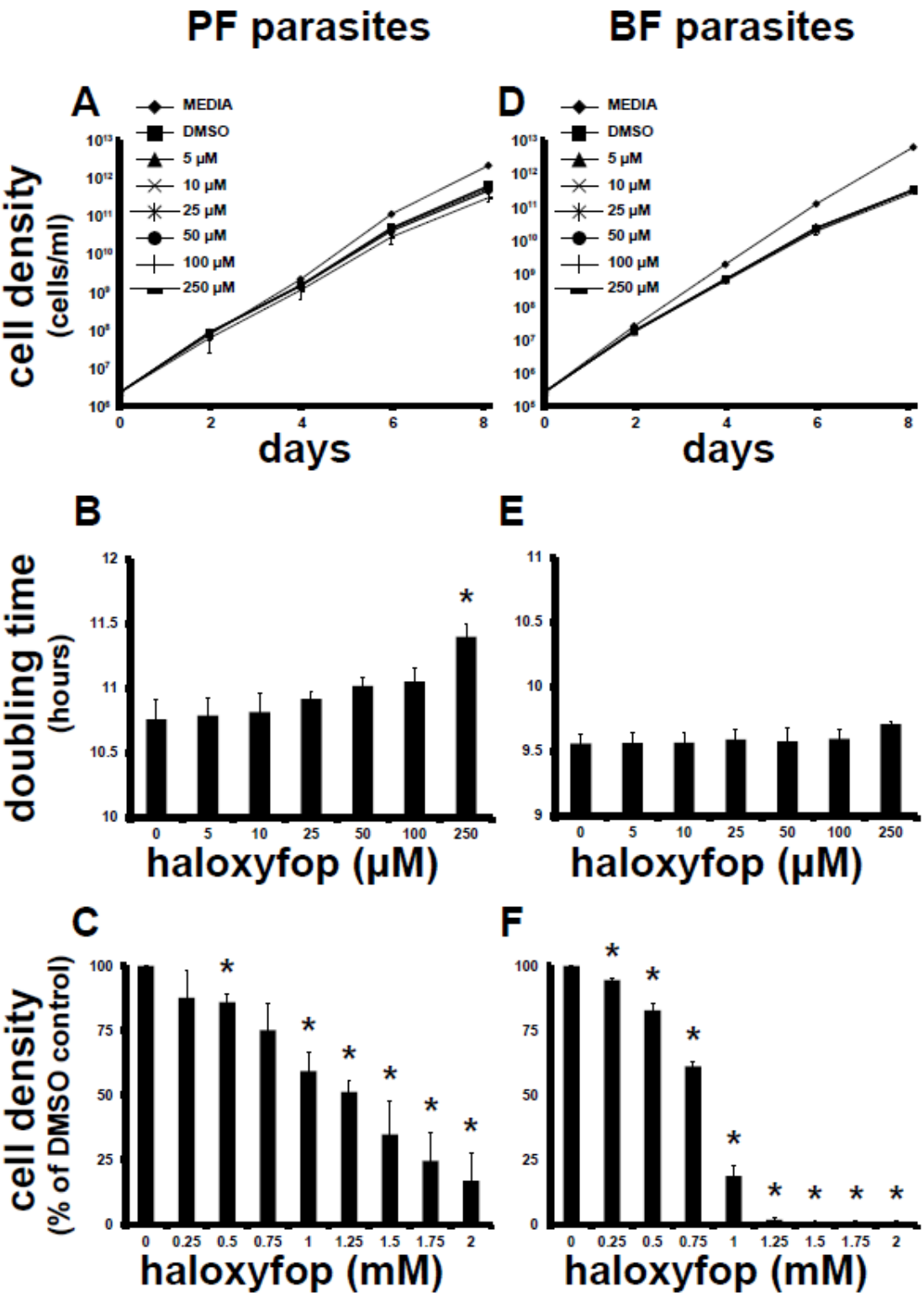
PF parasites
BF parasites
A
D
MEDIA
DMSO
5 µM
10 µM
25 µM
50 µM
100 µM
250 µM
cell density
(cells/ml)
days
B
E
doubling time
(hours)
haloxyfop (µM)
C
F
cell density
(% of DMSO control)
haloxyfop (mM)

Figure 3.4: Fatty acid incorporation and elongation in the presence of haloxyfop. WT PF cells were grown for 4 days in the presence of haloxyfop or DMSO. Cells were then incubated with 25 µCi of [^{3}H]laurate (C12) for 2 h. **A.** Total lipids were extracted and equal CPMs per lane were resolved by TLC. The origin (O) and relative migration of neutral lipids (NL), free fatty acids (FFA), and phospholipids (PL) are indicated on the right. Treatment conditions are indicated at the top. **B.** Fatty acid chain length analysis of FAMEs prepared from the total lipid extracts in (A). Equal CPMs per lane were resolved by C18 reverse-phase high-performance TLC. The origin (O) and markers for C12, C14, C16 and C18 FAMEs are indicated at the right. Treatment conditions are indicated at the top. A representative of two independent experiments is shown.

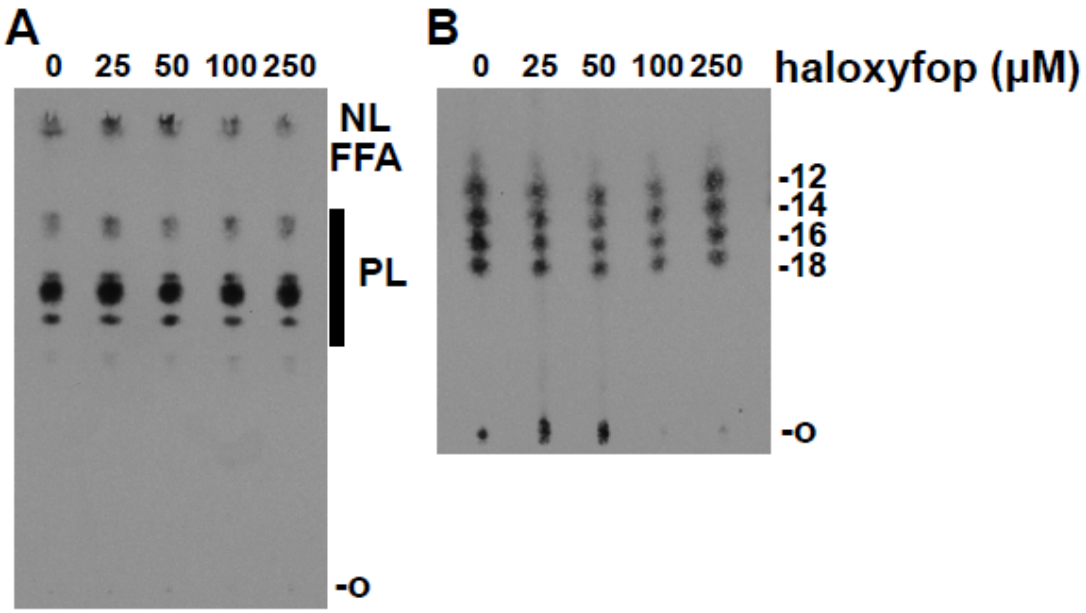

Figure 3.5: Effect of haloxyfop treatment on ACC protein levels. WT PF cells were grown for 4 days in the presence of 25–250 μM haloxyfop or DMSO. **A.** Total hypotonic lysates (20 μg protein) were probed for ACC by SA-HRP blotting, which recognizes the ACC biotin prosthetic group. The lower half of the blot was probed for tubulin as a loading control. Treatment conditions are indicated at the top. One representative of three independent blots is shown. **B.** Densitometric quantitation of ACC protein levels normalized to the α-tubulin loading control. Values are expressed as a percentage of the DMSO control. The mean of 3 independent replicates is shown. Error bars indicate the SD. No significant difference was observed between DMSO and haloxyfop-treated conditions ($p > 0.01$, Student's t-test).

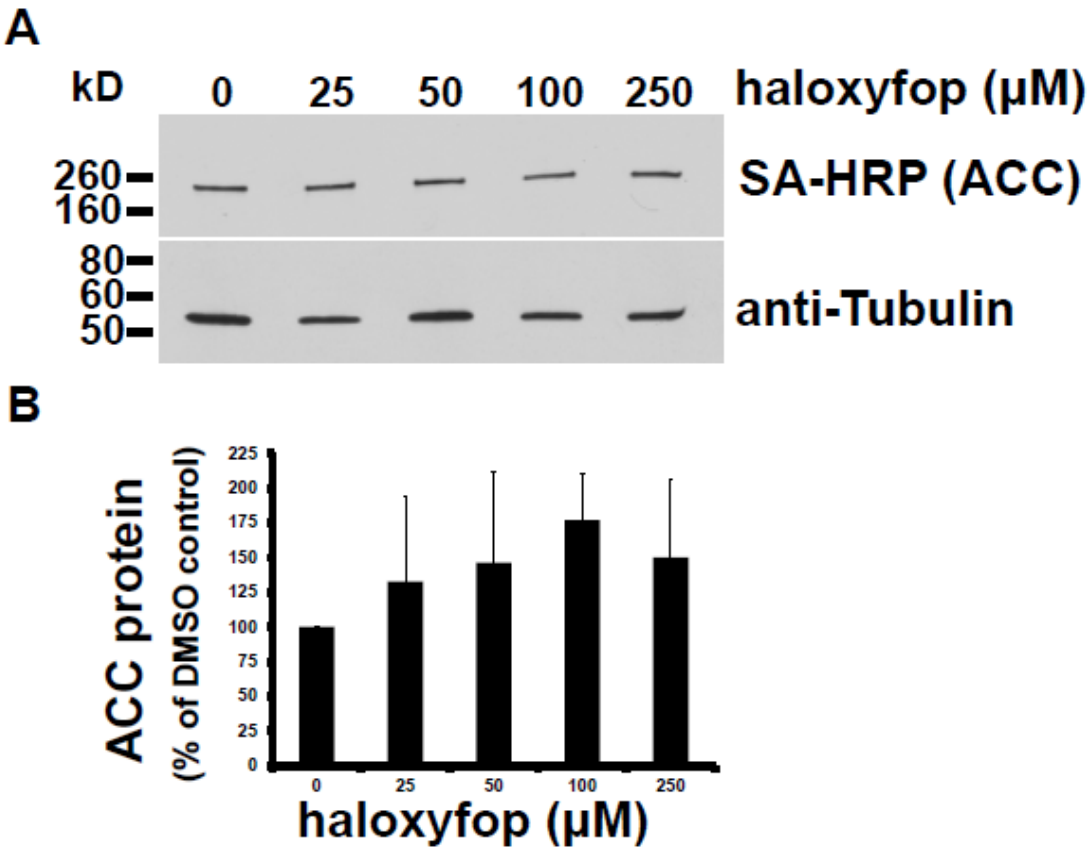
A
kD
0
25
50
100
250
haloxyfop (μM)
260
160
SA-HRP (ACC)
80
60
50
anti-Tubulin
B
ACC protein
(% of DMSO control)
225
200
175
150
125
100
75
50
25
0
0
25
50
100
250
haloxyfop (μM)

REFERENCES

Bartels M.J., and Smith F.A. (1989) Stereochemical inversion of haloxyfop in the fischer 344 rat. *Drug Metab Dispos* **17:** 286-291.

Brown A.C., Moss S.R., Wilson Z.A., and Field L.M. (2002) An isoleucine to leucine substitution in the ACCase of *Alopecurus myosuroides* (black-grass) is associated with resistance to the herbicide sethoxydim. *Pestic Biochem Physiol* **72:** 160-168.

Brun R., and Schonenberger M. (1979) Cultivation and *in vitro* cloning of procyclic culture forms of trypanosoma-brucei in a semi-defined medium. *Acta Trop* **36:** 289-292.

Burri C. (2010) Chemotherapy against human African trypanosomiasis: Is there a road to success? *Parasitology* **137:** 1987-1994.

Christoffers M.J., Berg M.L., and Messersmith C.G. (2002) An isoleucine to leucine mutation in acetyl-CoA carboxylase confers herbicide resistance in wild oat. *Genome* **45:** 1049-1056.

De Prado R., Gonzalez-Gutierrez J., Menendez J., Gasquez J., Gronwald J.W., and Gimenez-Espinosa R. (2000) Resistance to acetyl CoA carboxylase-inhibiting herbicides in *Lolium multiflorum*. *Weed Sci* **48:** 311-318.

Delye C., Zhang X.Q., Chalopin C., Michel S., and Powles S.B. (2003) An isoleucine residue within the carboxyl-transferase domain of multidomain acetyl-coenzyme A carboxylase is a major determinant of sensitivity to aryloxyphenoxypropionate but not to cyclohexanedione inhibitors. *Plant Physiol* **132:** 1716-1723.

Ditomaso J.M. (1994) Evidence against a direct membrane effect in the mechanism of action of graminicides. *Weed Sci* **42:** 302-309.

Doering T.L., Pessin M.S., Hoff E.F., Hart G.W., Raben D.M., and Englund P.T. (1993) Trypanosome metabolism of myristate, the fatty acid required for the variant surface glycoprotein membrane anchor. *J.Biol.Chem.* **268:** 9215-9222.

FAO, Food and Agricultural Organization of the United Nations. (2007) Ethiopian fly factory guns for "poverty insect".

Haneji T., and Koide S.S. (1989) Transblot identification of biotin-containing proteins in rat liver. *Anal Biochem* **177:** 57-61.

Hausler R.E., Holtum J.A., and Powles S.B. (1991) Cross-resistance to herbicides in annual ryegrass (*Lolium rigidum)*: IV. correlation between membrane effects and resistance to graminicides. *Plant Physiol* **97:** 1035-1043.

Hirumi H., and Hirumi K. (1989) Continuous cultivation of *Trypanosoma brucei* blood stream forms in a medium containing a low concentration of serum protein without feeder cell layers. *J.Parasitol.* **75:** 985-989.

Holtum J.A.M., Hausler R.E., Devine M.D., and Powles S.B. (1994) Recovery of transmembrane potentials in plants resistant to aryloxyphenoxypropanoate herbicides - a phenomenon awaiting explanation. *Weed Sci* **42:** 293-301.

Horn D., and McCulloch R. (2010) Molecular mechanisms underlying the control of antigenic variation in African trypanosomes. *Curr Opin Microbiol* **13:** 700-705.

Kemal C., and Casida J.E. (1992) Coenzyme A esters of 2-aryloxyphenoxypropionate herbicides and 2-arylpropionate antiinflammatory drugs are potent and stereoselective inhibitors of rat liver acetyl-CoA carboxylase. *Life Sci* **50:** 533-540.

Lee S.H., Stephens J.L., and Englund P.T. (2007) A fatty-acid synthesis mechanism specialized for parasitism. *Nat Rev Microbiol* **5:** 287-297.

Lee S.H., Stephens J.L., Paul K.S., and Englund P.T. (2006) Fatty acid synthesis by elongases in trypanosomes. *Cell* **126:** 691-699.

Liu W., Harrison D.K., Chalupska D., Gornicki P., O'donnell C.C., Adkins S.W.*, et al.* (2007) Single-site mutations in the carboxyltransferase domain of plastid acetyl-CoA carboxylase confer resistance to grass-specific herbicides. *Proc Natl Acad Sci U S A* **104:** 3627-3632.

Nikolau B.J., Wurtele E.S., and Stumpf P.K. (1985) Use of streptavidin to detect biotin-containing proteins in plants. *Anal Biochem* **149:** 448-453.

Paul K.S., Bacchi C.J., and Englund P.T. (2004) Multiple triclosan targets in *Trypanosoma brucei*. *Eukaryot Cell* **3:** 855-861.

Roberts C.W., McLeod R., Rice D.W., Ginger M., Chance M.L., and Goad L.J. (2003) Fatty acid and sterol metabolism: Potential antimicrobial targets in apicomplexan and trypanosomatid parasitic protozoa. *Mol Biochem Parasitol* **126:** 129-142.

Secor J., and Cseke C. (1988) Inhibition of acetyl-CoA carboxylase activity by haloxyfop and tralkoxydim. *Plant Physiol* **86:** 10-12.

Sharlow E.R., Lyda T.A., Dodson H.C., Mustata G., Morris M.T., Leimgruber S.S.*, et al.* (2010) A target-based high throughput screen yields *Trypanosoma brucei* hexokinase small molecule inhibitors with antiparasitic activity. *PLoS Negl Trop Dis* **4:** e659.

Shimabukuro R.H., and Hoffer B.L. (1992) Effect of diclofop on the membrane potentials of herbicide-resistant and -susceptible annual ryegrass root tips. *Plant Physiol* **98:** 1415-1422.

Singh A.P., Surolia N., and Surolia A. (2009) Triclosan inhibit the growth of the late liver-stage of plasmodium. *IUBMB Life* **61:** 923-928.

Surolia N., and Surolia A. (2001) Triclosan offers protection against blood stages of malaria by inhibiting enoyl-ACP reductase of *Plasmodium falciparum*. *Nat Med* **7:** 167-173.

Vigueira P.A., and Paul K.S. (2011) Requirement for acetyl-CoA carboxylase in *Trypanosoma brucei* is dependent upon the growth environment. *Mol Microbiol* **80:** 117-132.

White G.M., Moss S.R., and Karp A. (2005) Differences in the molecular basis of resistance to the cyclohexanedione herbicide sethoxydim in *Lolium multiflorum. Weed Res* **45:** 440-448.

WHO W.H.O. (2010) WHO fact sheet on African trypanosomiasis.

Wright J.P. (1994) Use of membrane-potential measurements to study mode action of diclofop-methyl. *Weed Sci* **42:** 285-292.

Wurtele E.S., and Nikolau B.J. (1990) Plants contain multiple biotin enzymes: Discovery of 3-methylcrotonyl-CoA carboxylase, propionyl-CoA carboxylase and pyruvate carboxylase in the plant kingdom. *Arch Biochem Biophys* **278:** 179-86.

Xiang S., Callaghan M.M., Watson K.G., and Tong L. (2009) A different mechanism for the inhibition of the carboxyltransferase domain of acetyl-coenzyme A carboxylase by tepraloxydim. *Proc Natl Acad Sci U S A* **106:** 20723-20727.

Zagnitko O., Jelenska J., Tevzadze G., Haselkorn R., and Gornicki P. (2001) An isoleucine/leucine residue in the carboxyltransferase domain of acetyl-CoA carboxylase is critical for interaction with aryloxyphenoxypropionate and cyclohexanedione inhibitors. *Proc Natl Acad Sci U S A* **98:** 6617-6622.

Zhang H., Tweel B., and Tong L. (2004) Molecular basis for the inhibition of the carboxyltransferase domain of acetyl-coenzyme-A carboxylase by haloxyfop and diclofop. *Proc Natl Acad Sci U S A* **101:** 5910-5915.

Zhang H., Yang Z., Shen Y., and Tong L. (2003) Crystal structure of the carboxyltransferase domain of acetyl-coenzyme A carboxylase. *Science* **299:** 2064-7.

Zhang X.Q., and Powles S.B. (2006a) Six amino acid substitutions in the carboxyl-transferase domain of the plastidic acetyl-CoA carboxylase gene are linked with resistance to herbicides in a *Lolium rigidum* population. *New Phytol* **172:** 636-645.

Zhang X.Q., and Powles S.B. (2006b) The molecular bases for resistance to acetyl co-enzyme A carboxylase (ACCase) inhibiting herbicides in two target-based resistant biotypes of annual ryegrass (*Lolium rigidum*). *Planta* **223:** 550-557.

Zuther E., Johnson J.J., Haselkorn R., McLeod R., and Gornicki P. (1999) Growth of *Toxoplasma gondii* is inhibited by aryloxyphenoxypropionate herbicides targeting acetyl-CoA carboxylase. *Proc Natl Acad Sci U S A* **96:** 13387-92.

CHAPTER 4

EFFECTS OF THE GREEN TEA CATECHIN EGCG ON *Trypanosoma brucei*

Patrick A. Vigueira, Ben A. Martin and Kimberly S. Paul

Department of Biological Sciences, Clemson University, Clemson, SC

ABSTRACT

Trypanosoma brucei, a eukaryotic pathogen that causes African sleeping sickness in humans and nagana in cattle, depends on the enzyme acetyl-CoA carboxylase (ACC) for full virulence in mice. ACC catalyzes the reaction that produces malonyl-CoA, the two carbon donor for fatty acid synthesis. We assessed the effect of the green tea catechin (−)-epigallocatechin-3-gallate (EGCG) on *T. brucei* ACC activity and growth in culture. EGCG inhibited TbACC in cell lysate (EC_{50} 55 μM). However, inhibition of TbACC by EGCG was dependent upon the presence of phosphatase inhibitors in the cell lysate. EGCG also reduced growth of bloodstream (BF) and procyclic form parasites at supraphysiological concentrations (EC_{50} of 33 μM and 27 μM), but BF growth was unaffected at physiologically relevant concentrations (<0.1 μM). Additionally, EGCG treatment did not affect *T. brucei* virulence in a mouse model.

RESULTS AND DISCUSSION

The protozoan parasite *Trypanosoma brucei* is the causative agent of African sleeping sickness, a fatal human disease that ranges across sub-Saharan Africa. In addition to causing substantial morbidity and mortality in humans, *T. brucei* is responsible for causing nagana, a livestock disease that results in wasting and death. Nagana imposes a tremendous economic burden on the region, causing 4.5 billion dollars in economic losses each year (FAO, Food and Agricultural Organization of the United Nations,2007). Vaccine development is confounded by the parasite's ability to switch its surface coat through antigenic variation (Horn *et al.*, 2010). Thus, chemotherapeutics are relied upon to battle to the disease, yet currently approved drugs cause undesirable side effects and can be too expensive for citizens of economically depressed regions (Castillo *et al.*, 2010). To meet this urgent need, investigations of existing compounds are an important avenue to identify potential new drugs that are effective, safe, and economical.

Green tea is among the most widely consumed beverages worldwide and is often touted for its wealth of medicinal effects (Moon *et al.*, 2007a; Khan *et al.*, 2008; Thielecke *et al.*, 2009; Ahmed,2010). The best studied active component of green tea is the catechin (−)-epigallocatechin-3-gallate (EGCG). While EGCG likely impacts a number of cellular pathways, it has been demonstrated to inhibit fatty acid synthesis (FAS) (Wang *et al.*, 2001; Brusselmans *et al.*, 2003; Huang *et al.*, 2009), through its effect on the regulation of acetyl-CoA carboxylase (ACC)

(Huang *et al.*, 2009). ACC catalyzes the first committed step in FAS, the ATP-dependent carboxylation of acetyl-CoA, which provides the two-carbon donor, malonyl-CoA, for FAS (Lee *et al.*, 2008). ACC is negatively regulated by phosphorylation by AMP-activated protein kinase (AMPK), a key regulator of cellular energy metabolism (Barber *et al.*, 2005; Brownsey *et al.*, 2006). EGCG treatment leads to increased phosphorylation of human ACC, resulting in its inhibition (Moon *et al.*, 2007b; Huang *et al.*, 2009).

In *T. brucei*, both the cytoplasmic and mitochondrial FAS pathways are important for parasite growth in culture and virulence in mouse models (Lee *et al.*, 2006; Stephens *et al.*, 2007; Vigueira *et al.*, 2011). In addition, we have demonstrated recently that RNA interference (RNAi)-mediated gene knockdown of ACC in *T. brucei* reduced fatty acid elongation activity in intact cells and nearly doubled the mean time until death in a mouse model of infection (Vigueira *et al.*, 2011). Taken together, these results suggest that fatty acid synthesis has the potential to be an effective drug target in *T. brucei*.

Here, we investigated whether EGCG could be used to target ACC and fatty acid synthesis in *T. brucei*. First, we tested EGCG for its ability to inhibit TbACC enzymatic activity in insect midgut stage, procyclic form (PF) lysate. TbACC activity is assayed in desalted cell lysate by measuring the incorporation of the [^{14}C]CO_2 from [^{14}C]$NaHCO_3$ into the acid resistant [^{14}C]malonyl-CoA product, which is then quantified by scintillation counting (Vigueira *et al.*, 2011). To preserve any changes in phosphorylation caused by EGCG, we added HALT,

a broad spectrum phosphatase inhibitor, to the cell lysate. In the presence of HALT, EGCG inhibited TbACC enzymatic activity with an EC_{50} of 55 μM (Fig. 4.1). However, in the absence of HALT we observed no inhibition of TbACC by EGCG. These observations are consistent with the previously reported mode of action of EGCG, inhibition of ACC by increasing its phosphorylation (Moon *et al.*, 2007b; Huang *et al.*, 2009). We contend that HALT, by inhibiting the parasite's native phosphatases, preserved an EGCG-driven increase in ACC phosphorylation, resulting in decreased TbACC activity. We have made multiple attempts to quantify EGCG-induced TbACC phosphorylation, but to date we have been unsuccessful.

We next examined the effect of EGCG on *T. brucei* growth in culture. In humans, the maximum reported EGCG plasma concentration achievable through oral consumption of concentrated green tea catechins ranges from 0.3–1 μM (Yang *et al.*, 1998; Umegaki *et al.*, 2001; Sugisawa *et al.*, 2002; Unno *et al.*, 2005). A 6-day treatment of mammalian bloodstream form (BF) parasites at these physiological EGCG concentrations (0.1–1 μM) caused no change in BF parasite growth or doubling time (Fig. 4.2A,B). At supraphysiological EGCG concentrations, we observed a statically significant reduction in cell growth over 48 h (Fig 4.2C,D), with an EC_{50} of 33 μM and 27 μM for BF and PF parasites, respectively. These values are consistent with the trypanocidal activity of EGCG previously reported for *T. brucei rhodesiense* (IC_{50} 20.3 μM) (Tasdemir *et al.*, 2006). Based on our previous data showing that TbACC is largely expendable in

BF parasites *in vitro* and is only required when PF parasites are cultured in low-lipid media (Vigueira *et al.*, 2011), we contend that inhibition of TbACC by EGCG should have little consequence on *T. brucei* growth in culture. Thus, the reduction in growth observed with EGCG concentrations >5 μM could be attributed to off-target effects, rather than inhibition of TbACC.

Finally, we examined the effect of EGCG treatment on the course of *T. brucei* infection in mice. Although the EC_{50} values for EGCG for growth in culture are greater than the maximum reported plasma concentrations in orally-dosed humans, there were two reasons to justify testing EGCG in a mouse model of infection. First, *T. brucei* exhibited condition-specific essentiality in the case of both TbACC and enoyl-CoA reductase (EnCR); PF ACC and EnCR RNAi cell lines exhibited slowed growth only when exogenous lipids were limited (Lee *et al.*, 2006; Vigueira *et al.*, 2011). In addition, TbACC RNAi and TbEnCR conditional knockout mutants had attenuated virulence in mice (Vigueira *et al.*, 2011 and Soo Hee Lee, personal communication). Second, previous studies of EGCG in mice yielded promising results for treatment of trypanosomiasis. *Trypanosoma cruzi* mortality in mice and parasite growth in culture was reduced with EGCG treatment (Paveto *et al.*, 2004; Guida *et al.*, 2007). In addition, inflammation caused by *T. brucei* infection was reduced with oral green tea supplementation in a mouse model (Karori *et al.*, 2008). Taken together, these observations suggest that the parasite's sensitivity to EGCG could be higher *in vivo*.

To test the ability of EGCG to clear a *T. brucei* infection in mice, we administered daily IP injections of 4.13 mg/kg EGCG in sterile H_2O two days prior to infection and over the course of the trial. This EGCG concentration had been previously demonstrated to not cause mouse liver damage, (Guida *et al.*, 2007). After 2 days of EGCG pre-treatment, Swiss mice were infected with $1x10^5$ BF wild-type 427 parasites as previously described (Bacchi *et al.*, 2009), and time to death (or humane end-point) was determined. In this model, EGCG treatment had no effect on infection duration or mouse mortality. Mean time until death was ~3.5 days for both treatment and control groups (data not shown). Thus, although EGCG has trypanocidal activity at supraphysiological concentrations, the compound did not attenuate virulence in an acute infection mouse model. EGCG concentrations may not have been sufficiently high in the mouse bloodstream to affect the parasite. Alternatively, it is possible that the course of infection was too rapid to allow EGCG to exert its effects. If so, then a chronic infection model might be better suited to examine the efficacy of EGCG as a possible anti-trypanosomiasis therapy.

In summary, we found that TbACC is inhibited by EGCG *in vitro,* and this inhibition was dependent upon the presence of phosphatase inhibitors in the cell lysate. This suggests that EGCG could be a useful tool for studying the effects of phosphorylation on TbACC activity. We also demonstrated that EGCG kills both PF and BF parasites in culture. However, EGCG treatment did not affect *T. brucei* virulence in one mouse model of acute infection.

FIGURES

Fig. 4.1: Inhibition of TbACC Activity by EGCG. ACC activity in PF cell lysates was measured in the presence of 5-100 μM EGCG (Sigma) in the absence (Grey bars) or presence (Black bars) of HALT phosphatase inhibitor cocktail (Thermo-Pierce). EGCG was prepared in filter-sterilized dimethyl sulfoxide (DMSO) and used as a 100X stock. HALT was added as a 100X stock per the manufacturer's instructions. The final reaction volume of 100 μL contained 5 mM ATP, 1 mM acetyl-CoA, 1% v/v DMSO and 5 mM [^{14}C]$NaHCO_3$ (14.9 mCi/mmol) and was incubated for 30 min at 30°C, mixing at 500 RPM. 6N HCl (50 μL) was added to terminate the reaction, and 50 μL of the acid-precipitated [^{14}C]malonyl-CoA product was collected on Whatman #1 filters, air-dried, and quantified by scintillation counting. Values are expressed as a percentage of the DMSO control. DMSO concentrations were maintained at 1% v/v for all conditions. The mean of 3 experiments is shown. Error bars indicate the SD. The * indicates $p < 0.01$ for the difference between DMSO control and EGCG-treated conditions (Student's t-test).

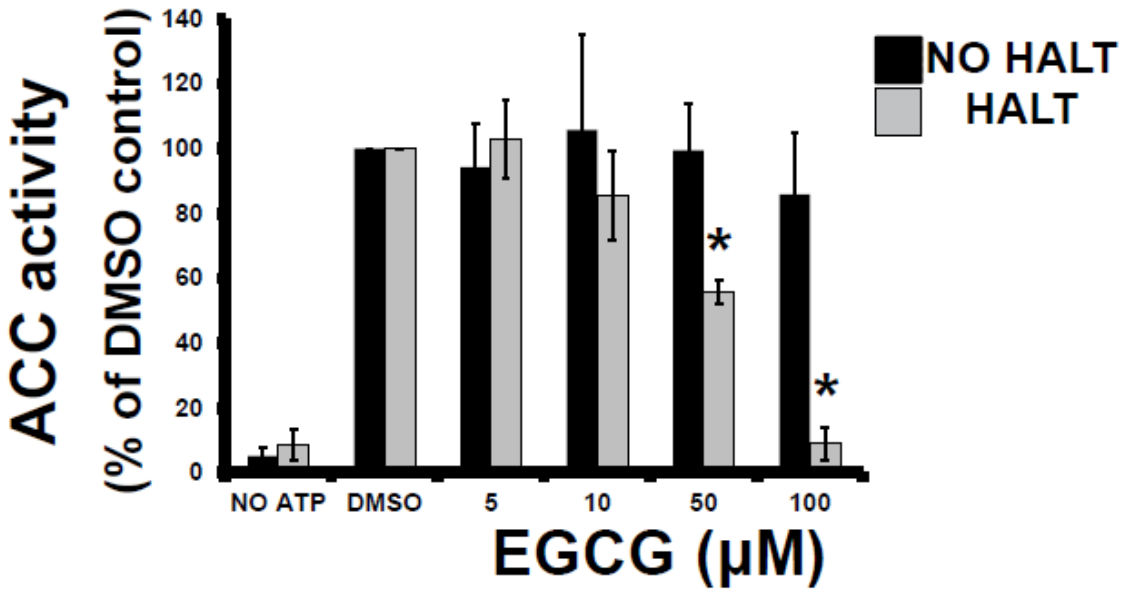
ACC activity
(% of DMSO control)
140
120
100
80
60
40
20
0
NO ATP
DMSO
5
10
50
100
EGCG (μM)
NO HALT
HALT
*
*

Fig. 4.2: Effect of EGCG on *in vitro* growth of *T. brucei*. A and B. WT BF cells were diluted into HMI-9 media (Hirumi *et al.*, 1989) containing 0.1-1 μM EGCG or DMSO as the solvent control, and the culture cell densities were monitored for 6 days. Following each cell count, cultures were diluted to maintain logarithmic phase growth, and EGCG/DMSO was added to maintain experimental concentrations. Cumulative culture densities are shown in A, and culture doubling times are shown in B. Please note in A, all points overlap and error bars are too small to be visible. **C and D** WT BF (C) and PF cells (D) were diluted into HMI-9 or SDM-79 media (Brun *et al.*, 1979) containing 5–50μM EGCG or DMSO control, and the culture cell densities were determined after 48 h. Values are expressed as a percentage of the DMSO control. For all panels, EGCG was prepared in filter-sterilized DMSO and used as a 100X stock. The mean of three replicates is shown. Error bars show SD. The * indicates $p < 0.01$ for the difference between DMSO and EGCG-treated conditions (Student's t-test).

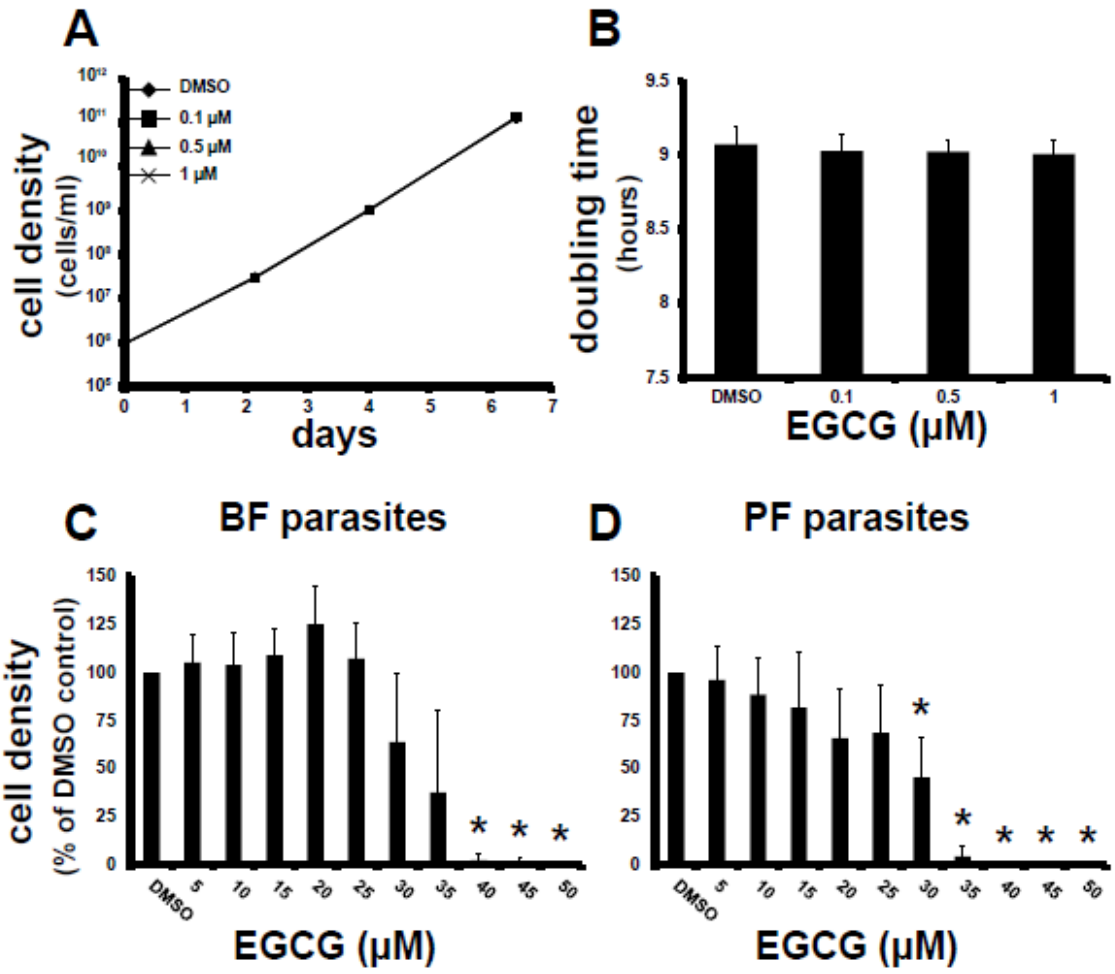
A
cell density
(cells/ml)
DMSO
0.1 µM
0.5 µM
1 µM
days
B
doubling time
(hours)
DMSO
0.1
0.5
1
EGCG (µM)
C
BF parasites
cell density
(% of DMSO control)
EGCG (µM)
D
PF parasites
EGCG (µM)

REFERENCES

Ahmed S. (2010) Green tea polyphenol epigallocatechin 3-gallate in arthritis: Progress and promise. *Arthritis Res Ther* **12:** 208.

Bacchi C.J., Barker R.H.,Jr, Rodriguez A., Hirth B., Rattendi D., Yarlett N.*, et al.* (2009) Trypanocidal activity of 8-methyl-5'-{[(Z)-4-aminobut-2-enyl]-(methylamino)}adenosine (genz-644131), an adenosylmethionine decarboxylase inhibitor. *Antimicrob Agents Chemother* **53:** 3269-3272.

Barber M.C., Price N.T., and Travers M.T. (2005) Structure and regulation of acetyl-CoA carboxylase genes of metazoa. *Biochim Biophys Acta* **1733:** 1-28.

Brownsey R.W., Boone A.N., Elliott J.E., Kulpa J.E., and Lee W.M. (2006) Regulation of acetyl-CoA carboxylase. *Biochem Soc Trans* **34:** 223-7.

Brun R., and Shonenberger M. (1979) Cultivation and *in vitro* cloning of procyclic culture forms of *Trypanosoma brucei* in a semi-defined medium. *Acta Tropica* **36:** 289-292.

Brusselmans K., De Schrijver E., Heyns W., Verhoeven G., and Swinnen J.V. (2003) Epigallocatechin-3-gallate is a potent natural inhibitor of fatty acid synthase in intact cells and selectively induces apoptosis in prostate cancer cells. *Int J Cancer* **106:** 856-862.

Castillo E., Dea-Ayuela M.A., Bolas-Fernandez F., Rangel M., and Gonzalez-Rosende M.E. (2010) The kinetoplastid chemotherapy revisited: Current drugs, recent advances and future perspectives. *Curr Med Chem* **17:** 4027-4051.

FAO, Food and Agricultural Organization of the United Nations. (2007) Ethiopian fly factory guns for "poverty insect".

Guida M.C., Esteva M.I., Camino A., Flawia M.M., Torres H.N., and Paveto C. (2007) Trypanosoma cruzi: *in vitro* and *in vivo* antiproliferative effects of epigallocatechin gallate (EGCg). *Exp Parasitol* **117:** 188-194.

Hirumi H., and Hirumi K. (1989) Continuous cultivation of *Trypanosoma brucei* blood stream forms in a medium containing a low concentration of serum protein without feeder cell layers. *J.Parasitol.* **75:** 985-989.

Horn D., and McCulloch R. (2010) Molecular mechanisms underlying the control of antigenic variation in African trypanosomes. *Curr Opin Microbiol* **13:** 700-705.

Huang C.H., Tsai S.J., Wang Y.J., Pan M.H., Kao J.Y., and Way T.D. (2009) EGCG inhibits protein synthesis, lipogenesis, and cell cycle progression through activation of AMPK in p53 positive and negative human hepatoma cells. *Mol Nutr Food Res* **53:** 1156-1165.

Karori S.M., Ngure R.M., Wachira F.N., Wanyoko J.K., and Mwangi J.N. (2008) Different types of tea products attenuate inflammation induced in *Trypanosoma brucei* infected mice. *Parasitol Int* **57:** 325-333.

Khan N., and Mukhtar H. (2008) Multitargeted therapy of cancer by green tea polyphenols. *Cancer Lett* **269:** 269-280.

Lee C.K., Cheong H.K., Ryu K.S., Lee J.I., Lee W., Jeon Y.H., and Cheong C. (2008) Biotinoyl domain of human acetyl-CoA carboxylase: Structural insights into the carboxyl transfer mechanism. *Proteins* **72:** 613-24.

Lee S.H., Stephens J.L., Paul K.S., and Englund P.T. (2006) Fatty acid synthesis by elongases in trypanosomes. *Cell* **126:** 691-699.

Moon H.S., Lee H.G., Choi Y.J., Kim T.G., and Cho C.S. (2007a) Proposed mechanisms of (-)-epigallocatechin-3-gallate for anti-obesity. *Chem Biol Interact* **167:** 85-98.

Moon H.S., Chung C.S., Lee H.G., Kim T.G., Choi Y.J., and Cho C.S. (2007b) Inhibitory effect of (-)-epigallocatechin-3-gallate on lipid accumulation of 3T3-L1 cells. *Obesity (Silver Spring)* **15:** 2571-2582.

Paveto C., Guida M.C., Esteva M.I., Martino V., Coussio J., Flawia M.M., and Torres H.N. (2004) Anti-*trypanosoma cruzi* activity of green tea (*Camellia sinensis*) catechins. *Antimicrob Agents Chemother* **48:** 69-74.

Stephens J.L., Lee S.H., Paul K.S., and Englund P.T. (2007) Mitochondrial fatty acid synthesis in *Trypanosoma brucei*. *J Biol Chem* **282:** 4427-36.

Sugisawa A., and Umegaki K. (2002) Physiological concentrations of (-)-epigallocatechin-3-O-gallate (EGCg) prevent chromosomal damage induced by reactive oxygen species in WIL2-NS cells. *J Nutr* **132:** 1836-1839.

Tasdemir D., Kaiser M., Brun R., Yardley V., Schmidt T.J., Tosun F., and Ruedi P. (2006) Antitrypanosomal and antileishmanial activities of flavonoids and their analogues: *in vitro, in vivo*, structure-activity relationship, and quantitative structure-activity relationship studies. *Antimicrob Agents Chemother* **50:** 1352-1364.

Thielecke F., and Boschmann M. (2009) The potential role of green tea catechins in the prevention of the metabolic syndrome - a review. *Phytochemistry* **70:** 11-24.

Umegaki K., Sugisawa A., Yamada K., and Higuchi M. (2001) Analytical method of measuring tea catechins in human plasma by solid-phase extraction and HPLC with electrochemical detection. *J Nutr Sci Vitaminol (Tokyo)* **47:** 402-408.

Unno T., Sagesaka Y.M., and Kakuda T. (2005) Analysis of tea catechins in human plasma by high-performance liquid chromatography with solid-phase extraction. *J Agric Food Chem* **53:** 9885-9889.

Vigueira P.A., and Paul K.S. (2011) Requirement for acetyl-CoA carboxylase in *Trypanosoma brucei* is dependent upon the growth environment. *Mol Microbiol* **80:** 117-132.

Wang X., and Tian W. (2001) Green tea epigallocatechin gallate: A natural inhibitor of fatty-acid synthase. *Biochem Biophys Res Commun* **288:** 1200-1206.

Yang C.S., Chen L., Lee M.J., Balentine D., Kuo M.C., and Schantz S.P. (1998) Blood and urine levels of tea catechins after ingestion of different amounts of green tea by human volunteers. *Cancer Epidemiol Biomarkers Prev* **7:** 351-354.

CHAPTER FIVE

KNOCKDOWN OF *Trypanosoma brucei* ACYL-COA SYNTHETASE GENES BY RNA INTERFERENCE

Patrick A. Vigueira and Kimberly S. Paul

Department of Biological Sciences, Clemson University, Clemson, SC

INTRODUCTION

Acyl-CoA synthetases (ACS) are a class of enzymes that catalyze the thioesterification of free fatty acids (FA) to Coenzyme A (CoA). This process activates the fatty acids for use in metabolic processes (e.g., α/β-oxidation) and synthesis of phospholipids, cholesterol esters, ceramides and triglycerides (Watkins,1997; Soupene *et al.*, 2008; Li *et al.*, 2010). The irreversible, two-step ping-pong reaction occurs as follows. First, the FA is converted to an acyl-adenylate, forming AMP and PPi from ATP. Second, the reaction is completed by esterification of the acyl-adenylate intermediate to CoA through hydrolysis of PPi, forming the final fatty acyl-CoA product (Watkins,1997; Li *et al.*, 2010).

The human genome codes for five long chain ACS genes (ACSL). The enzymes' FA substrates include saturated and unsaturated species ranging from 14-24 carbons. Each ACSL has a unique hierarchy of substrate preferences. However, many of their substrates overlap, creating redundancy in enzymatic activity (Soupene *et al.*, 2008). Subcellular localization of the human ACSL1 and ACSL6 proteins are the best characterized. Both are located on the plasma membrane, and ACSL1 is tightly associated with fatty acid transport protein 1

(FATP1) in many cell types. The ACSL1/FATP1 interaction is believed to enhance FA uptake through vectorial acylation, the coordinated import and activation of FAs (Soupene *et al.*, 2008).

In addition to the annotated ACS genes, other proteins have been demonstrated to exhibit ACS activity. Mammalian FATP4 exhibits an intrinsic ACS activity and has been found to be involved in FA uptake. Despite being localized to the endoplasmic reticulum rather than the plasma membrane, expression of FATP4 was reported to correlate with increased fatty acid uptake. Increased fatty acyl-CoA retention is the proposed mechanism for this observation. While free FAs can diffuse across membranes and out of the cell, fatty acyl-CoAs are membrane impermeant and therefore cannot leave the cell by diffusion (Milger *et al.*, 2006).

The *Trypanosoma brucei* genome codes for 5 ACS genes based on homology to previously characterized genes for *Leishmania* ACS and yeast free fatty acid receptor 2. Each TbACS contains the characteristic ACS active site that controls FA binding and enzymatic specificity (Black *et al.*, 1997; Jiang *et al.*, 2000; Smith *et al.*, 2010). Sequence alignments of TbASC1-4 measured 46-95% similarity at the nucleotide level and 53-96% similarity at the protein level (Jiang *et al.*, 2000). The TbASC1-4 genes are organized in a tandem array on chromosome 9 and the TbACS5 gene resides on chromosome 10 (Jiang *et al.*, 2000; Aslett *et al.*, 2010). Northern blot analysis revealed that all TbACS1-4

genes are expressed in both bloodstream (BF) and procyclic (PF) form parasites (Jiang *et al.*, 2000).

Recombinant versions of the TbACS1-4 genes have been expressed, purified, and assayed for ACS enzymatic activity (Jiang *et al.*, 2001). TbACS1 had preferences for saturated FAs C11:0 to C14:0. TbACS2 had the highest specificity, working mainly on C10:0 and C11:0. TbACS3 and TbACS4 had a very similar substrate preference, not surprisingly because of their 95% sequence identity; they accommodated a broad range of substrates and exhibited high affinity for saturated fatty acids C14:0 to C17:0. The substrate preference of TbACS5 has been less extensively characterized, but early studies suggest it has the highest affinity for C14:0 (Smith *et al.*, 2010). TbACS1, TbACS3, and TbACS4 also exhibited high activity on a range of unsaturated FA substrates; however, TbACS2 activity was restricted to saturated fatty acids (Jiang *et al.*, 2001).

Here I present experiments that further the characterization of the TbACS genes. I investigated the collective functional role of the ACS genes in *T. brucei* FA uptake and growth. RNA interference (RNAi) of the TbACS genes in PF parasites had a profound effect on FA uptake and caused a minor reduction in parasite growth.

RESULTS

Generation of panTbACS RNAi cell line

Due to the high level of similarity among the TbACS genes, attempts to create an RNAi construct for single TbACS gene would likely be unsuccessful. Therefore, we elected to study the result of simultaneously knocking down all five of the currently-annotated TbACS genes. To do so, we chose a ~700-bp region with high homology among the TbACS genes. This region was amplified by PCR, cloned into the pZJM RNAi vector and stably transfected into PF parasites, creating a panTbACS RNAi cell line (Wang *et al.*, 2000).

Knockdown of TbACS reduced FA uptake

In order to determine the effect of panTbACS RNAi on *T. brucei* FA uptake, cells were incubated with C12:0 or C16:0 FAs conjugated to a non-polar green fluorescent fluorophore (4,4-difluoro-5,7-dimethyl-4-bora-3a,4a-diaza-*s*-indacene) (BODIPY), allowing FA uptake to be monitored by measuring cell-associated fluorescence. Upon induction of RNAi, BODIPY-C12:0 (B-C12) and BODIPY-C16:0 (B-C16) FA uptake was assayed at 48 h intervals (Fig. 5.1). Induction of RNAi for 2 days caused a 34% reduction in B-C12 uptake ($p < 0.05$) but had no effect on B-C16 uptake. B-C12 uptake was further reduced after 4 days of RNAi to almost half of the uninduced control (47% reduction, $p < 0.01$). This was accompanied by a 24% increase in B-C16 uptake ($p < 0.05$). By day 6 of RNAi induction, B-C12 uptake was reduced further (58% reduction, $p < 0.01$),

while B-C16 uptake was further increased by 48% relative to the uninduced control ($p < 0.01$).

Knockdown of TbACS reduced T. brucei growth.

RNAi of panTbACS caused only a small reduction in growth over 6 days of induction (Fig. 5.2A). This reduction in growth was most evident in a comparison of cumulative cell densities at the 6-day time point (30% reduction, $p < 0.01$) (Fig. 5.2B). Additionally, doubling time over the 6 days of panTbACS RNAi induction was increased by ~0.8 h ($p < 0.05$) (Fig. 5.2C).

DISCUSSION

Knockdown of the TbACS genes by RNAi caused a progressive reduction in uptake of B-C12 and a corresponding progressive increase in B-C16 uptake (Fig. 5.1). The former observation is likely due to reduced FA activation by TbACS, thereby reducing FA retention in the form of activated, membrane-impermeant fatty acyl-CoAs.

The increase in B-C16 uptake was somewhat unexpected and cannot be directly attributed to TbACS RNAi. We fully expected uptake of B-C12 and B-C16 to respond similarly to TbACS RNAi because both FAs are highly suitable substrates for TbACS1, TbACS3, and TbACS4 (Jiang *et al.*, 2001). It was clear that uptake efficiency was very different between the two chain lengths; B-C12 was taken up at a rate ~10 times greater than B-C16 (data not shown). This was not unexpected, as B-C16 likely does not partition into the plasma membrane as efficiently due to its longer chain length. Additionally, the rate constant of the rate-limiting flip-flop reaction is decreased when FA chain lengths are increased (Kleinfeld *et al.*, 1997).

One possible explanation for the differential consequences of TbACS RNAi on B-C12 and B-C16 uptake is that the FAs are taken up through two distinct mechanisms. The parasite, sensing a reduction in FA acquisition due to TbACS knockdown compensated by up-regulating another FA uptake mechanism (currently undescribed in *T. brucei*). This could occur through increased expression or posttranslational modification of proteins involved in the

pathway. Assuming B-C12 enters the cell predominately through passive diffusion and subsequent activation by ACS and B-C16 is taken up primarily through the presumed upregulated mechanism, this could result in a net decrease in B-C12 uptake and increase in B-C16 uptake.

These observations represent significant progress towards understanding the mechanisms of FA uptake in *T. brucei*. Based on kinetic experiments, it has long been suspected that the parasite's FA uptake mechanisms mimic that found in mammals (Voorheis,1980). However, this is the first direct experimental evidence that FA uptake is mediated by multiple mechanisms in *T. brucei*.

The reduction in parasite growth caused by 6 days of panTbACS RNAi induction was fairly mild (Fig. 5.2A). However, both cumulative cell density and doubling time showed statistically significant reductions after 6 days of panTbACS RNAi (Fig. 5.2B,C). This observation is in conflict with the previous report that TbASC5 is not essential for growth in either PF or BF parasites (Smith *et al.*, 2010), however it is possible that no single TbACS gene is essential in isolation because the overlapping activities of the ACS family can compensate for the loss.

It is also important to note that we detected changes in FA uptake prior to reduction in parasite growth. This suggests that the observed FA uptake phenotypes were likely a direct result of, or an immediate response to, TbACS knockdown and not due to non-specific complications associated with cell death.

FUTURE DIRECTIONS

In the future, the panTbACS RNAi mutant should be tested for growth in low-lipid media and FA synthesis rates measured. Evidence from previously characterized genes involved in *T. brucei* FA metabolism demonstrates that the parasite is adaptable to changes in lipid availability. For example, the rate of fatty acid synthesis was increased when the parasites were cultured in low-lipid media (Lee *et al.*, 2006). Additionally, RNAi mutants for genes involved in FA synthesis only exhibited a growth phenotype when cultured in low-lipid media (Lee *et al.*, 2006; Vigueira *et al.*, 2011). I anticipate that FA synthesis will be upregulated due to the parasite's reduced capacity to acquire FA from the environment.

In addition to causing a reduction in B-C12 uptake, presumably TbACS knockdown also reduced the activation of FAs to CoA esters. This reduction could be quantified using high-performance liquid chromatography. Because FAs require activation in order to be incorporated into more complex lipid species, I anticipate that TbACS knockdown will also lead to an increase in the levels of free FAs in the parasite. This could be examined by labeling parasites with [^{3}H]C12:0 and measuring incorporation into complex lipids using densitometric analysis of total cellular lipid content resolved by thin layer chromatography.

One likely and potentially exciting consequence of panTbACS knockdown is the reduction in glycophosphatidylinositol (GPI) anchor synthesis. BF *T. brucei* depends on the production of copious amounts of a dimyristoyl GPI anchor to attach its dense surface coat (10^{7} copies per cell) to the plasma membrane. The

variant surface glycoprotein coat is critical to the parasites ability to evade the adaptive immune system, and therefore perturbations in the GPI biosynthesis pathway could compromise the parasites virulence in the mammalian host. This highlights the importance of extending my studies of TbACS into BF parasites.

Protein modifications by acetylation are also important to the survival of the parasite. Recently, N-myristoylation has been validated as a drug target. The myristoyl-CoA:protein N-myristoyltransferase (NMT) is essential for virulence in a mouse model (Price *et al.*, 2010). The TbACS genes are potentially involved in generating the myristoyl-CoA used by NMT and could therefore represent drug targets.

I have provided the first glimpse into the role of ACS in *T. brucei's* FA uptake pathway. However, my studies have barely scratched the surface of what can be learned about these genes. Many experimental questions pertaining to TbACS remain unasked. I hope that this work and my thoughts provide a future Paul Lab student the opportunity to extend our knowledge of these exciting genes.

MATERIALS AND METHODS

Trypanosome strains, cell lines, and media

PF *T. brucei* transgenic cell lines containing genomically integrated Tetracycline (TET) repressor and T7 polymerase [29-13 (Wirtz *et al.*, 1999)] were generously provided by Dr. George Cross (Rockefeller University). PF parasites were grown in SDM-79 medium (Brun *et al.*, 1979) containing 10% heat-inactivated FBS and supplemented with 15 mg/ml G418, 50 mg/ml hygromycin and 2.5 mg/ml phleomycin.

Generation of panTbACS RNAi cell line

To make the panTbACS RNAi construct, an ~700-bp fragment containing a highly homologous region among the TbACS genes was amplified by PCR from WT 427 PF genomic DNA using a forward primer containing a 5′ XhoI site (5′-ctcgagTACTGCGCTTACCTGC-3′) and a reverse primer containing a 5′ HindIII site (5′-aagcttGCCAATGATGCGAAGGGT-3′). This amplicon was first cloned into pCR2.1 TOPO prior to subcloning into the TET-inducible RNAi vector pZJM (Wang *et al.*, 2000). The resulting pZJM.panTbACS plasmid was confirmed by sequencing.

The pZJM.panTbACS plasmid DNA was isolated from 10 mL of overnight *Escherichia coli* culture using 2 QIAprep Miniprep columns (Qiagen). 100 µL of the purified plasmid DNA was linearized in a 200 µL restriction digest containing 20 U of Not1 restriction enzyme (New England Biolabs) for 3 h at 37° C. The

linearized DNA was then cleaned up using 2 MinElute Reaction Cleanup columns (Qiagen). Linearized DNA was eluted from the columns in warm sterile H_2O and quantified using a BioPhotometer spectrometer (Eppendorf).

For transfection, $1x10^8$ PF 29-13 parasites were harvested by centrifugation (10 min, 2500 x G). The parasites were then resuspended in 500 µL of prewarmed Cytomix (van den Hoff *et al.*, 1992) and mixed with 20 µg of linearized pZJM.panTbACS. A mock transfection that included H_2O rather than DNA was prepared to ensure proper drug selection. The cells were then electroporated in a 4 mm gap cuvette under the following conditions: exponential decay mode, 2 pulses with a 10 second interval, capacitance 25 µF, voltage 1.5kV (Djikeng *et al.*, 2004). The cells were then transferred to 40 mL of prewarmed SDM-79 containing G418 and hygromycin. Phleomycin was added to the cultures 18 h later to select for successful transfectants. Following drug selection, clonal populations were established by limiting dilution.

In vitro Growth Experiments

For growth curves, panTbACS RNAi cells were diluted into SDM-79 media, induced for RNAi by the addition of TET (1 mg/ml final) (Wang *et al.*, 2000). Cell density was monitored using a FACScan flow cytometer approximately every 48 h (Becton Dickinson). For comparison purposes, doubling times were calculated for each experimental condition. Following each cell count, cultures were diluted to maintain logarithmic phase growth.

Fatty Acid Uptake

FA uptake was monitored at approximately 48 h intervals. To assay FA uptake, cells were incubated for 20 min at room temperature in a solution of 50% SDM-79 and 50% Cytomix containing 20 μM B-C12 or B-C16. Following the incubation, 300 μL of ice-cold Cytomix was added and tubes were chilled on ice for 2 min. Cells were then washed by centrifugation (2 min, 8000 x g) and resuspension in Cytomix. Cell-associated fluorescence was measured using a FACScan flow cytometer (Becton Dickinson). The values were corrected for background fluorescence by subtracting values collected from an unstained population of cells. Final values are expressed as a percentage of the uninduced control.

Statistics

One-tailed Student's t-test analyses between control and treatments were performed using Microsoft Excel. We judged statistical significance to be $p < 0.05$. Error bars represent standard deviation from the mean.

FIGURES

Figure 5.1: Effect of panTbACS RNAi on *T. brucei* FA Uptake. PF panTbACS RNAi parasites were grown in uninduced (no RNAi) or induced (panTbACS RNAi) conditions and assayed for uptake of B-C12 (A) and B-C16 (B) every other day for 6 days. All values are expressed as a percentage of the uninduced control. For both panels, the mean of three replicates is shown. Error bars show SD. The * indicates $p < 0.05$ and ** indicates $p < 0.01$ for the difference between uninduced and induced RNAi conditions, Student's t-test.

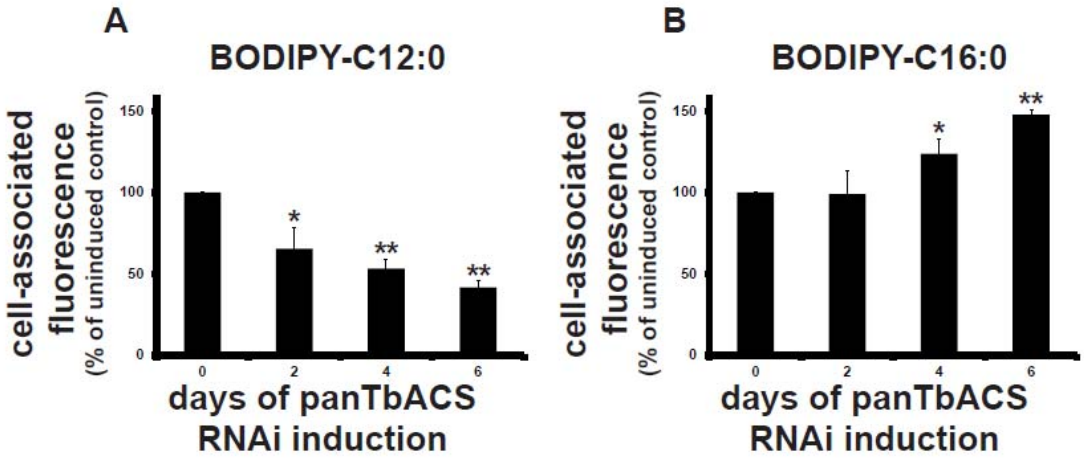

Figure 5.2: Effect of panTbACS RNAi on *in vitro* growth of *T. brucei*. PF panTbACS RNAi parasites were grown in uninduced (no RNAi) or induced (panTbACS RNAi) conditions and cell densities of the cultures were recorded every other day for 6 days. **A.** Cumulative culture densities over 6 days. **B.** Final cumulative culture densities after 6 days. **C.** Parasite doubling times. For all panels, the mean of three replicates is shown. Error bars show SD. Please note in A, error bars are too small to be visible. The * indicates $p < 0.05$ and ** indicates $p < 0.01$ for the difference between uninduced and induced RNAi conditions, Student's t-test.

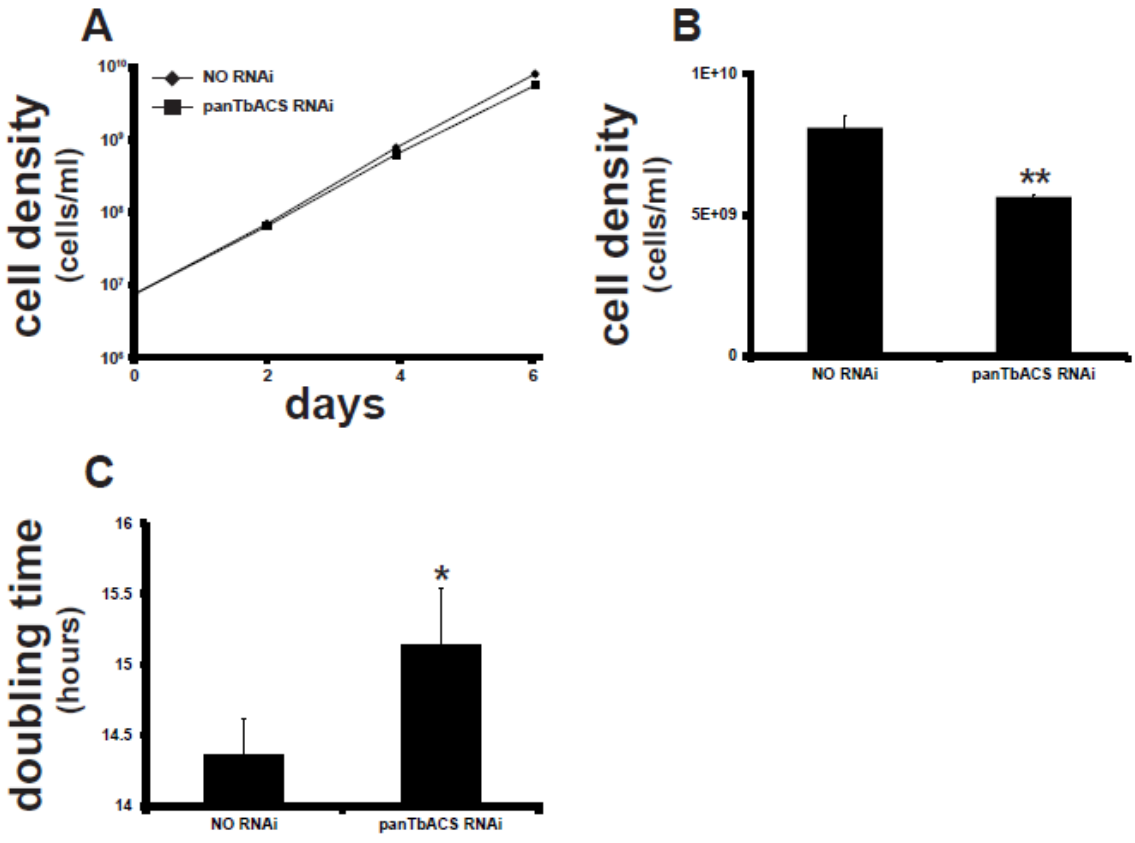

REFERENCES

Aslett M., Aurrecoechea C., Berriman M., Brestelli J., Brunk B.P., Carrington M.*, et al.* (2010) TriTrypDB: A functional genomic resource for the Trypanosomatidae. *Nucleic Acids Res* **38:** D457-62.

Black P.N., Zhang Q., Weimar J.D., and DiRusso C.C. (1997) Mutational analysis of a fatty acyl-coenzyme A synthetase signature motif identifies seven amino acid residues that modulate fatty acid substrate specificity. *J Biol Chem* **272:** 4896-4903.

Brun R., and Schonenberger M. (1979) Cultivation and *in vitro* cloning of procyclic culture forms of *Trypanosoma brucei* in a semi-defined medium. *Acta Trop* **36:** 289-292.

Djikeng A., Shen S., Tschudi C., and Ullu E. (2004) Analysis of gene function in *Trypanosma brucei* using RNA interference. In Parasite Genomics Protocols. Melville, S.E. (ed). Totowa, New Jersey: Humana Press, pp. 287.

Jiang D.W., and Englund P.T. (2001) Four *Trypanosoma brucei* fatty acyl-CoA synthetases: Fatty acid specificity of the recombinant proteins. *Biochem J* **358:** 757-761.

Jiang D.W., Ingersoll R., Myler P.J., and Englund P.T. (2000) *Trypanosoma brucei*: Four tandemly linked genes for fatty acyl-CoA synthetases. *Exp Parasitol* **96:** 16-22.

Kleinfeld A.M., Chu P., and Romero C. (1997) Transport of long-chain native fatty acids across lipid bilayer membranes indicates that transbilayer flip-flop is rate limiting. *Biochemistry* **36:** 14146-14158.

Lee S.H., Stephens J.L., Paul K.S., and Englund P.T. (2006) Fatty acid synthesis by elongases in trypanosomes. *Cell* **126:** 691-699.

Li L.O., Klett E.L., and Coleman R.A. (2010) Acyl-CoA synthesis, lipid metabolism and lipotoxicity. *Biochim Biophys Acta* **1801:** 246-251.

Milger K., Herrmann T., Becker C., Gotthardt D., Zickwolf J., Ehehalt R.*, et al.* (2006) Cellular uptake of fatty acids driven by the ER-localized acyl-CoA synthetase FATP4. *J Cell Sci* **119:** 4678-4688.

Price H.P., Guther M.L., Ferguson M.A., and Smith D.F. (2010) Myristoyl-CoA:Protein N-myristoyltransferase depletion in trypanosomes causes avirulence and endocytic defects. *Mol Biochem Parasitol* **169:** 55-58.

Smith T.K., and Butikofer P. (2010) Lipid metabolism in *Trypanosoma brucei*. *Mol Biochem Parasitol* **172:** 66-79.

Soupene E., and Kuypers F.A. (2008) Mammalian long-chain acyl-CoA synthetases. *Exp Biol Med (Maywood)* **233:** 507-521.

van den Hoff M.J., Moorman A.F., and Lamers W.H. (1992) Electroporation in 'intracellular' buffer increases cell survival. *Nucleic Acids Res* **20:** 2902.

Vigueira P.A., and Paul K.S. (2011) Requirement for acetyl-CoA carboxylase in *Trypanosoma brucei* is dependent upon the growth environment. *Mol Microbiol* **80:** 117-132.

Voorheis H.P. (1980) Fatty acid uptake by bloodstream forms of *Trypanosoma brucei* and other species of the kinetoplastida. *Mol Biochem Parasitol* **1:** 177-186.

Wang Z., Morris J.C., Drew M.E., and Englund P.T. (2000) Inhibition of *Trypanosoma brucei* gene expression by RNA interference using an integratable vector with opposing T7 promoters. *J Biol Chem* **275:** 40174-9.

Watkins P.A. (1997) Fatty acid activation. *Prog Lipid Res* **36:** 55-83.

Wirtz E., Leal S., Ochatt C., and Cross G.A. (1999) A tightly regulated inducible expression system for conditional gene knock-outs and dominant-negative genetics in *Trypanosoma brucei*. *Mol Biochem Parasitol* **99:** 89-101.

CHAPTER 6

A FORWARD-GENETIC SCREEN FOR GENES INVOLVED IN *Trypanosoma brucei* FATTY ACID UPTAKE

Patrick A. Vigueira, Marianne M. Ligon, Ben A. Martin and Kimberly S. Paul

Department of Biological Sciences, Clemson University, Clemson, SC

INTRODUCTION

In both procyclic (PF) and bloodstream (BF) life stages *Trypanosoma brucei* relies on dense glycoprotein surface coats for survival. Procyclin covers the PF parasite and is believed to protect the parasite from proteolytic degradation while in the midgut of the tsetse (Richardson *et al.*, 1988; Roditi *et al.*, 1989). The BF form relies on variant surface glycoprotein (VSG) to evade the mammalian host's adaptive immune system (Horn *et al.*, 2010). Both procyclin (10^6 copies per cell) and VSG (10^7 copies per cell) are very densely arranged on the cells surface. Each glycoprotein is attached to the parasite's outer membrane by specialized glycolipids called glycosylphosphatidylinositol (GPI) anchors, each including two fatty acid (FA) moieties. The high density of essential, GPI-anchored surface coat proteins imposes a tremendous requirement for FAs.

The parasite has two options for satisfying its requirement for FAs: synthesis or uptake. Evidence from previous studies suggests that FA uptake is preferred over synthesis (Doering *et al.*, 1993; Lee *et al.*, 2006; Vigueira *et al.*, 2011). Compared to FA synthesis, uptake is highly energetically favorable. For example, a C16:0 FA that diffuses into a cell and is subsequently activated by

esterification to a Coenzyme A (CoA) molecule requires the hydrolysis of a single ATP. In comparison, synthesis of the same C16:0 FA *de novo* would require 6 ATPs and 12 NADH/NADPH reducing equivalents (Morita *et al.*, 2000; Lee *et al.*, 2006; Stephens *et al.*, 2007). Despite their importance in the FA metabolism of the parasite, little is known about the mechanisms or genes involved in *T. brucei* FA uptake. I therefore set out to conduct an RNA interference (RNAi)-based genetic screen to identify genes involved in *T. brucei* FA uptake.

The creation of an RNAi library by a group of visionary scientists opened the door to forward-genetic experiments in *T. brucei* (Morris *et al.*, 2002). The library was created by cloning sheared fragments of *T. brucei* genomic DNA (gDNA) into the pZJM RNAi vector (Wang *et al.*, 2000). The resulting plasmid library was then stably transfected into procyclic form (PF) parasites. The coverage of the RNAi library is ~5 fold (Morris *et al.*, 2002; Morris *et al.*, 2005; Alsford *et al.,* 2011). Thus, upon expansion of the library, each gene in genome should be represented by multiple parasites. The library has proven to be a useful tool in identifying novel parasite genes and revealing uncharacterized biological functions of described genes (Morris *et al.*, 2002; Drew *et al.*, 2003; Zhao *et al.*, 2008).

To measure FA uptake we utilized a commercially available FA conjugated to a non-polar green fluorescent fluorophore (4,4-difluoro-5,7-dimethyl-4-bora-3a,4a-diaza-*s*-indacene) (BODIPY). BODIPY-FAs have been previously validated as useful tools for the study of FA uptake (Li *et al.*, 2005)

and exhibit properties very similar to unlabeled fatty acids (Zou *et al.*, 2003; Thumser *et al.*, 2007; Hostetler *et al.*, 2010). Previous studies in our lab have also validated BODIPY-FAs for use in *T. brucei*. Cell associated fluorescence increases with incubation time and FA concentration. My studies of the *T. brucei* acyl-CoA synthetases (Chapter 5) demonstrated that RNAi of known FA uptake genes reduced uptake of BODIPY-C12:0 (B-C12), further validating the basis of the screen.

In brief, following 4 days of RNAi induction, the library population of cells were incubated with B-C12 and the dim parasites (those taking up less FA) were isolated using fluorescence activated cell sorting. Dim parasites were then subjected to a second round of RNAi induction and FA uptake screening. Clones with the lowest capacity for uptake were expanded and the RNAi insert was identified by PCR amplification and subsequent sequencing. Many genes were identified, but an initial attempt to validate the role of these genes in FA uptake was unsuccessful. Here I describe the screen in detail and offer suggestions for future work and screens.

MATERIALS AND METHODS

Primary FA Uptake Screen

The *T. brucei* 660-bp RNAi library was thawed from six 1 mL liquid nitrogen stabilates and allowed to expand for 2 days. In order to achieve the theoretical 5-fold genome coverage, 200 µL of the expanded RNAi library culture were seeded into 4 mL of fresh SDM-79 media. Induction of RNAi was initiated by addition of 1 mg/mL tetracycline (TET) to the media (Wang *et al.*, 2000). The culture volume was expanded as needed to maintain logarithmic growth, but no dilutions were made. Following 4 days of RNAi induction, 5 mL of culture ($6.3x10^6$ cells/mL) were utilized for fluorescence activated cell sorting.

The parasites were incubated for 20 min at room temperature in a solution of 50% SDM-79 and 50% Cytomix (van den Hoff *et al.*, 1992) containing 20 µM B-C12. Following the incubation, cells were washed twice by centrifugation (2 min, 8000 x g) and resuspension in Cytomix. Cell sorting was conducted in the Clemson University Cell Analysis Laboratory by the lovely and talented Dr. Meredith Morris using the Cytopeia Influx fluorescence-activated cell sorter. The parasites were analyzed using a dot plot (yellow channel, Y-axis and green channel, X-axis) and gated for normal cellular morphology using the forward and side scatter detectors. Parasites in the dimmest 1% of the population were distributed into individual wells of 96-well plates. In total, sixty 96-well plates were collected.

Secondary FA Uptake Screen

The 96-well plates were monitored daily for parasite growth. After ~2 weeks of incubation, parasites that had grown to density were diluted into fresh media in ten 96-well plates. These clonal populations were then subjected to a second round of screening to further isolate clones that exhibited the strongest FA uptake phenotype. Prior to RNAi induction, replica plates were generated to maintain uninduced cell populations for further analysis. RNAi was induced for 4 days prior to FA uptake analysis using a Guava Flow Cytometer. In an attempt to maximize the dynamic range of the FA uptake assay, cells were incubated with 40 μM B-C12, double the concentration used in the original sort. Following 20 min of incubation, the cells were transferred to a 30 μM filter plate (Millipore) positioned above a v-bottom 96-well plate. The plates were centrifuged at 4° C for 10 min at a speed of 3200xG. As the cultures passed through the filter plate, cellular aggregations were eliminated and individual cells pelleted in the v-bottom 96-well plate. The staining solution was removed by aspiration, and parasites were resuspended in 200 μL Cytomix. Histogram plots of cell-associated fluorescence were generated using the 408 nm (yellow channel) detector. The geometric means of each histogram were used to determine the dimmest 24 clones from each of the ten 96-well plates. The corresponding clonal populations were transferred from the replica plates into ten 24-well plates for culture expansion.

PCR and Sequencing

gDNA was purified from each of the expanded clonal populations using an STE buffer protocol. Parasites were harvested from 1 mL of dense culture by centrifugation (3 min, 8,000xG), washed once in Cytomix and resuspended in 200 µL of STE buffer (10 mM Tris-HCl, 1 mM EDTA and 100 mM NaCl). The cell suspension was then incubated for 10 min in a 95° C heat block and transferred to ice for 5 min. The lysed cells were then subjected to RNAse treatment (125 µg/mL) for 5 min in a 37° C thermomixer at a speed of 500 RPM. Proteins were then degraded by proteinase K treatment (250 µg/mL) for 15 min in a 60° C thermomixer at a speed of 500 RPM. The RNAse and proteinase K were subsequently inactivated by heating the samples for 5 min in a 95° C heat block. Following a 5 min incubation on ice, cellular debris was removed by centrifugation (5 min, 16,000xG).

To determine the gene responsible for causing reduction in FA uptake, the pZJM insert was amplified from the gDNA using a nested PCR approach described previously (Morris *et al.*, 2005). The first PCR contained 5 µL of GoTaq Colorless Mastermix (Promega), 1 µL of each primer PhleoF and AldoR (Morris *et al.*, 2005) (diluted 1:10 in sterile H_2O), 1 µL of freshly-purified gDNA, and 2 µL of sterile H_2O. Thermocycling conditions were as follows: initial denaturation, 94° C for 2 min; 40 cycles of denaturation, 94° C for 20 sec, annealing, 55° C for 30 sec, extension, 72° C for 2.5 min; final extension 72° C for 5 min. The second PCR using the internal primers contained 10 µL of GoTaq Colorless Mastermix, 1

μL of each primer XlinkF and BetaLow (Morris *et al.*, 2005) (diluted 1:10 in sterile H_2O), 1 μL of PCR product from the first reaction and 7 μL of sterile H_2O. Thermocycling conditions were as follows: initial denaturation, 94° C for 2 min; 40 cycles of denaturation, 94° C for 20 sec, annealing, 61° C for 30 sec, extension, 72° C for 2.5 min; final extension 72° C for 5 min. The PCR products were then subjected to DNA electrophoresis on a 1% w/v agarose gel. The quantity and purity of the PCR products were assessed by examining the size and number of bands from each reaction. Reactions that contained a single product were prepared for direct sequencing.

In order to perform direct sequencing on PCR products, the primers used in the PCR must be removed. This was accomplished by treatment with Exonuclease I and Antarctic Phosphatase (exo-AP) (Fisher). A working stock of exo-AP was prepared by diluting Exonuclease I 1:100 and Antarctic Phosphatase 1:10 in sterile H_2O. 1 μL of each PCR product was combined with an equal volume of the exo-AP enzyme mixture. Samples were then incubated at a temperature of 37ºC for 30 min and subsequently 80ºC for 15 min.

Following exo-AP treatment, 1 μL of XlinkF primer (diluted 1:10 in sterile H_2O) was added to each sample. PCR products determined to be larger than 1000 bp by DNA electrophoresis were included in a second sequencing reaction using the BetaLow primer. Sequencing reactions were performed by the Clemson University Genomics Institute (CUGI). Sequencing results were analyzed using Sequencher (Gene Codes) and trimmed manually to include only

high quality sequence. The TriTryp database was utilized to perform BLAST searches against the *T. brucei* strain 927 genome (Aslett *et al.*, 2010).

RNAi Cell Line Generation

Four genes were chosen to rebuild RNAi constructs for uptake phenotype verification: Tb927.7.1310, Tb927.7.6550, Tb11.47.0009, and Tb927.10.14430 identified from clones 1F11, 3B12, 5F10, 6G5, respectively. Primers were designed to amplify ~ 500 bp region from each of the genes. These genes fragments were amplified by PCR from wild-type PF 427 genomic DNA using a forward primer containing a 5′ XhoI site and a reverse primer containing a 5′ HindIII. Each primer also included 4 additional 5' nucleotides to allow direct digestion of PCR products. The primer sequences for each gene are as follows: Tb927.7.1310, pv1F11f.XhoI 5' –GATCctcgagCGGAGCATCCTAACCAACAG – 3' and pv1F11r.HindIII 5' – GATCaagcttTCCCAGGACCAGCCGGAGCG – 3'; Tb927.7.6550, pv3B12f.XhoI 5' –GATCctcgagCCATTCTGTGCAATGTGGGG – 3' and pv3B12r.HindIII 5' – GATCaagcttTCAAGGTCTCGGTGATGTTG – 3'; Tb11.47.0009, pv5F10f.XhoI 5' –GATCctcgagCCTCACGGAGTGTATTAAAC– 3' and 5F10r.HindIII 5' – GATCaagcttCAGCCCGAACAACCGGTGAG – 3'; Tb927.10.14430, pv6G5f.XhoI 5' – ATCctcgagGGTGGGAATCACCGAGATTG– 3' and pv6G5r.HindIII 5' – GATCaagcttCGTGATGTTGTCGCACGACG – 3'. Following a restriction digest with XhoI and HindIII, the amplicons were ligated into the TET-inducible RNAi vector pZJM. The resulting plasmids were confirmed by sequencing.

Each RNAi construct plasmid was isolated from 10 mL of overnight *Escherichia coli* culture using 2 QIAprep Miniprep columns (Qiagen). 100 µL of the purified plasmid DNA was linearized in a 200 µL restriction digest containing 20 U of Not1 restriction enzyme (New England Biolabs) for 3 h at 37° C. The linearized DNA was then cleaned up using 2 MinElute Reaction Cleanup columns (Qiagen). Linearized DNA was eluted from the columns in warm sterile H_2O and quantified using a BioPhotometer spectrometer (Eppendorf). For transfection $1x10^8$ PF 29-13 parasites were harvested by centrifugation (10 min, 2500 x G). The parasites were then resuspended in 500 µL of prewarmed Cytomix and mixed with 20 µg of linearized RNAi construct. A mock transfection that included water rather than DNA was prepared to ensure proper drug selection. The cells were then electroporated in a 4 mm gap cuvette under the following conditions: exponential decay mode, 2 pulses with a 10 second interval, capacitance 25 µF, voltage 1.5kV (Djikeng *et al.*, 2004). Following electroporation, the cells were transferred to 40 mL of prewarmed SDM-79 containing G418 and hygromycin. Phleomycin was added to the cultures 18 h later to select for successful transfectants.

Fatty Acid Uptake Experiments

FA uptake was monitored at 2 or 4-day intervals. To assay FA uptake, cells were incubated for 20 min at room temperature in a solution of 50% SDM-79 and 50% Cytomix containing 20 µM B-C12. Cells were then washed by centrifugation (2 min, 8000 x g) and resuspension in Cytomix. Cell-associated

fluorescence was measured using a FACScan flow cytometer (Becton Dickinson). The values were corrected for background fluorescence by subtracting values collected from an unstained population of cells. Alternatively, cells were incubated for 10 min at room temperature in a solution of 50% SDM-79 and 50% Cytomix containing 20 μM [^{3}H]-C12. Cells were then washed twice by centrifugation (2 min, 8000 x g) and resuspension in Cytomix. Cell-associated radioactivity was measured using an LS-6500 liquid scintillation counter (Becton Dickinson). Final values are expressed as a percentage of the uninduced or 29-13 control.

RESULTS

In total, BLAST searches identified 99 clones containing pZJM inserts with high homology to annotated genes from the *T. brucei* strain 927 genome (Table 6.1). 12 genes were represented multiple times (Table 6.2). One gene, Tb927.4.1320, was particularly enriched, identified from 32 clones.

I independently assessed 4 of the clonal cell lines (3B12, 3C4, 5B6, 6G5) for reduced FA uptake following 4 and 6 days of RNAi induction (Fig. 6.2). These clones were particularly interesting because they contained predicted transmembrane domains and/or signal peptides, both features of proteins involved in FA uptake in other organisms. Compared to uninduced controls, only clone 3B12 exhibited reduced FA uptake on day 4 and 6 of induction. However, each of the clones exhibited greater than 40% reduction in uptake when compared to the parental 29-13 control.

Based on the predicted attributes of the genes identified by BLAST searches, we chose 4 candidates we were interested in further characterizing (1F11, 3B12, 5F10, 6G5). To generate independent RNAi cell lines for each candidate gene I cloned a new target sequence that was different from the original target sequence in the RNAi library into pZJM. Induction of RNAi for 8 days resulted in a 41% reduction in uptake of B-C12 in the pv5F10 cell line (Fig. 6.3B). This reduction in uptake was accompanied by a 56% reduction in growth (data not shown). RNAi induction in the remaining 3 cones (pv1F11, pv3B12, pv6G5) did not reduce B-C12 uptake relative to the uninduced controls (Fig. 6.3).

DISCUSSION AND FUTURE DIRECTIONS

The two most common genes isolated from the screen were Tb927.4.1320 (32 hits) and Tb11.02.2810 (17 hits), both annotated as conserved hypothetical proteins. According to the InterPro protein analysis and classification database, Tb927.4.1320 contains a SMAD/FHA domain and Tb11.02.2810 contains an RNA-binding domain. Thus, both genes are likely involved in gene expression. While knockdown of these genes may cause reduction in FA uptake, they are of limited interest to this project because it is unlikely that they are directly involved in FA uptake. Most likely, these genes cause broad changes in gene expression that, among other effects, reduces FA uptake.

The screen yielded many potentially interesting genes that should be independently characterized in the future. For the initial follow-up experiments, I used a fairly loose set of criteria for prioritizing interest in genes. Genes that contained predicted transmembrane domains were considered high priority because many FA uptake genes in other organisms code for integral membrane proteins. Genes with predicted signal peptides were also of particular interest because many FA uptake proteins are localized to the cell membrane or endoplasmic reticulum, both destinations of the secretory pathway.

It is very curious and somewhat disturbing that neither the isolated clones nor the rebuilt RNAi mutants exhibited consistently reduced FA uptake. Because we selected the dimmest 1% of the population in the primary sort and then further narrowed the candidates by 75% in the secondary screen, we should

have isolated the dimmest 0.25% of the RNAi library at 4 days of RNAi induction. However, when the clones or genes are tested independently and compared to uninduced controls, I observed no consistent reductions in FA uptake. It is difficult to reconcile this observation with the methodology of the screen.

In the 4 tested clones, [^{3}H]-C12 uptake was consistently reduced when induced RNAi conditions were compared to 29-13 parental controls, but not uninduced controls (Fig. 6.2). This could potentially be explained by leaky expression of dsRNA in the uninduced controls, causing a constant induction of RNAi in the absence of TET in the media. Theoretically, uninduced RNAi mutants should exhibit phenotypes identical to that of the 29-13 parental parasites, but in this experiment they do not. This could potentially result in an apparent dampening or masking of the phenotype upon induction. Leaky expression did not impact the primary or secondary screen because I did not select clones based on comparison to uninduced controls. Instead, I chose clones exhibiting low B-C12 uptake under induced RNAi conditions.

Another possibility is that we selected for clones that were deficient in FA uptake on the basis of the location of the RNAi vector integration rather that the RNAi target gene fragment. Typically, linearization of the RNAi construct plasmid by Not1 restriction digest results in integration into the transcriptionally-inactive ribosomal spacer region. However, errant integration into alternative genomic loci could cause the disruption of non-target genes and influence gene-expression patterns in the surrounding regions. This concept has been demonstrated

previously (Motyka *et al.*, 2004). This phenomenon has the potential to create parasites that are deficient in FA uptake and not responsive to RNAi. This is consistent with my observation that each of the isolated clones exhibited reduced FA uptake compared to parental 29-13 parasites (Fig. 6.2).

Future screens should avoid this potential problem by using an alternative methodology for the secondary screen. Rather than utilizing the secondary screen to select for the dimmest clones, one should compare the uptake of induced and uninduced RNAi clones. The clones with the greatest reduction in B-C12 uptake compared to uninduced controls should be maintained for further screening. This will help to ensure that the reduced uptake phenotype is a result of RNAi of the target gene rather than gene disruptions due to errant RNAi construct integration.

Of the four genes I chose to target with independently constructed RNAi vectors, only pv5F10 caused a reduction in B-C12 uptake (Fig. 6.3). Clone 5F10 isolated from the screen targeted Tb11.47.0009, annotated as a conserved hypothetical protein in the TriTryp database. The sequence codes for a protein with a predicted molecular weight of ~94kD and contains no predicted signal peptides or transmembrane domains. However, it was of interest to this screen because it contains a peroxisomal targeting signal and is therefore predicted to be localized to the glycosome, though it was not included in the report of glycosome proteomics (Colasante *et al.*, 2006). It is also important to note that RNAi of Tb11.47.0009 caused a reduction in parasite growth (data not shown).

While I have demonstrated that RNAi of genes involved in FA uptake can potentially cause a slowed-growth phenotype (Chapter 5), it is possible that in the case of Tb11.47.0009, reduced FA uptake was a consequence rather than a cause of unhealthy cells. Both the reduced FA uptake and growth phenotypes became apparent following 8 days of pv5F10 RNAi induction, but neither was detected on day 4. Thus, future studies should include an additional time point at 6 days post-induction to determine which of the phenotypes (reduced uptake or growth) are exhibited first.

Despite not exhibiting an uptake phenotype, the independently constructed RNAi cell lines I have generated (pv1F11, pv3B12, pv6G5) should not be abandoned. The experiments I have presented in this chapter represent a single experiment using non-clonal cell lines. Clonal cell lines should be established for each mutant, and the resulting cell lines should be used to repeat the uptake experiments I have described. In addition, the efficiency of RNAi knockdown has not been assessed in any of the discussed cell lines.

Recognizing the shortcomings of this RNAi screen, there remains great potential to find genes involved in FA uptake from the data we have generated. Within the list there are a number of interesting candidates currently annotated as hypothetical proteins. These genes should be targeted by conducting FA uptake and growth assays with independently constructed RNAi mutant cell lines. Sequencing of RNAi target genes from many of the dim clones was either not attempted or proved unsuccessful. However, I created liquid nitrogen stabilates

for all of the clones selected in the secondary screen, so they are available for further analysis when funding becomes available.

TABLES AND FIGURES

Table 6.1: FA Uptake Screen Results. Gene annotations, TriTryp gene IDs, BLAST fragment homology scores, predicted signal peptides (SP) and transmembrane domains (TMD) from the clones isolated in the FA uptake screen.

Clone ID	Gene Annotation	TriTryp Gene ID	BLAST Homology Score	SP, TMD
up1A1	hypothetical protein, conserved	Tb927.4.1320	Positives = 378/378 (100%)	
up1A8	hypothetical protein, conserved	Tb11.02.2810	Positives = 284/286 (99%)	
up1B3	hypothetical protein, conserved	Tb11.02.2810	Positives = 284/286 (99%)	
up1B12	hypothetical protein, conserved	Tb11.02.2810	Positives = 284/286 (99%)	
up1C6	hypothetical protein, conserved	Tb11.02.2810	Positives = 284/286 (99%)	
up1C10	hypothetical protein, conserved	Tb927.4.1320	Positives = 378/378 (100%)	
up1D7	hypothetical protein, conserved	Tb927.4.1320	Positives = 378/378 (100%)	
up1E10	hypothetical protein, conserved	Tb11.02.2810	Positives = 284/286 (99%)	
up1E12	hypothetical protein, conserved	Tb11.01.0950	Positives = 856/1105 (77%)	
up1F3	hypothetical protein, conserved	Tb927.4.1320	Positives = 378/378 (100%)	
up1F11	hypothetical protein, conserved	Tb927.7.1310	Positives = 471/491 (95%)	
up1G1	hypothetical protein, conserved	Tb927.4.1320	Positives = 378/378 (100%)	
up1G2	hypothetical protein, conserved	Tb11.02.2810	Positives = 284/286 (99%)	
up1G3	hypothetical protein, conserved	Tb927.4.1320	Positives = 378/378 (100%)	
up1G5	hypothetical protein, conserved	Tb11.02.2810	Positives = 284/286 (99%)	
up1G8	hypothetical protein, conserved	Tb927.4.1320	Positives = 378/378 (100%)	
up2A6	hypothetical protein, conserved	Tb927.4.1320	Positives = 378/378 (100%)	
up2A8	hypothetical protein, conserved	Tb927.4.1320	Positives = 293/364 (80%)	
up2C6	hypothetical protein, conserved	Tb927.4.1320	Positives = 378/378 (100%)	
up2D3	hypothetical protein, conserved	Tb927.4.1320	Positives = 378/378 (100%)	
up2D6	hypothetical protein, conserved	Tb11.02.2810	Positives = 287/360 (79%)	
up2E2	hypothetical protein, conserved	Tb11.01.0950	Positives = 679/710 (95%)	
up2E3	hypothetical protein, conserved	Tb11.02.2810	Positives = 284/286 (99%)	
up2E8	hypothetical protein, conserved	Tb927.4.1320	Positives = 378/378 (100%)	
up2F2	hypothetical protein, conserved	Tb11.01.0950	Positives = 679/710 (95%)	
up2F4	hypothetical protein, conserved	Tb11.02.2810	Positives = 284/286 (99%)	
up2F6	hypothetical protein, conserved	Tb11.02.2810	Positives = 284/286 (99%)	
up2G5	hypothetical protein, conserved	Tb927.4.1320	Positives = 261/336 (77%)	
up2H2	hypothetical protein, conserved	Tb11.02.2810	Positives = 282/332 (84%)	
up2H3	hypothetical protein, conserved	Tb927.4.1320	Positives = 258/335 (77%)	
up2H8	hypothetical protein, conserved	Tb927.4.1320	Positives = 176/197 (89%)	
up3A3	hypothetical protein, conserved	Tb927.4.1320	Positives = 378/378 (100%)	
up3B12	hypothetical protein, conserved	Tb927.7.6550	Positives = 524/615 (85%)	SP, 1 TMD
up3C4	hypothetical protein, conserved	Tb927.7.6550	Positives = 567/614 (92%)	SP, 1 TMD
up3C7	hypothetical protein, conserved	Tb927.4.1320	Positives = 378/378 (100%)	
up3D9	hypothetical protein, conserved	Tb927.4.1320	Positives = 378/378 (100%)	
up3E1	hypothetical protein, conserved	Tb927.4.1320	Positives = 378/378 (100%)	
up3E9	hypothetical protein, conserved	Tb11.02.2810	Positives = 284/286 (99%)	
up3F2	hypothetical protein, conserved	Tb927.4.1320	Positives = 306/379 (80%)	
up3F5	hypothetical protein, unlikely	Tb927.1.200	Positives = 139/196 (70%)	2 TMDs
up3F6	hypothetical protein, conserved	Tb11.02.2810	Positives = 319/332 (96%)	
up3F9	hypothetical protein, conserved	Tb927.4.1320	Positives = 378/378 (100%)	
up3G2	EP1 procyclin	Tb927.10.10260	Positives = 127/175 (72%)	
up3G10	hypothetical protein, unlikely	Tb09.160.1350	Positives = 104/143 (72%)	1 TMD

Clone ID	Gene Annotation	TriTryp Gene ID	BLAST Homology Score	SP, TMD
up4A2	hypothetical protein, unlikely	Tb927.1.200	Positives = 118/149 (79%)	2 TMDs
up4B4	hypothetical protein, conserved	Tb927.4.1320	Positives = 378/378 (100%)	
up4B6	hypothetical protein, conserved	Tb927.4.1320	Positives = 378/378 (100%)	
up4B10	hypothetical protein, unlikely	Tb09.160.1350	Positives = 93/143 (65%)	1 TMD
up4C4	hypothetical protein, unlikely	Tb927.1.460	Positives = 82/116 (70%)	2 TMDs
up4C10	hypothetical protein, unlikely	Tb927.1.460	Positives = 84/118 (71%)	2 TMDs
up4D4	hypothetical protein, conserved	Tb927.4.1320	Positives = 378/378 (100%)	
up4D11	hypothetical protein, unlikely	Tb927.1.200	Positives = 61/93 (65%)	2 TMDs
up4E6	hypothetical protein, conserved	Tb927.4.1320	Positives = 378/378 (100%)	
up4F7	hypothetical protein, conserved	Tb927.4.1320	Positives = 378/378 (100%)	
up4G2	hypothetical protein, conserved	Tb927.4.1320	Positives = 378/378 (100%)	
up4G8	hypothetical protein, conserved	Tb11.02.2810	Positives = 284/286 (99%)	
up4H11	hypothetical protein, conserved	Tb927.4.1320	Positives = 378/378 (100%)	
up4H12	hypothetical protein, conserved	Tb927.4.1320	Positives = 349/378 (92%)	
up5B6	hypothetical protein, conserved	Tb11.18.0010	Positives = 95/107 (88%)	SP, 7 TMDs
up5D2	DNA topoisomerase ii	Tb09.160.4090	Positives = 501/522 (95%)	
up5E8	hypothetical protein, conserved	Tb927.5.700	Positives = 756/885 (85%)	
up5E10	hypothetical protein, conserved	Tb11.01.5780	Positives = 227/282 (80%)	
up5F10	hypothetical protein, conserved	Tb11.47.0009	Positives = 840/895 (93%)	
up5G5	hypothetical protein, conserved	Tb11.01.5780	Positives = 251/251 (100%)	
up6A10	hypothetical protein, conserved	Tb11.01.6610	Positives = 294/327 (89%),	
up6D10	hypothetical protein, conserved	Tb11.02.2810	Positives = 330/334 (98%)	
up6F1	hypothetical protein, conserved	Tb11.01.0950	Positives = 998/1065 (93%)	
up6G5	hypothetical protein, conserved	Tb927.10.14430	Positives = 813/1014 (80%)	2 TMDs
up7B4	hypothetical protein, conserved	Tb927.4.1320	Positives = 381/387 (98%)	
up7C8	succinyl-coA:3-ketoacid-coenzyme A transferase, putative	Tb11.02.0290	Positives = 35/37 (94%)	
up7D2	hypothetical protein, conserved	Tb927.5.2610	Positives = 225/225 (100%)	
up7F4	hypothetical protein, conserved	Tb11.01.6610	Positives = 300/333 (90%)	
up7G4	variant surface glycoprotein, pseudogene	Tb11.v4.0020	Positives = 162/238 (68%)	
up7G9	hypothetical protein, unlikely	Tb09.160.0590	Positives = 69/69 (100%)	SP, 3 TMDs
up7G10	variant surface glycoprotein, pseudogene	Tb11.57.0045	Positives = 198/267 (74%)	
up7H12	expression site-associated gene, pseudogene	Tb927.2.910	Positives = 571/1006 (56%)	
up8A12	hypothetical protein, conserved	Tb927.6.620	Positives = 102/102 (100%)	
up8B11	hypothetical protein, conserved	Tb11.02.2810	Positives = 284/286 (99%)	
up8B12	variant surface glycoprotein-related, putative	Tb09.244.2240	Positives = 219/294 (74%)	
up8C12	hypothetical protein, conserved	Tb927.3.1550	Positives = 114/114 (100%)	
up8D9	hypothetical protein, conserved	Tb927.4.1320	Positives = 344/387 (88%)	
up8F10	leucine-rich repeat protein, putative	Tb927.3.1490	Positives = 136/137 (99%)	
up8F12	hypothetical protein	Tb927.3.1230	Positives = 379/393 (96%)	
up8G8	hypothetical protein,chrXI additional, unordered contigs	Tb11.1770	Positives = 247/293 (84%)	
up8H7	hypothetical protein, conserved	Tb927.4.1320	Positives = 121/148 (81%)	
up8H10	SL RNA	Tb09_SLRNA_0004	Positives = 55/58 (94%)	
up8H11	RNA-editing complex protein,KREPB6	Tb927.3.3990	Positives = 74/74 (100%)	
up9B9	UDP-Gal or UDP-GlcNAc-dependent glycosyltransferase	Tb10.v4.0244	Positives = 258/264 (97%)	
up9B12	hypothetical protein, unlikely	Tb09.160.0590	Positives = 51/53 (96%)	SP, 3 TMDs
up9D12	hypothetical protein, conserved	Tb927.5.2610	Positives = 208/221 (94%)	
up9E4	ARP2/3 complex subunit, putative	Tb927.2.2900	ositives = 530/546 (97%)	
up9H2	hypothetical protein, conserved	Tb927.5.3550	Positives = 688/740 (92%)	SP
up10C8	hypothetical protein, conserved	Tb09.244.0440	Positives = 62/81 (76%)	
up10F1	Variant surface glycoprotein, pseudogene	Tb09.160.0220	Positives = 812/895 (90%)	
up10F2	helicase, putative	Tb927.5.3940	Positives = 77/96 (80%)	
up10F8	hypothetical protein, unlikely	Tb09.160.0590	Positives = 64/65 (98%)	SP, 3 TMDs
up10G2	hypothetical protein, conserved	Tb11.18.0010	Positives = 108/110 (98%)	SP, 7 TMDs
up10G9	hypothetical protein, unlikely	Tb09.160.0590	Positives = 64/65 (98%)	SP, 3 TMDs
up10H8	retrotransposon hot spot protein, pseudogene	Tb927.1.240	Positives = 764/846 (90%)	

Table 6.2: Genes Isolated Multiple Times. Gene annotations, TriTryp gene IDs, and number of isolated clones.

Gene Annotation	TriTryp Gene ID	# of hits
hypothetical protein, conserved	Tb927.4.1320	32
hypothetical protein, conserved	Tb11.02.2810	17
hypothetical protein, unlikely	Tb09.160.0590	4
hypothetical protein, conserved	Tb11.01.0950	4
hypothetical protein, unlikely	Tb927.1.200	3
hypothetical protein, unlikely	Tb09.160.1350	2
hypothetical protein, conserved	Tb11.01.5780	2
hypothetical protein, conserved	Tb11.01.6610	2
hypothetical protein, conserved	Tb11.18.0010	2
hypothetical protein, unlikely	Tb927.1.460	2
hypothetical protein, conserved	Tb927.5.2610	2
hypothetical protein, conserved	Tb927.7.6550	2

Figure 6.1: FA Uptake RNAi Screen Flowchart.

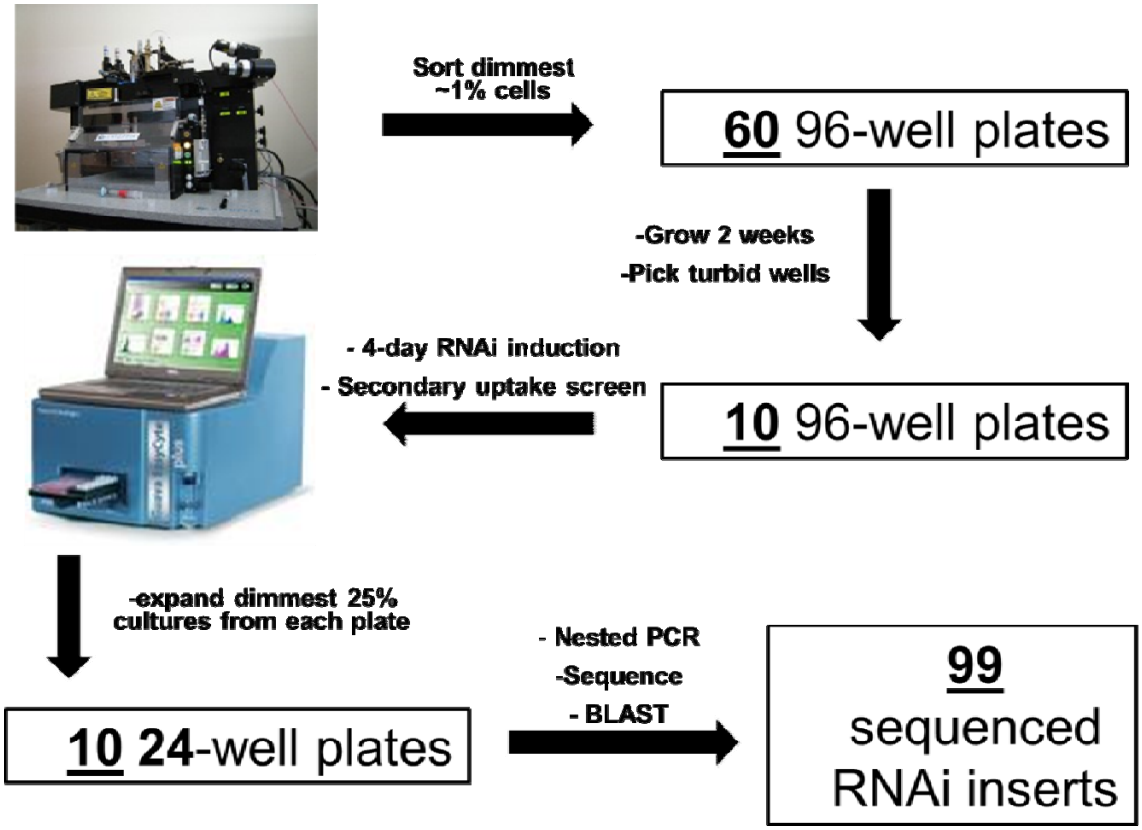

Figure 6.2: FA Uptake in Clones Isolated From the Screen. 29-13 parental cell lines and clonal parasite populations isolated from the screen were grown in uninduced or induced conditions for 4 (A) or 6 (B) days and assayed for uptake of [^{3}H]-C12. All values are expressed as a percentage of uninduced (black bars) or 29-13 (grey bars) controls.

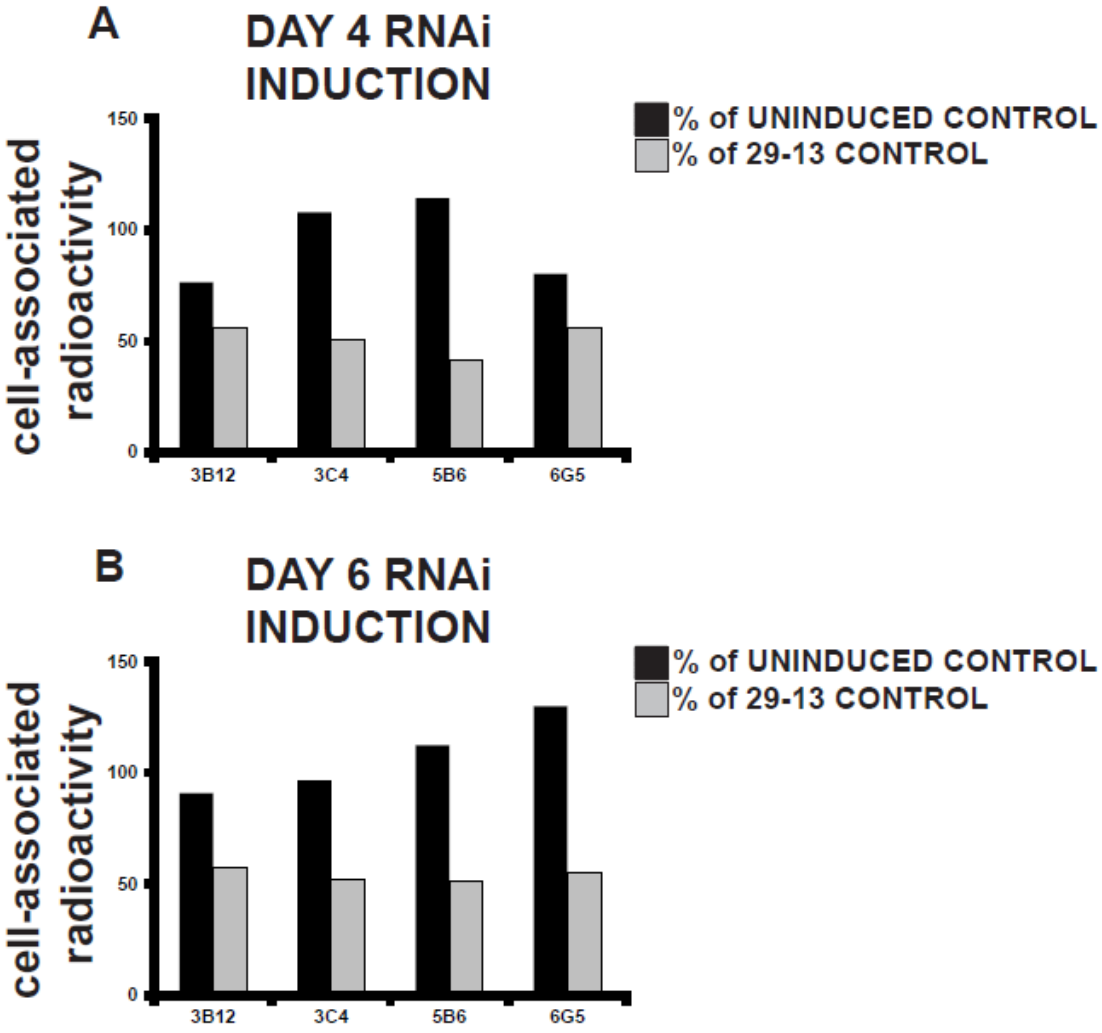

Figure 6.3: FA Uptake in Independently Constructed RNAi Parasites.

Independently constructed RNAi parasites were grown in uninduced or induced conditions for 4 (black bars) or 8 (grey bars) days and assayed for uptake of B-C12. All values are expressed as a percentage of uninduced controls.

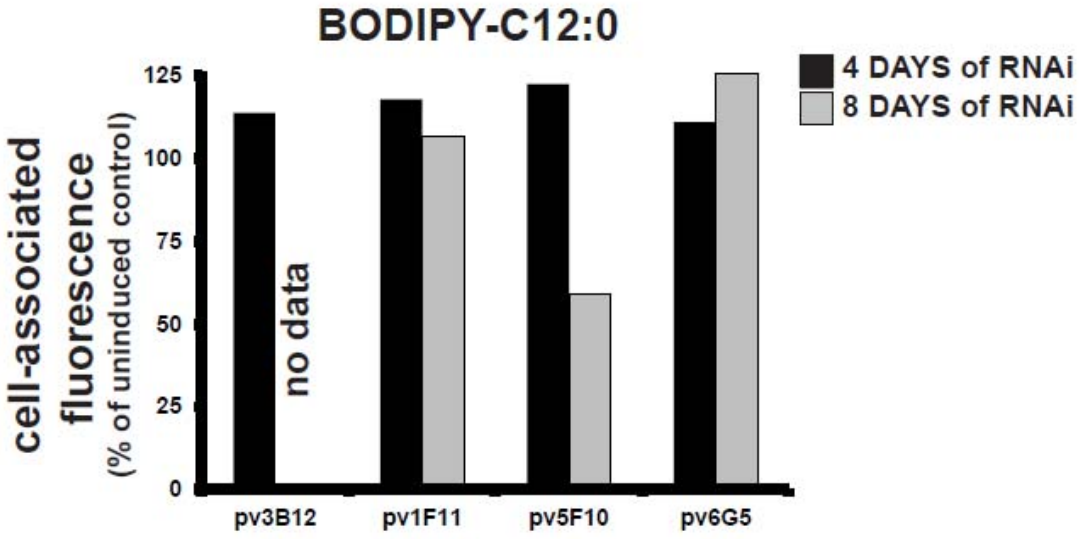

REFERENCES

Alsford S., Turner D.J., Obado S.O., Scnchez-Flores A., Glover L., Berriman M., Hertz-Fowler C., and Horn D. (2011) High-throughput phenotyping using parallel sequencing of RNA interference targets in the African trypanosome. Genome Res **21:** 915-924.

Aslett M., Aurrecoechea C., Berriman M., Brestelli J., Brunk B.P., Carrington M., *et al.* (2010) TriTrypDB: A functional genomic resource for the Trypanosomatidae. *Nucleic Acids Res* **38:** D457-62.

Colasante C., Ellis M., Ruppert T., and Voncken F. (2006) Comparative proteomics of glycosomes from bloodstream form and procyclic culture form *Trypanosoma brucei brucei*. *Proteomics* **6:** 3275-3293.

Djikeng A., Shen S., Tschudi C., and Ullu E. (2004) Analysis of gene function in T*rypanosma brucei* using RNA interference. In Parasite Genomics Protocols. Melville, S.E. (ed). Totowa, New Jersey: Humana Press, pp. 287.

Doering T.L., Pessin M.S., Hoff E.F., Hart G.W., Raben D.M., and Englund P.T. (1993) Trypanosome metabolism of myristate, the fatty acid required for the variant surface glycoprotein membrane anchor. *J.Biol.Chem.* **268:** 9215-9222.

Drew M.E., Morris J.C., Wang Z., Wells L., Sanchez M., Landfear S.M., and Englund P.T. (2003) The adenosine analog tubercidin inhibits glycolysis in *Trypanosoma brucei* as revealed by an RNA interference library. *J Biol Chem* **278:** 46596-600.

Horn D., and McCulloch R. (2010) Molecular mechanisms underlying the control of antigenic variation in African trypanosomes. *Curr Opin Microbiol* **13:** 700-705.

Hostetler H.A., Balanarasimha M., Huang H., Kelzer M.S., Kaliappan A., Kier A.B., and Schroeder F. (2010) Glucose regulates fatty acid binding protein interaction with lipids and peroxisome proliferator-activated receptor alpha. *J Lipid Res* **51:** 3103-3116.

Lee S.H., Stephens J.L., Paul K.S., and Englund P.T. (2006) Fatty acid synthesis by elongases in trypanosomes. *Cell* **126:** 691-699.

Li H., Black P.N., and DiRusso C.C. (2005) A live-cell high-throughput screening assay for identification of fatty acid uptake inhibitors. *Anal Biochem* **336:** 11-19.

Morita Y.S., Paul K.S., and Englund P.T. (2000) Specialized fatty acid synthesis in African trypanosomes: Myristate for GPI anchors. *Science* **288:** 140-3.

Morris J.C., Wang Z., Motyka S.A., Drew M.E., and Englund P.T. (2005) An RNAi-based genomic library for forward genetics in the African trypanosome. In Gene Silencing by RNA Interference: Technology and Application. Sohali, M. (ed). Boca Raton, FL: CRC Press, pp. 241.

Morris J.C., Wang Z., Drew M.E., and Englund P.T. (2002) Glycolysis modulates trypanosome glycoprotein expression as revealed by an RNAi library. *Embo J* **21:** 4429-38.

Motyka S.A., Zhao Z., Gull K., and Englund P.T. (2004) Integration of pZJM library plasmids into unexpected locations in the *Trypanosoma brucei* genome. *Mol Biochem Parasitol* **134:** 163-7.

Richardson J.P., Beecroft R.P., Tolson D.L., Liu M.K., and Pearson T.W. (1988) Procyclin: An unusual immunodominant glycoprotein surface antigen from the procyclic stage of African trypanosomes. *Mol.Biochem.Parasitol.* **31:** 203-216.

Roditi I., Schwarz H., Pearson T.W., Beecroft R.P., Liu M.K., Richardson J.P.*, et al.* (1989) Procyclin gene expression and loss of the variant surface glycoprotein during differentiation of *Trypanosoma brucei*. *J.Cell.Biol.* **108:** 737-746.

Stephens J.L., Lee S.H., Paul K.S., and Englund P.T. (2007) Mitochondrial fatty acid synthesis in *Trypanosoma brucei*. *J Biol Chem* **282:** 4427-36.

Thumser A.E., and Storch J. (2007) Characterization of a BODIPY-labeled fluorescent fatty acid analogue. binding to fatty acid-binding proteins, intracellular localization, and metabolism. *Mol Cell Biochem* **299:** 67-73.

van den Hoff M.J., Moorman A.F., and Lamers W.H. (1992) Electroporation in 'intracellular' buffer increases cell survival. *Nucleic Acids Res* **20:** 2902.

Vigueira P.A., and Paul K.S. (2011) Requirement for acetyl-CoA carboxylase in *Trypanosoma brucei* is dependent upon the growth environment. *Mol Microbiol* **80:** 117-132.

Wang Z., Morris J.C., Drew M.E., and Englund P.T. (2000) Inhibition of *Trypanosoma brucei* gene expression by RNA interference using an integratable vector with opposing T7 promoters. *J Biol Chem* **275:** 40174-9.

Zhao Z., Lindsay M.E., Roy Chowdhury A., Robinson D.R., and Englund P.T. (2008) p166, a link between the trypanosome mitochondrial DNA and flagellum, mediates genome segregation. *EMBO J* **27:** 143-154.

Zou Z., Tong F., Faergeman N.J., Borsting C., Black P.N., and DiRusso C.C. (2003) Vectorial acylation in saccharomyces cerevisiae. Fat1p and fatty acyl-CoA synthetase are interacting components of a fatty acid import complex. *J Biol Chem* **278:** 16414-16422.

CHAPTER 7

CONCLUSIONS

Lipid metabolism in *Trypanosoma brucei* is an often-overlooked aspect of the parasite's biology. The existing body of research is outstanding and provides a solid theoretical and methodological foundation on which to design future studies. However, many genes that are likely involved in lipid metabolism remain unstudied. This is surprising because of the unique and essential nature of these metabolic pathways. The parasite's utilization of microsomal elongases as a *de novo* fatty acid synthesis pathway is novel and many of the characterized genes represent potential drug targets.

The research I have presented in this dissertation has added to our growing knowledge of *Trypanosoma brucei's* lipid metabolism. In the process we have established acetyl-CoA carboxylase (ACC) as a potential drug target. Knockdown of ACC caused a doubling in the mean time until death in a mouse model. However, we did not cure the mice of the infection and they eventually succumbed. In the future, conditional knockouts for ACC should be generated and tested for virulence in mice.

Beyond adding to a long list of potential drug targets, our study has also demonstrated the importance of experimental flexibility when investigating potentially essential genes. Many investigations of individual genes and even genetic screens targeting essential genes examine parasite growth in normal culture media. This methodology leaves many essential genes unidentified. I

realize that investigating each gene's contribution to virulence in a mouse model is not feasible and would be a foolish endeavor. Instead, media components can be altered to more closely mimic physiological conditions in the mammalian bloodstream and cerebrospinal fluid. I fully anticipate that subtle changes in media composition would influence the outcome of many experiments.

As a follow-up to the ACC characterization, the consequences of ACC knockdown by RNA interference should be defined. This is the focus of an ongoing project in the lab. The metabolic or functional consequences of ACC RNAi, rather than loss of ACC, were the direct causes of reduced parasite virulence. Defining these consequences would allow us to expand our investigation to other genes potentially involved in that particular cellular process. For example, if we determine that ACC RNAi causes of reduced endocytosis rates, other genes involved in endocytosis could potentially result in a similar reduction in parasite virulence.

This concept is not unique, as many researchers attempt to identify the cause of cell death brought on by RNAi. However, because RNAi of most essential genes results in cell death *in vitro*, this endeavor is often fruitless. When a cell is dying, it becomes difficult to define whether a phenotype is a cause, direct consequence, or indirect consequence of cell death. In the case of ACC we can avoid this potential problem because the gene is essential for growth only under certain conditions. Thus, the elaborated phenotypes brought on by RNAi of ACC can be studied in isolation of cell death.

I hope that the information and thoughts I have shared in this dissertation will be useful to future researchers. With a little hard work and a lot of luck this work could lead to a treatment for African trypanosomiasis, resulting in the economic revitalization of Sub-Saharan Africa, a region of the world too long oppressed by the shadow of the tsetse.